

**UNIVERSIDAD AUTÓNOMA DE NUEVO LEÓN
FACULTAD DE CIENCIAS BIOLÓGICAS**



**SYNTHESIS AND PHYSICOCHEMICAL CHARACTERIZATION OF
PHOTO CROSSLINKED HYDROGELS OF ALGINATE/GELATIN AND
 α -TOCOPHEROL NANOCAPSULES FOR THEIR POTENTIAL
USE AS BIOMATERIALS**

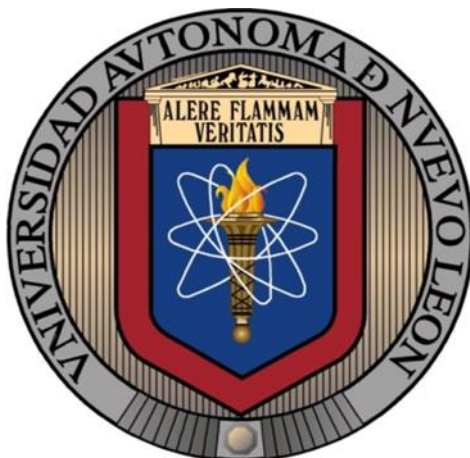
POR

JOSÉ ERNESTO PALACIOS SANTOS

**COMO REQUISITO PARCIAL PARA OBTENER EL GRADO DE
DOCTOR EN CIENCIAS CON ORIENTACIÓN EN BIOTECNOLOGÍA**

NOVIEMBRE, 2019

UNIVERSIDAD AUTÓNOMA DE NUEVO LEÓN
FACULTAD DE CIENCIAS BIOLÓGICAS
SUB-DIRECTORATE OF POSTGRADUATE STUDIES



**SYNTHESIS AND PHYSICOCHEMICAL CHARACTERIZATION OF
PHOTO CROSSLINKED HYDROGELS OF ALGINATE/GELATIN AND
 α -tocopherol NANOCAPSULES FOR THEIR POTENTIAL USE AS
BIOMATERIALS**

BY

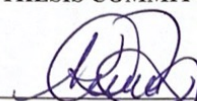
JOSÉ ERNESTO PALACIOS SANTOS

**AS A PARTIAL REQUIREMENT TO OBTAIN THE DEGREE OF
DOCTOR IN SCIENCES WITH ORIENTATION IN BIOTECHNOLOGY**

NOVEMBER, 2019

**SYNTHESIS AND PHYSICOCHEMICAL
CHARACTERIZATION OF PHOTO CROSSLINKED HYDROGELS
OF ALGINATE/GELATIN AND α -TOCOPHEROL
NANOCAPSULES FOR THEIR POTENTIAL USE AS
BIOMATERIALS**

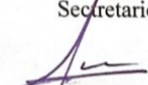
THESIS COMMITTEE



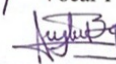
Dra. Katiushka Arevalo Niño
Director



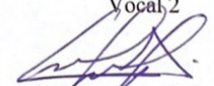
Dra. Verónica Almaguer Cantú
Secretario



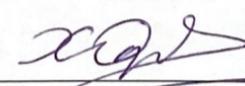
Dr. Sergio A. Galindo Rodríguez
Vocal 1



Dr. Juan Gabriel Báez González
Vocal 2



Dra. Roelío Alvarez Román
Vocal 3



Dra. Oksana Vasilievna Kharissova
Asesor Externo 1



Dr. Alberto Gómez Treviño
Asesor Externo 2

ACKNOWLEDGMENTS

Primero me gustaría agradecer a mi familia, a mi mama Nelly Santos García y a mi papa Oziel Chapa Martínez, por apoyarme durante todo este tiempo y guiarme hasta llegar a culminar este momento tan importante en mi vida, sin ustedes no hubiera podido lograr culminar ninguna meta que me hubiera propuesto en la vida; a mi hermanita, Marisol Palacios, ya que siempre as sido un lucero en mis días mas tristes.

A Andrés Flores, por siempre apoyarme en cada uno de los pasos que di durante esta etapa y que siempre me alentó a ser una mejor persona todos los días.

A mis compañeros de laboratorio (Eugenia, Héctor, Mayra, Katita, Renatito, Valentina e Isabel) ya que sin su amistad y su apoyo, no lo hubiese logrado y mis días en el laboratorio no hubieran sido lo mismo.

A mis compañeros de generación, Exiquio Maldonado, Claudio Guajardo, Martha Espinoza y Ana Herrera.

A la Dra. Katiushka Arévalo, por brindarme esta gran oportunidad que me formo como persona y como profesional.

Muchas Gracias

DEDICATORIES

Este trabajo lo dedico a todas las personas que creyeron en mi y a mi
mama; sin ti yo no seria nada.

CONTENT INDEX

	Page
Introduction.....	1
Background.....	2
Skin Structure.....	2
Epidermis.....	2
Dermis.....	3
Hypodermis.....	3
Wounds.....	4
Pressure ulcers.....	4
Epidemiology.....	5
Treatment.....	6
Wound Care Cost.....	6
Tissue Regeneration.....	7
Cicatrization.....	7
Biomaterials.....	8
Biopolymers.....	8
Alginate.....	9
Alginate Properties.....	9
Alginate Production.....	10
Alginate Degradation.....	10
Alginate Current Uses.....	10
Gelatin.....	11
Gelatin Properties.....	11
Gelatin Production.....	11
Gelatin Degradation.....	11
Current Uses of Gelatin.....	12
Hydrogels.....	13
Uses of Hydrogels.....	13
Type of Hydrogels.....	13

	Page
Physical Stimuli.....	14
Thermal Crosslinking.....	14
Chemical Stimuli.....	14
Photo crosslinking.....	14
Photoreceptors.....	15
Irgacure 2959.....	15
Properties of Hydrogels.....	16
Physicochemical Properties.....	16
Swelling.....	16
Mechanism of De-Swelling.....	17
Morphology (Porosity).....	18
Wettability (Contact Angle)	18
Rheological Behavior.....	19
Classic Rheological Models.....	20
Model of Ostwald-de Waele.....	20
Water Vapor Permeability.....	21
Permeation Theory.....	21
Drug Entrapment.....	22
Nanotechnology.....	23
Type of Nanosynthesis.....	24
Nanoprecipitation.....	24
Mechanism of Nanoprecipitation.....	24
Aqueous phase.....	25
Organic Phase.....	25
Most used Polymers.....	25
Polycaprolactone (PCL).....	26
Properties of PCL.....	25
Degradation of PCL.....	25
Current uses of PCL.....	25
Characterization of Nanocapsules.....	27

	Page
Particle Size.....	27
Surface Load (Z potential)	27
Polydispersity Index (PDI)	27
Drug Release and Encapsulation Efficiency.....	28
Oxidative Stress.....	28
Free radicals in Chronic Wounds.....	28
Antioxidants.....	30
Vitamins.....	30
Vitamin E.....	30
Functions of α -tocopherol.....	31
α -tocopherol Degradation.....	31
Current uses of α -tocopherol.....	31
Justification.....	32
Hypothesis.....	33
Objectives.....	34
General Objective.....	34
Specific Objective.....	34
Methodology.....	35
Thermal Crosslinking of Hydrogels (Alginate or Gelatin).....	35
Physical Characterization of Hydrogels.....	36
Swelling.....	36
Solubility.....	37
Rheological Behavior.....	38
Consistency Index.....	38
Chemical Characterization.....	38
pH.....	38
Contact Angle.....	39
Fourier Infrared Transform Spectroscopy (FTIR)	39
Water Vapor Permeability.....	40
Synthesis of Nanocapsules.....	41

	Page
Physical Characterization.....	42
Chemical Characterization.....	42
Antioxidant Activity by DPPH.....	42
α -Tocopherol quantification.....	43
Direct (HPLC).....	43
Indirect (DPPH).....	43
Stability of α -tocopherol after UV exposure.....	44
Quantification.....	44
Antioxidant Activity.....	44
Results.....	45
Thermal crosslinked Hydrogels (Alginate or Gelatin)	45
Physical Characterization.....	45
Swelling Behavior.....	45
Alginate Hydrogels.....	45
Gelatin Hydrogels.....	46
Solubility Behavior.....	47
Alginate Hydrogels.....	47
Gelatin Hydrogels.....	47
Rheological Analysis of Thermo crosslinked Hydrogels.....	49
Rheological behavior	49
Alginate Hydrogels.....	49
Gelatin Hydrogels.....	50
Thermal and Photo crosslinked Hydrogels.....	52
Physical Characterization.....	52
Swelling Behavior.....	52
Thermal crosslinked Hydrogels.....	52
Photo crosslinked Hydrogels.....	53
Solubility Behavior.....	54
Thermal crosslinked Hydrogels.....	54
Photo crosslinked Hydrogels.....	54

	Page
Rheological Analysis of (Thermal and photo) Hydrogels.....	56
Rheological Behavior of Thermal crosslinked Hydrogels.	56
Rheological Behavior of Photo crosslinked Hydrogels...	57
Consistency Index.....	58
Thermal crosslinked Hydrogels.....	58
Photo crosslinked Hydrogels.....	58
Fourier Transform Infrared Spectroscopy (FTIR).....	59
FTIR of Photo crosslinked Hydrogels.....	59
Porosity by SEM.....	60
Chemical Characterization.....	61
pH.....	61
Thermal and Photo crosslinked Hydrogels.....	61
Water Vapor Permeability.....	61
Thermal crosslinked Hydrogels.....	61
Photo crosslinked Hydrogels.....	62
Contact Angle (Wettability).....	63
Thermal crosslinked Hydrogels.....	63
Photo crosslinked Hydrogels.....	64
Nanoprecipitation of PCL nanocapsules with 20 mg of PCL.....	65
Physical Characterization.....	65
Chemical Characterization.....	66
Antioxidant Activity by DPPH.....	66
Quantification of α -tocopherol by HPLC.....	66
Nanoprecipitation of PCL with 10 mg of PCL.....	67
Physical characterization.....	67
Nanoprecipitation using different solvent concentration.....	67
Physical Characterization.....	67
Chemical characterization.....	68
Antioxidant Activity by DPPH.....	68
Quantification of α -tocopherol of NCs obtained Acetone:Metanol 1:1...	68

	Page
Direct (HPLC).....	68
Indirect (DPPH).....	68
Stability of α -tocopherol after UV light exposure.....	70
HPLC.....	70
Antioxidant Activity after UV light exposure.....	70
Discussion.....	71
Alginate or Gelatin Hydrogels.....	71
Physical characterization.....	71
Swelling.....	71
Solubility.....	71
Rheological Analysis.....	72
Thermal and Photo crosslinked Hydrogels.....	73
Physical Characterization.....	73
Swelling.....	73
Solubility.....	73
Rheological Analysis.....	74
Chemical Characterization.....	74
pH.....	74
Water Vapor Permeability.....	74
Contact Angle (Wettability).....	75
Effect of the concentration of PCL, α -tocopherol and different solvents in the synthesis of nanocapsules.....	76
PCL Concentration.....	76
Physical characterization.....	76
Chemical characterization.....	76
α -tocopherol Concentration.....	76
Physical characterization.....	76
Solvent concentration.....	76
Physical characterization.....	76
Chemical characterization.....	77

	Page
Protection of UV.....	77
Conclusion.....	78
Perspectives.....	79
Bibliography.....	80
Appendix.....	97

FIGURES INDEX

		Page
Figure 1	Skin Structure	1
Figure 2	Pressure Ulcer Process	4
Figure 3	Alginate Structure	9
Figure 4	Method of Alginate Purification	10
Figure 5	Gelatin Structure	11
Figure 6	Diagram of Photo crosslinking Types	15
Figure 7	Chemical Structure of Irgacure 2959	15
Figure 8	Physical states of Water within Hydrogels	17
Figure 9	Different contact angles	19
Figure 10	Superficial Tension	20
Figure 11	Types of Rheological Behaviors	20
Figure 12	Representation of Pseudoplastic Behavior	21
Figure 13	Diagram of Vapor or Gas permeation on membrane	22
Figure 14	Representation of drug entrapment	23
Figure 15	Different approaches in nanotechnology	24
Figure 16	Nanoprecipitate process	25
Figure 17	Synthesis of Polycaprolactone	27
Figure 18	Hydroxyl Radical	29
Figure 19	Phases of a normal Wound repair	30
Figure 20	Chemical structures of α -tocopherol and α -tocotrienol	31
Figure 21	Swelling test representation	37
Figure 22	Solubility test representation	38
Figure 23	Cone-plate sensor representation	39
Figure 24	Water Vapor Permeability test representation	41
Figure 25	Antioxidant activity by DPPH test	43
Figure 26	Swelling Behavior of Alginate Hydrogels	48
Figure 27	Swelling Behavior of Gelatin Hydrogels	49
Figure 28	Solubility Behavior of Alginate Hydrogels	50

	Page
Figure 29 Solubility Behavior of Gelatin Hydrogels	51
Figure 30 Rheological Behavior of Alginate Hydrogels	52
Figure 31 Rheological Behavior of Gelatin Hydrogels	53
Figure 32 Swelling Behavior of Thermal crosslinked Hydrogels	55
Figure 33 Swelling Behavior of Photo crosslinked Hydrogels	56
Figure 34 Solubility Behavior of Thermal crosslinked Hydrogels	57
Figure 35 Solubility Behavior of Photo crosslinked Hydrogels	58
Figure 36 Rheological Behavior of Thermal crosslinked Hydrogels	59
Figure 37 Rheological Behavior of Photo crosslinked Hydrogels	60
Figure 38 Consistency Index of Thermal crosslinked Hydrogels	61
Figure 39 Consistency Index of Crosslinked Hydrogels	61
Figure 40 FTIR of Photo crosslinked Hydrogels	63
Figure 41 SEM images.	
Figure 42 Permeability behavior of thermal crosslinked hydrogels	72
Figure 43 Permeability behavior of photo crosslinked hydrogels	73
Figure 44 Contact angle of Thermal crosslinked hydrogels	74
Figure 45 Contact angle of Photo crosslinked hydrogels	75
Figure 46 Antioxidant Activity by DPPH of the supernatant and the precipitate of the nanocapsules suspension of 20 mg of PCL	77
Figure 47 Antioxidant activity by DPPH of the supernatant and the precipitate of the nanocapsule suspension of different solvents	
Figure 48 Antioxidant activity by DPPH of nanocapsules suspension after being exposed to different times of UV light exposure	85

TABLE INDEX

	Page	
Table 1	Skin Stratifications	3
Table 2	Stages of Pressure Ulcers	5
Table 3	Pharmaceutical applications of Hydrogels	13
Table 4	Examples of Polymer most used in the nanoprecipitation technique	25
Table 5	Alginate and Gelatin hydrogel formulations	35
Table 6	Experimental design of Thermal and photo crosslinked hydrogels	39
Table 7	Formulation of Nanocapsules	41
Table 8	Physical characteristics of 20 mg of PCL nanocapsules	65
Table 9	Physical characteristics of 10 mg of PCL nanocapsules	67
Table 10	Physical characteristics of nanocapsules with different solvents	67
Table 11	Quantification of α -Tocopherol by HPLC of nananocapsules with different solvents	69
Table 12	Antioxidant activity of nanocapsules after being exposed to UV light	70

EQUATION INDEX

		Page
Equation 1	Formula for calculating the Density of Dry Hydrogels	18
Equation 2	Power Law formula	21
Equation 3	Fick's first Law	22
Equation 4	Drug Loading formula	23
Equation 5	Percentage of Swelling formula	37
Equation 6	Percentage of Solubility formula	38
Equation 7	Linear regression formula	39
Equation 8	Water Vapor Permeability Formula	41
Equation 9	Antioxidant activity formula	43

AVREBIATION LIST

USA	United States of America
INER	Instituto Nacional de Enfermedades Respiratorias
MXN	Mexican Pesos
NPUAP	National Pressure Ulcer Advisory Panel
DM	Diabetes Mellitus
UPP	Pressure Ulcers
USD	United States Dollars
EUR	Euros
GBP	Pounds
IL-1	Interlucín-1
IPN	Interpenetrated polymers
SIPN	Semi-interpenetrating polymers networks
PIPn	Pseudo-interpenetrating polymer networks
MPPs	Metalloproteinases
ROS	Reactive Oxygen Species
PI	Photoinitiators
µm	Micrometers
°	Degree
$\dot{\gamma}$	Shear rate
η	Viscosity
τ	Shear stress
<i>K</i>	Consistency Index
WVTR	Water Vapor Transmission Rate
mMol	Millimolar
nm	Nanometers
PCL	Polycaprolactone
IUPAC	Union of Pure Applied Chemistry
°C	Degrees Celsius

ζ	Z Potential
DLS	Dynamic Light Scattering
PDI	Polydispersity Index
HPLC	High Performance Liquid Chromatography
NCs	Nanocapsules
FR	Free Radicals
PKC	Protein Kinase C
PLGA	Poly(lactic-co-glycolic acid)
w/v	Weight/volume
RPM	Revolutions per minute
PEG	Polyethylene glycol
g	grams
mL	milliliters
Pa.s	Pascals per second
FTIR	Fourier Infrared Transform Spectroscopy

APPENDIX LIST

- Appendix A** Thermo crosslinked hydrogels
- Appendix A.1** Photo crosslinked hydrogels
- Appendix B** Effect on the swelling behavior of Alginate or Gelatin hydrogels
- Appendix C** Effect on the solubility behavior of Alginate or Gelatin hydrogels
- Appendix D** Effect on the swelling behavior of Thermal and Photo crosslinked hydrogels
- Appendix E** Effect on the solubility behavior of Thermal and Photo crosslinked hydrogels
- Appendix F** Effects on the water vapor permeability of the Thermal and Photo crosslinked hydrogels
- Appendix G** Microscopic analysis of AG1 Thermal crosslinked hydrogels)
- Appendix G.1** Microscopic analysis of AG1 Photo crosslinked hydrogels)
- Appendix H** Microscopic analysis of GA1 Thermal crosslinked hydrogels)
- Appendix H.1** Microscopic analysis of GA1 Photo crosslinked hydrogels)
- Appendix I** Elemental analysis of Thermo crosslinked hydrogels
- Appendix J** Elemental analysis of Photo crosslinked hydrogels
- Appendix K** Nanocapsule suspension batch
- Appendix L** Nanocapsules microscopic (SEM) analysis

SUMMARY

In recent years, great advances have been made in the development of biomaterials for wound healing and tissue regeneration, so they can cover the necessary requirements to be ideal treatments for wounds of difficult healing. Current treatments are materials focused on the protection, absorption of wound exudate and wound healing, however, there are different types of wounds which due to the complexity of healing of the damage tissue, diseases such as diabetes and arterial hypertension or the type of accident that caused them, such as burns or necrosis, the regeneration of the new tissue is more complicated.

Therefore, this project proposes the developments of photo crosslinked hydrogel matrices of alginate and gelatin and nanocapsules of polycaprolactone loaded with α -tocopherol that have a potential use for a natural regenerative response of the skin by eliminating excessive free radicals.

Based on what previously explained the question was raised: Will hydrogels made with biopolymers and loaded with nanoencapsulated α -tocopherol promotes a faster and more effective cell proliferation response?

During this investigation, the synthesis of the hydrogels was made by photo crosslink and their physicochemical characteristics were analyzed by gravimetric, spectrophotometric and rheological techniques, while the nanocapsules were formed using nanoprecipitation method and their physicochemical characteristics were also analyzed.

In this work, 12 hydrogel formulations were made and analyzed using different crosslinking methods, and it was observed that Photo-crosslinking had no negative effect on its physicochemical characteristics, due to its firmness and its solubility rate are further improved. Also, 13 nanocapsule formulations were made and analyzed employing the nanoprecipitation technique, where it was observed that by modifying the concentrations of the solvents, smaller diameters of the nanocapsules were obtain and using different extraction methods, its encapsulation efficiency and antioxidant activity were improved

RESUMEN

En los últimos años se han realizado grandes avances en el desarrollo de biomateriales para la curación de heridas y la regeneración de tejidos, de tal modo que puedan cubrir los requisitos necesarios para ser tratamientos ideales para heridas crónicas de difícil cicatrización. Los tratamientos actuales son materiales enfocados en la protección, absorción de exudado de las heridas y curación de estas mismas. Sin embargo, existen diferentes tipos de heridas crónicas que, debido a la complejidad de la curación del tejido dañado por enfermedades tales como la Diabetes y la Hipertensión arterial o el tipo de accidente que las causó, como quemaduras o necrosis, la regeneración del nuevo tejido se vuelve más complicado.

Por lo tanto, este proyecto propone el desarrollo de matrices de hidrogel de alginato y gelatina, incorporando nanocápsulas de policaprolactona con α -tocoferol para crear un microambiente óptimo y servir como guía para una respuesta regenerativa natural de la piel al eliminar el exceso de radicales libres.

Con base en lo que se explicó anteriormente, se planteó la pregunta: ¿Los hidrogeles hechos con biopolímeros y cargados con α -tocoferol nanoencapsulado promueven una respuesta de proliferación celular más rápida y efectiva?

Durante esta investigación, la síntesis de los hidrogeles se realizó mediante Foto entrecruzamiento y sus características fisicoquímicas se analizaron mediante técnicas gravimétricas, espectrofotométricas y reológicas, mientras que las nanocápsulas se formaron utilizando el método de nanoprecipitación y también se analizaron sus características fisicoquímicas.

En este trabajo, se realizaron y analizaron 12 formulaciones de hidrogeles utilizando diferentes métodos de entrecruzamiento y se observó que la foto entrecruzamiento no tuvo un efecto negativo sobre sus características fisicoquímicas, ya que su firmeza y su tasa de solubilidad mejoraron. Además, se realizaron y analizaron 13 formulaciones de nanocápsulas empleando mediante nanoprecipitación y se observó que al modificar las concentraciones de los solventes, se obtuvieron diámetros más pequeños y utilizando diferentes métodos de extracción, su eficiencia de encapsulación y actividad antioxidante mejorado.

INTRODUCTION

Chronic wounds represent a latent problem in health systems affecting around 5.7 million patients and costing around 20 billion dollars annually in the United States of America (USA) alone, while in Mexico, there are no specific statistical studies, the Instituto Nacional de Enfermedades Respiratorias (INER), reported an incidence of ulcers by 80 % of its patients. Diseases such as diabetes have a surprisingly high correlation with wounds in Mexico, diabetes affects 9.2 % of the population, of which 7.2. % of these patients have ulcers that can be complicated and increase the mortality of affected people.

The most common chronic wounds in the USA are; diabetic foot ulcers, burns, venous ulcers and pressure ulcers. During the second day for the prevention of pressure ulcers by the Ministry of Health, it was pointed out that the treatments of these wounds at the outpatient level have a cost of \$ 1,259 Mexican pesos (MXN) a week and \$ 5,036 MXN a month and at the hospital level it has a weekly cost of \$ 41,046 MXN and monthly of \$ 175,552 MXN.

Currently, the first instance treatments are based on the use of wet occlusive or semi-occlusive dressings so that they can promote cell proliferation and tissue regeneration, however, these do not grant an ideal healing, since at the time of changing or cleaning them, they bring with them novo-tissue and do not produce an adequate absorption of exudate, however, tissue engineering is frequently used to create autologous graft, but these are very expensive and have a probability of being rejected by the host.

For these reasons, the possible use as an adjunctive treatment for chronic wounds, the application of hydrogels with biocompatible polymers as an environmental and mechanical protection system, absorption of exudate and release of active agents in nanocapsules will be evaluated to be evaluated as an accelerating agent for cell proliferation and an oxidative stress reducer product of chronic wounds.

BACKGROUND

Skin Structure

The skin (Fig. 1) is known as the “Integumentary System”, this being the skin and its accessory organs (e.g. Hair, nails and glands), this consists of three layers: Epidermis, Dermis and Hypodermis (Saladin *et al.*, 2015), some of the most important functions of the skin are: barrier function, Vitamin D synthesis, sensation and thermoregulation (Kolarsick *et al.*, 2011).

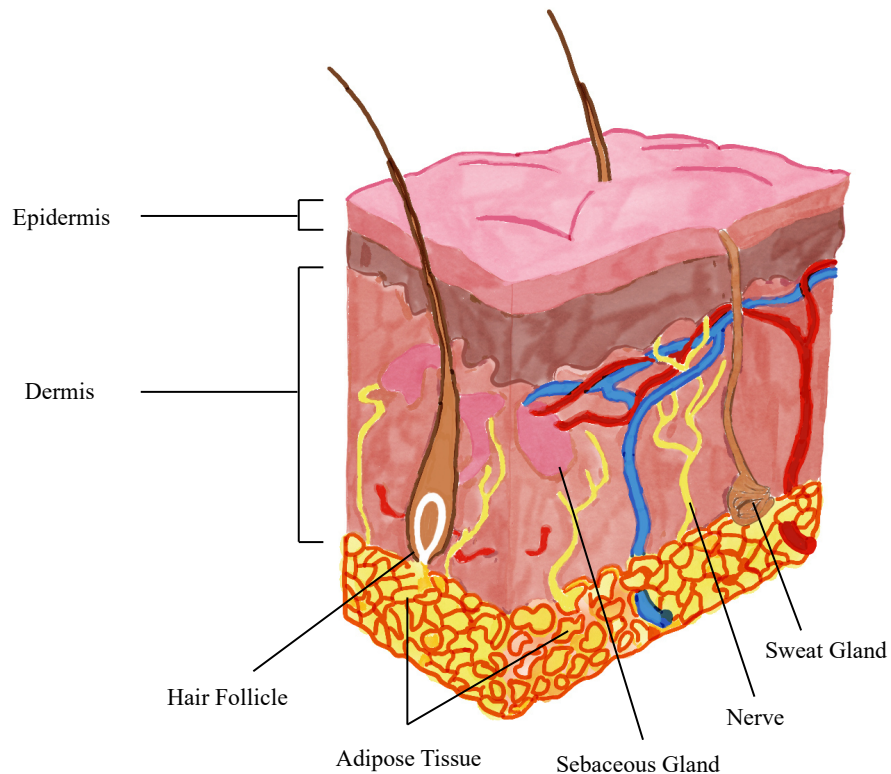


Figure 1. Skin Structure

Epidermis

It is a stratified keratinized squamous epithelium, since its surface consists of dead cells packed with a hard protein (Keratin), lacks blood vessels and depends on the diffusion of nutrients from connective tissues (Saladin *et al.*, 2015). It consists of five types of cells: Cytoblasts (divide and give rise to Keratinocytes), Keratinocytes (perform keratin synthesis), Melanocytes (perform melanin synthesis), Merkel cells (sensory receptors) and Langerhans cells (immune cells) (Kolarsick *et al.*, 2011).

Dermis

A layer of connective tissue composed mainly of: Collagen, elastic fibers and reticular fibers (Saladin *et al.*, 2015), it has a wide supply of blood vessels, skin glands and nerve endings (Kolarsick *et al.*, 2011) consists of two layers: the papillary layer and the reticular layer (Saladin *et al.*, 2015).

Hypodermis

Also called subcutaneous tissue, its main function is to serve as an energy deposit and thermal insulation (Saladin *et al.*, 2015), since it is composed of adipose tissue and joins the skin with adjacent tissue (Kolarsick *et al.*, 2011). Next, in Table 1, a summary of the characteristics of the epidermal layers is presented:

Table 1. Skin Stratifications (Saladin *et al.*, 2015)

Layer	Description
Epidermis	Keratinized stratified squamous epithelium
Stratum corneum	Keratinized and dead skin Surface cells
Lucid layer	Narrow, clear area, without features, which is only seen on thick skin
Granular layer	Two to five layers of cells with keratohyalin granules that stain them dark.
Stratum Spinosum	Many layers of keratinocytes that flatten as they move away from the dermis and abundant dendritic cells
Basal Stratum	Single layer of cubic to cylindrical cells, melanin is notorious in the keratinocytes of this layer
Dermis	Fibrous connective tissue, with abundant blood vessels and nerve endings
Papillary Layer	It consists of areolar tissue and covers a fifth of the surface of the dermis
Reticular layer	It is irregular dense connective tissue
Hypodermis	Adipose tissue between the skin and muscle

Wounds

According to the National Pressure Ulcer Advisory Panel (NPUAP) a wound is defined as “Any disruption of normal anatomical and functional structures” and these can be classified as acute or chronic. According to the NPUAP, if a wound does not restore the anatomy and functionality of the affected skin within a period of less than thirty days, it is considered an evolving chronic wound (Heasler 2014).

Pressure Ulcers

Diseases such as diabetes mellitus (DM), have a correlation with chronic wounds, in Mexico, DM affects 9.2 % of the Mexican population, of which 7.2 % of these, have ulcers that can complicate and increase mortality of affected people (Guitierrez *et al.*, 2012).

This type of chronic wound is caused by the lack of blood supply in an area, due to a vascular pathology of a constant weight in the area (Fig. 2), resulting in a necrosis due to the lack of oxygen irrigation (Talens 2016). Chronic ulcers can be classified according to the degree of epithelial loss, their etiology (Vela-anaya 2013). The most common chronic ulcers are pressure ulcers (UPP) (Monsonis 2013), this type of wounds lacked interest for health professionals, being assumed as “Irremediable situations of the disease” (Talens 2016) being the reasons for which, at the time, did not favor the development of studies on this condition.

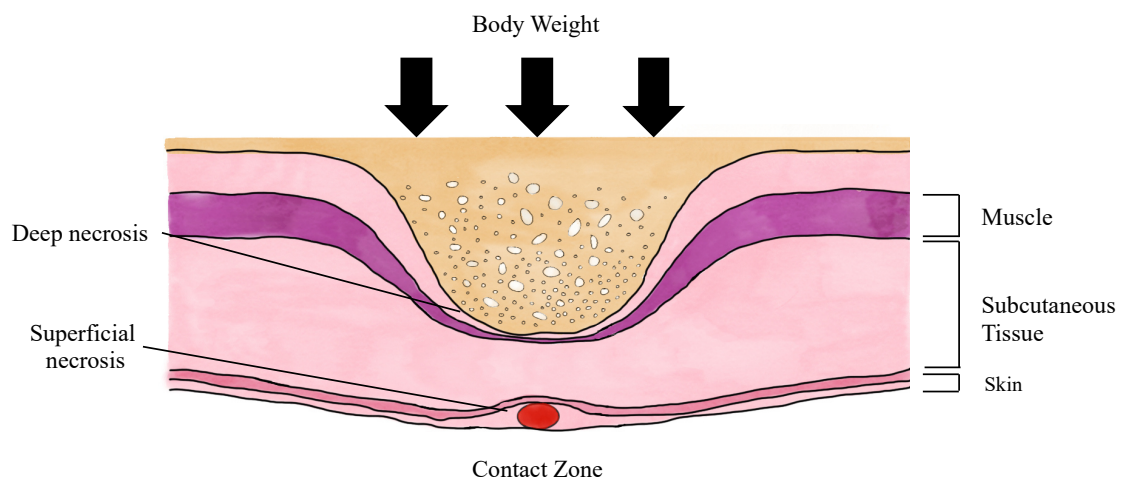


Figure 2. Pressure Ulcer Process

The NPUAP created a classification according to the extent of the ulceration by dividing it into different stages, as explained in Table 2:

Table 2. Stages of Pressure Ulcers

Stages	Characteristics	Examples
Stage I. Non-Bleaching Erythema	Intact skin with non-bleachable redness of a localized area, usually on a bony prominence. The area can be painful, firm, soft, hotter or colder compared to adjacent tissues.	
Stage II. Partial thickness ulcer	Loss of partial thickness of the dermis, it presents as a shallow open ulcer. It can also be presented as an intact ampoule filled with serum (sometimes bloody) or open.	
Stage III: Total loss of skin thickness	Complete tissue loss. Subcutaneous fat may be visible, but bones, tendons or muscles are not exposed. The depth of the ulcer by Stage III pressure varies according to the anatomical location of the wound.	
Stage IV: Total loss of tissue thickness	Total loss of tissue thickness with exposed bone, tendon or muscle. Stage IV ulcers may spread to muscle and/or support structures and osteomyelitis or osteitis may be likely to occur.	

Epidemiology

The main risk factor for this pathology are; age, sedentary lifestyle, overweight, chronic degenerative diseases and vascular diseases (Cañon *et al.*, 2005).

Treatment

Currently, two healing systems are established for this type of wounds: the traditional treatment, which is based on the use of antiseptics and “Leaving the wound in the open air” and on the other hand the wet treatments, being the use of products that generate the wound area is a humid environment that controls exudate and stimulates healing (Talens 2016). Falanga (2004) was the one who developed the term “Preparation of the wound bed” and defines it as “A form of global wound treatments, which accelerates endogenous healing and facilitates the efficiency of other therapeutic measures”.

Experimental studies have shown that maintaining a moist microenvironment in a wound, either through occlusive or semi-occlusive dressings, accelerates reepithelization twice as much as that obtained by traditional treatment (Winter, 1962, 1963; Falanga 2004).

Wound Care Cost

Regarding studies related to the issue of the cost of the care service for these wounds in Mexico, one study (Mejía *et al.*, 2015) indicated that, in 14 units of first level of care, the cost of treatment of UPP can amount up to \$ 30,194.19 MXN for these units, but the data are not available as a nation of said condition. However, in the United States of America (USA), this type of injury represents an annual expenditure of 25 billion US dollars (USD) (Sen *et al.*, 2009) while in Spain and the United Kingdom it is estimated more than 1,687 million euros (EUR) (Agreda Soldevilla *et al.*, 2008) and 1769 million pounds (GBP) (Bennett *et al.*, 2004) annually respectively.

Tissue Regeneration

The epithelia are always in permanent regeneration due to the continuous wear to which they are subjected (Saladin *et al.*, 2015), when a wound occurs, the regeneration process is activated and goes hand in hand with the healing process (Kolarsick *et al.*, 2011).

Cicatrization

The repair of a wound is a set of processes that comprises three phases: Inflammatory, Proliferative and Tissue remodeling, which are explained below:

- **Inflammatory Phase:** Platelet adhesion to damaged tissue are activated by thrombin and fibrillar collagen and as a result, degranulation occurs that intervene in platelet aggregation (Gonzales *et al.*, 2016); Neutrophils release enzymes (hydrolases, proteases and lysozymes).
- **Proliferative phase:** There are four important processes: (A) Fibroplasia; the arrival of fibroblast to the wound to create a mold of collagen, (B) Angiogenesis; starts simultaneously with fibroplasia to create new capillary vessels, (C) Re-epithelialization; Keratinocytes migrate from the wound edges to restore skin integrity activated by Interlucin-1 (IL-1) and (D) Wound contraction; Myoblast are rich in actin microfilaments and will establish cell-cell binding (Gonzales *et al.*, 2016).
- **Tissue remodeling phase:** Fibroblasts will produce fibronectin, hyaluronic acid, proteoglycans and collagen (Gonzales *et al.*, 2016).

Biomaterials

Biomaterials can be defined as “Materials with the functions of repairing, replacing or improving an existing tissue in the body” (H. A. Currie *et al.*, 2007), the biomaterials that are most used are polymers, such as polysaccharides and proteins (H. A. Currie *et al.*, 2007). In general, the use of polymeric materials in the regeneration of tissue and organs has had a use in many different applications, such as in the use of polymeric biomaterials for drug delivery (Pohlman *et al.*, 2013), regeneration of striated (Kwee and Mooney 2017) and cardiac (Sewell-Loftin *et al.*, 2011) muscles and tendon reconstruction (Walden *et al.*, 2017) to name a few.

Biopolymers

Biopolymers are polymers produced by living organisms, they contain monomers that are covalently linked to form larger structures (Mohanty *et al.*, 2005). There are three main classes of biopolymers based on the different monomer units used and the structure of the biopolymer formed, like;

- Polynucleotides are long polymers that consist of 13 or more nucleotide monomers.
- Polypeptides are short polymers of amino acids
- Polysaccharides are often linearly linked polymeric carbohydrate structures (Mayers *et al.*, 2008)

A network of interpenetrated polymers (IPN) is a polymer that comprises two or more networks that are intertwined or at least partially, but are not covalently bonded together (Thomas *et al.*, 2012) the simple mixing of two or more polymers does not create an IPN, since there are semi-interpenetrating polymer networks (SIPN) and pseudo-interpenetrating polymer networks (PIPn) (Thomas *et al.*, 2012).

Alginate

Alginate Properties

It is an anionic polymer of natural origin and is widely researched and used for many biomedical applications due to its biocompatibility, low toxicity, relatively low cost and gentle gelation by adding divalent cations (e.g. Ca⁺) according to (Szakalska *et al.*, 2016), and is made up of Glucuronic and Mannuronic monomers (Fig. 1)

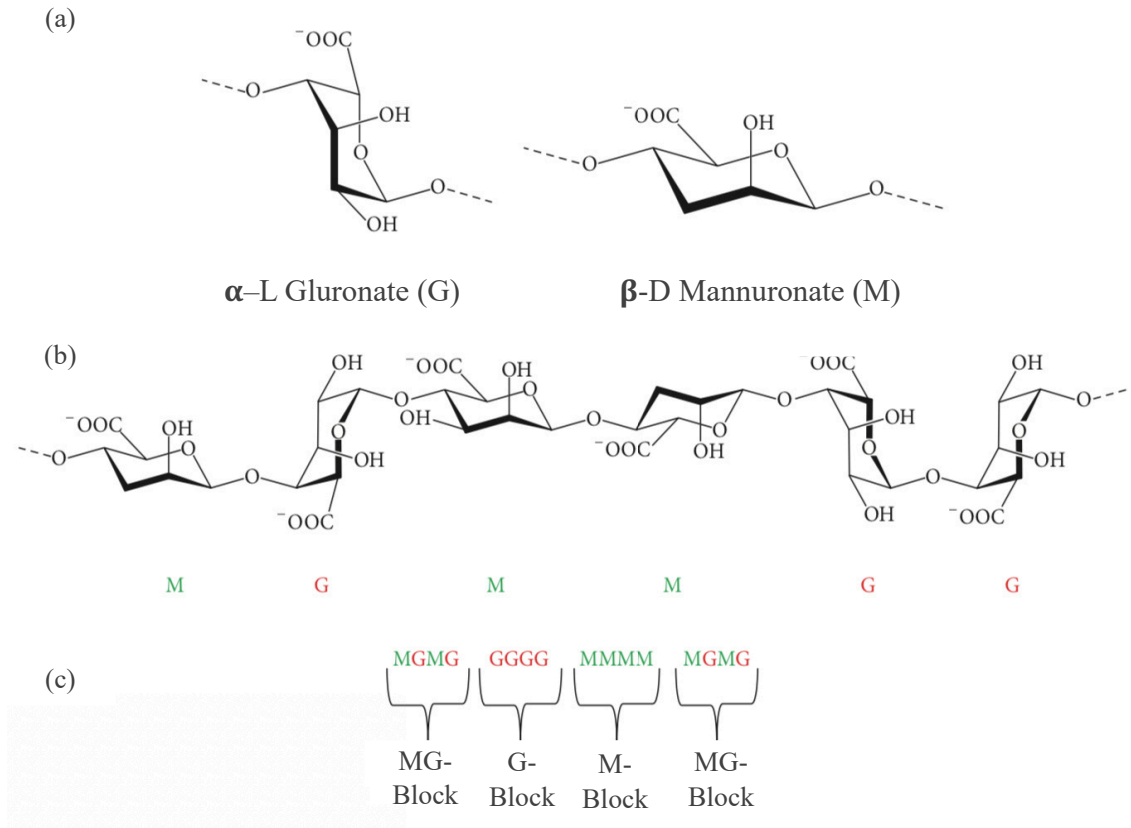


Figure 3. Alginate Structure. Where (a) are the monomers (B) is the conformation of the chain, (c) is the distribution of the blocks.

Alginate Production

Commercial alginate is typically extracted from brown algae, mainly *Phaeophyceae* by treatments with alkaline solutions, typically Sodium Hydroxide (NaOH) (Szekalska *et al.*, 2016) and other acid solutions (Fig. 2).

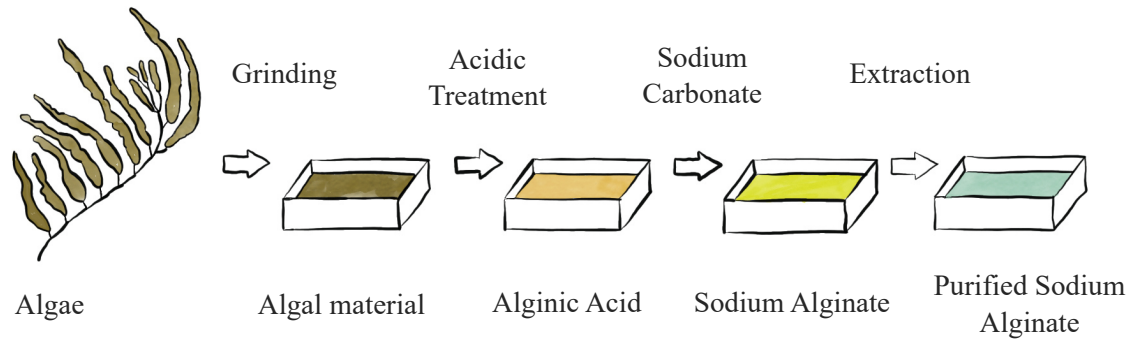


Figure 4. Method of Alginate Purification.

Alginate Degradation

Alginate is not degradable in mammals, since they lack the enzyme Alginase (Remminghorst and Rehm, 2006) but there are methods to make alginate degradable under physiological conditions, as (Bouhadir *et al.*, 2001) explained by a partial oxidation of the alginate chains in an aqueous medium, in the same way (Yang *et al.*, 2011) showed that the degradation rate and its mechanical properties can be controlled by modifying the molecular weight distribution of the polymer.

Alginate Current Uses

Alginate has been used in the food, textile, printing and chemical industries (Szekaskla *et al.*, 2016) and one of the most frequent use is in the field of regenerative medicine, it is the creation of hydrocolloids that can be prepared by various method of crosslinking, since, due to its similarity with the extracellular structures of living tissues, it allows wide applications in the field of tissue engineering and wound healing (Szekalska *et al.*, 2016).

Gelatin

Gelatin Properties

Gelatin is a Polypeptide (Fig. 3) of greater molecular weight and an important polymer as it is a mixture of different polypeptide chains, including α , β and γ chains, with a molar mass, approximately of 90, 180 and 300 g/M respectively (Mariod and Fadul, 2013).

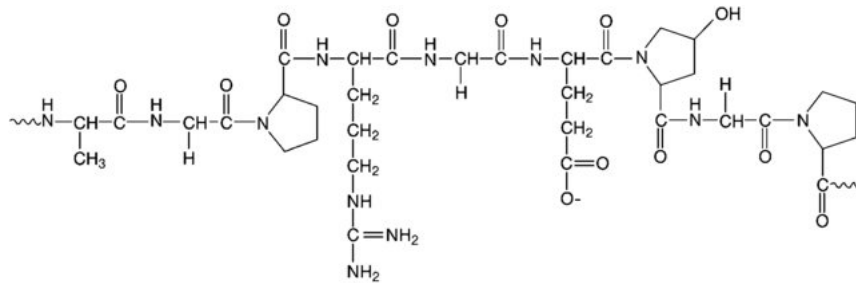


Figure 5. Gelatin Structure

Gelatin Production

It can be contained from different sources of collagen such as; cattle bones, pig and fish skin, that are the main commercial sources (Djagny *et al.*, 2001) and their extraction can be by two different processes, either by acid or alkaline methods (Djagny *et al.*, 2001).

Gelatin Degradation

Matrix metalloproteinases (MPPs) are zinc-dependent endopeptidases and have an important role in tissue development and repair (Perez-Garcia 2004). MPPs or also called “Gelatinases” are enzyme responsible for the natural degradation of denatured collagen and collagen IV (Perez-Garcia 2004).

Current Uses of Gelatin

Gelatin is commonly used as a stabilizer in yogurt (Karim and Bhat, 2008) both as an emulsifier and preservative in the food industry (Manbeck *et al.*, 2017) and also in pharmaceutical applications due to its active surface properties (Mironova and Kovaleva, 2017).

In a study exposed by (Saarai *et al.*, 2012) it was shown that gelatin hydrogels have the ideal rheological characteristics to be used in tissue engineering, where the results showing comparisons of crosslinked hydrogels are shown, where the comparison of crosslinked hydrogels are shown, when varying polymer concentrations, significant differences were observed in water absorption, morphology and viscosity, concluding the polymeric relationships has a great influence on these biomaterials characteristics.

Hydrogels

They are one of the most used biomaterials, since they have viscoelastic properties and network structure caused by the crosslinker and solvent (Ahmed 2015).

Uses of Hydrogels

Hydrogels are present in daily life in different forms such as soap, shampoo, toothpaste and contact lenses (Gulrez *et al.*, 2011) and in advances industrial applications such as oil recovery, agriculture, water treatment and pharmaceutical products (Peppas *et al.*, 200). Due to the ability to absorb water and its high biocompatibility, hydrogels are used in tissue engineering and wound regeneration (Nho *et al.*, 2014) in Table 1 you can see a list of the pharmaceutical applications given to the hydrogels:

Table 3. Pharmaceutical applications of Hydrogels

Applications	Polymers	Reference
Wound Healing	Tragacanth gum	(Singh <i>et al.</i> , 2016)
	Gelatin	(Yue <i>et al.</i> , 2015)
	Alginate	(Hooper <i>et al.</i> , 2012)
	Agar	(Benamer, 2006)
	Polyethylene Glycol	(Dutta 2012)
Tissue Engineering	Chitin	(Mi <i>et al.</i> , 2002)
	Polyvinyl alcohol,	(Yu <i>et al.</i> , 2006)
	Hyaluronic Acid	(Fahmy <i>et al.</i> , 2015)
Injectable Polymers	Alginate	(Li <i>et al.</i> , 2012)
	Dextran	(Cascone <i>et al.</i> , 1999)

Type of Hydrogels

Hydrogels can be classified in different ways as their morphology; particles, powders, spherical, fiber, membrane and emulsion (Gulrez *et al.*, 2011), the type of material; Natural macromolecules, semi-synthesized polymers and synthesized polymers (Ahmed 2015) and the type of crosslinking agents, but can also be classified according to the type of crosslinking.

Physical Stimuli

These types of hydrogels are generally created by reversible molecular interactions (Vorhaar and Hoogenboom 2016) such as: ionic (electrostatic) interactions, hydrogen bonds, hydrophobic/hydrophilic interactions and crystallization (Berger *et al.*, 2004) (Kuo and Ma *et al.*, 2001).

Thermal Crosslinking

The balance between the hydrophobic and hydrophilic segments is the key to controlling the properties of a thermal crosslinking (Chai *et al.*, 2017). The temperature has a remarkable effect on the hydrophobic interactions between the hydrophobic polymer segments and the hydrophilic interaction between the hydrophilic polymer segments and the water molecules, whereby a temperature change can disrupt the original equilibrium and induce the solitary of sol-gel transition (Bajpai *et al.*, 2008).

Chemical Stimuli

Hydrogel that are chemically crosslinked have covalent bonds between the polymer chains (Hu *et al.*, 2019). So far, several methods of chemical crosslinking, have been reported and typically involve free radical-induced, enzymatic, “Click” crosslinking with Diels-Alder reactions and Schiff base formation (Li *et al.*, 2018). In comparison to the physical crosslinking hydrogels, these demonstrate better stability and better mechanical properties.

Photo crosslinking

It is a process where a liquid formulation is transformed into a hydrocolloidal solution by means of photoreceptor and its reactions with light (Li *et al.*, 2013). Photoreceptors break into C-C, C-CL, C-O or C-S bonds to form radicals when exposed to light and can have two types of reactions; radical by rupture or radical by hydrogen extraction. The advantage of this method is the rapid formation of IPN at room temperature and the control of mechanical properties by the crosslink agent (Nguyen and West 2002). Photo crosslinking is related to the presences of unsaturated groups and in most cases, they are methacrylate (Dijk-Wolthuis *et al.*, 1995).

Photoreceptors

Also known as photo initiators (PI), they are light sensitive (Fouassier and Laleva, 2012) that after absorbing it suffer a photochemical breakdown that produces free radicals (Li *et al.*, 2013) that interact with the formulations. There exist two types of PI: Type I (Fig. 7 A) they are those that absorb photons and decompose into radicals to initiate crosslinking and Type II (Fig. 7 B), they extract a hydrogen from a co-initiator to generate radicals and initiate crosslinking (Shih and Lin, 2013), only few PIs are considered cytocompatible such as: lithium arylphosphanate (Fairbanks *et al.*, 2009), eosin Y (Elbert and Hubell 2001) and Irgacure-2959 (I-2959) (Williams *et al.*, 2005).

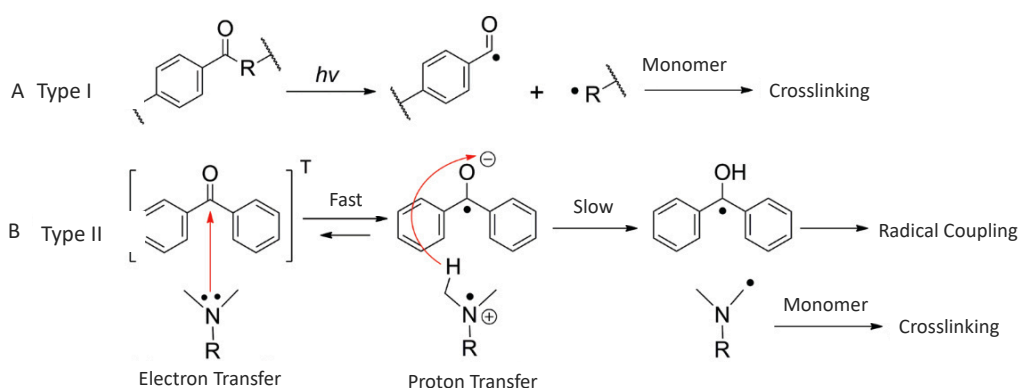


Figure 6. Diagram of Photo crosslinking types. Where (A) is the reaction of radical crosslinking by rupture, since after exposure to light, PI forms radicals. (B) The radical photo crosslinking by extraction of hydrogen, after irradiation, these PI go through an extraction of hydrogen by a donor to generate radicals and create links with the components of the formulation (Fouassier and LalevÁ, 2012).

Irgacure 2959

1-[4-(2-Hydroxyethoxy)-phenyl]-2-hydroxy-2-methyl-1-propane-1-one best known as I-2959 (Fig. 8) is a highly efficient Type I radical PI used for UV crosslinking, which is also suitable for use in water-based systems (Coimbra *et al.*, 2008), due to its properties and its low cellular toxicity this PI can also be used in the polymerization of polymers and copolymers intended for biomedical and tissue engineering applications (Leach and Smith 2005).

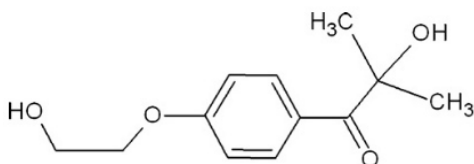


Figure 7. Chemical Structure of Irgacure 2959 ®.

Properties of Hydrogels

Hydrogels have a wide variety of properties that make them promising materials for a wide variety of applications.

Physicochemical Properties

Swelling

The mechanisms of swelling in hydrogels, can be explained when hydrogels encounter water, the latter, hydrates the polar groups and starts to make bounds with water (Barbucci and Pasqui 2013), when the groups are hydrated, the network starts to swell. There exist some characteristics that improve the swelling in hydrogels, for example; increasing the ionic groups, the amount and type of crosslinking and porosity.

The properties and characteristics of a gel depend on the organization of the water (Singh *et al.*, 2018), while in hydrogels is classified by different classes, such as Freezing and non-freezing mobile or stationary and free or trapped water (Khalid *et al.*, 2002). The best classification (Singh *et al.*, 2018), considers that the water in the hydrogel can exist in three physical states (Fig. 10):

- 1.- Free Water; it is not bound to the polymer chain and freezes at 0 °C.
- 2.- Interstitial Water; weakly bound to a polymer chain or interacts with bound water. It freezes at a temperature lower than the usual freezing point.
- 3.- Bound Water; it is tightly bound with the hydrophilic segments of the polymers and does not freeze at a usual freezing point.

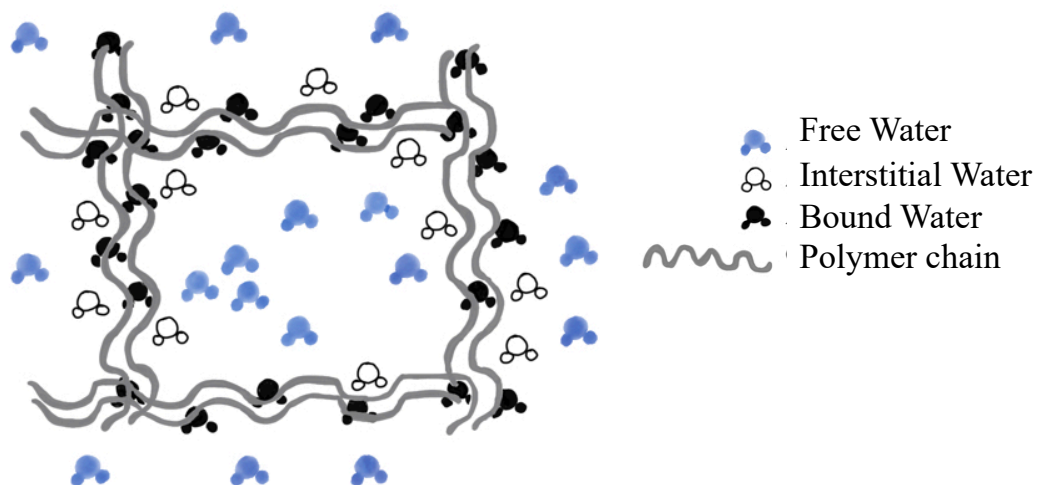


Figure 8. Physical states of Water within Hydrogels

The water content is affected by the polymer and the nature of the crosslinking (Singh *et al.*, 2018), therefore, it is assumed that the bound water content increases with the proportion of hydrophilic groups (Valles *et al.*, 2000) and decreases with the increases of hydrophobic groups (Kim and Peppas 2003).

This capacity of the hydrogels depends on the amount of carboxylic group present in the polymers, since they remain free after crosslinking and these are responsible for their swelling (Vashuk *et al.*, 2001). These characteristics can also be determined by the density of the hydrogel using a pycnometer with a non-polar solvent (e.g. N-hexane). The density of the dry hydrogel ($P\rho$) and the density of the swollen hydrogel (P_s), are calculated using the following equation (Ganji *et al.*, 2010):

$$P\rho(P_s) = \frac{M_s}{M_1 - M_2 + M_s} \times P_i$$

Equation 1. Formula for calculating the Density of Dry Hydrogels. Where P_i is the density of the solvent, M_s is the weight of the dry hydrogel (for the density of the dry hydrogel) or the weight of the swollen hydrogel (for the density of the swollen hydrogel), M_1 is the weight of the pycnometer with the solvent and M_2 is the weight of the pycnometer with the sample and solvent.

The diffusion of a solvent into the hydrogel, has three different models of swelling process, and was propose by (George *et al.*, 2004);

- Case I or Fickian Diffusion: The diffusion is slower than the rate of relaxation of the polymer chains. The mass uptake is proportional to the square root of diffusion time, $Q \sim t^{1/2}$
- Case II Diffusion: The rate of diffusion is higher that the relaxation rate of the polymer chains. The mass solvent uptake is proportional to the time, $Q \sim t$.
- Case III or Anomalous Diffusion: Both rates are comparable, $Q \sim t^a$.

Mechanism of De-Swelling

The de-swelling mechanisms occurs through three different process; the loss of free water, the loss of interstitial water and only partially the loss of bound water (Barbucci and Pasqui 2013).

Morphology (Porosity)

A hydrogel is composed of distributed microchannels or pores created by the mobility of the polymer segments within an IPN in the presence of a solvent (Dorkoosh *et al.*, 2002). These pores are formed as a result of the thermal movement of the chain, the presence of pores in the hydrogels is relevant for the application that is intended to give the biomaterial, for example tissue regeneration (Gasperini *et al.*, 2014), since the size of the pores strongly affects the ability of the cells to adhere and proliferate. The porosity of hydrogels may be divided into four main classes:

- Non-porous hydrogels; show a molecular size pores equal to the macromolecular correlation length (10-100 Å)
- Microporosity Hydrogels; found on a scale from 100 to 1000 Å and the
- Macroporosity Hydrogels; they enter a scale of .1 to 1 μm
- Super-porous hydrogels; porosity bigger than 1 μm

The porosity is the restoring of the solvation of the hydrophilic polymer with water, which induces the polymer chains to swell, Some studies have shown the optimal size for neovascularization, which is 5 μm , from 5 – 15 μm for fibroblast growth, 20 – 125 μm for mammalian skin regeneration and for bone regeneration from 100 – 350 μm (Whang *et al.*, 1999). The degree of porosity of the biomaterial influences the mechanical properties, since increasing porosity decreases the stiffness (Gerecht *et al.*, 2007).

Wettability (Contact Angle)

The contact angle is a common measure that determines the hydrophobicity of a surface (Chau *et al.*, 2009), it can be defined as the “Angle formed by the intersection of the liquid-solid interface and the liquid-vapor interface” (Lafuma and Quéré 2003). The small contact angles ($< 90^\circ$) correspond to those of high wettability, while the angles ($> 90^\circ$) correspond to those of low wettability (ref) (Fig. 11).



Figure 9. Different contact angles

Ideally, the shape of a drop of liquid is determined by the surface tension of the liquid. In a pure liquid, each molecule in the volume is attracted equally in each direction by the neighboring liquid molecules, resulting in a net force of zero, however, the molecules exposed on the surface do not have adjacent molecules in all directions to provide a balanced net force, instead are pushed inwards by the neighboring molecules (Fig. 12), creating an internal pressure (Lafuma and Quéré 2003).

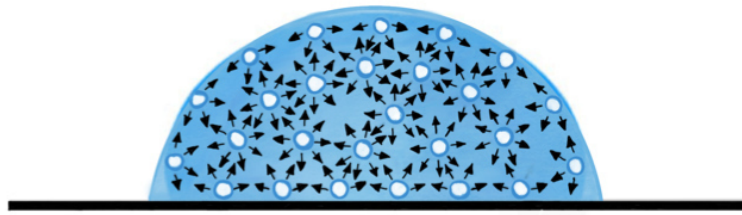


Figure 10. Superficial Tension. its caused for unbalance forces or liquid molecules on the surface

Rheological Behavior

A “Fluid” is a substance that cannot stand an effort without moving, we can say that the rheology is “The science of flow and deformation” (Cherizol *et al.*, 2015). As much as the rheological properties and the flow behavior of the suspensions, depends on parameters such as: particle shape, size and concentration, particle-particle interactions and particle surface properties (Datt and Elfring 2018). Fluids can be divided in two types (Brookfiel Engineering Labs 2017):

- Newtonian Fluids; which are fluids that its viscosity (η) remains constant as the shear rate ($\dot{\gamma}$) is varied.
- Non-Newtonian Fluids; the relationship between Shear stress (τ) and Shear Rate ($\dot{\gamma}$) is not constant

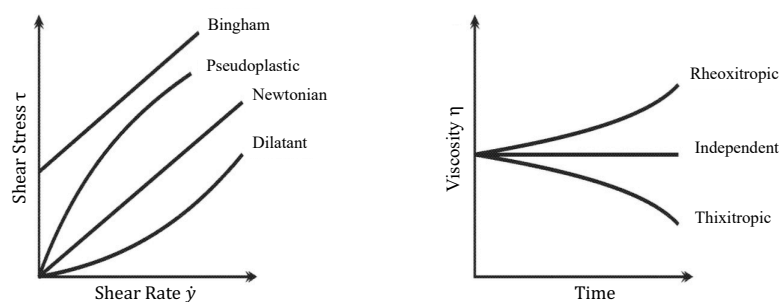


Figure 11. Types of Rheological Behaviors

Classic Rheological Models

A rheological model is an empirical mathematical expression that relates the shear stress to the speed of deformation (Cherizol *et al.*, 2015). There are several models, such as the Newton Model (Krizek and Pepper 2004), Bingham Model (Sevssiecg *et al.*, 2003), Carreau Model (Li *et al.*, 2009), Maxwell Model (Larson 2013) and Ostwald-de Waele Model or better known as Power Law (Ng *et al.*, 2011)

Model of Ostwald – de Waele (Power Law)

This model is applied to shear thinning fluids, those which do not present yield stress (Pevere *et al.*, 2006), the Flow Performance Index (η), gives fluid behavior according to:(Eq. 2):

$$\eta = K\dot{\gamma}^{n-1}$$

Equation 2. Power Law formula. Where η is the apparent viscosity, $\dot{\gamma}$ is the shear rate and K represent the Power Index or flow behavior, respectively.

When the values of n are greater than 1, this model predicts a Pseudoplastic behavior and when they are less than 1 predicts a Dilatant behavior, when the value of n is equal to 1, the model is reduced to Newton Law, where the viscosity is equal to the consistency index (Pevere *et al.*, 2006).

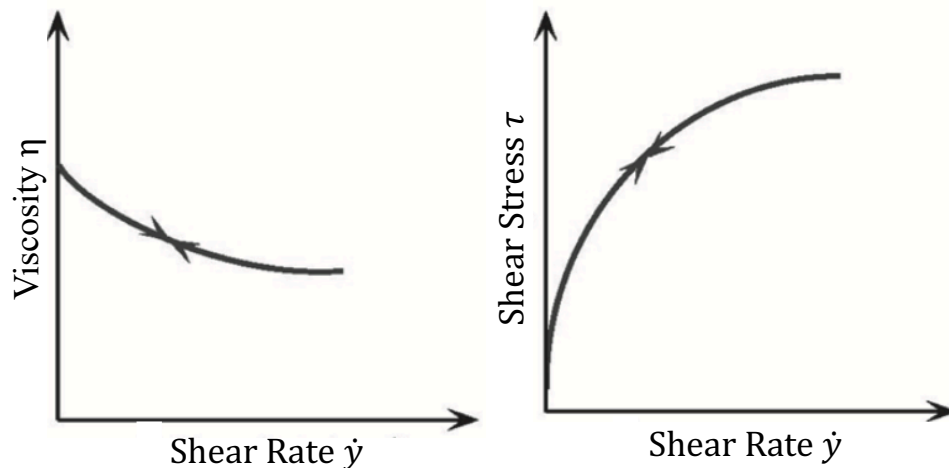


Figure 12. Representation of Pseudoplastic behavior

Water vapor permeability

One of the basic physical properties of biomaterials for wound healing, which can influence the healing process, is the rate of water vapor transmission (WVTR), which directly regulates the moisture microenvironment of wound (Xu *et al.*, 2016). Diffusion across a film or membrane is influenced by; the structure, permeability to a specific gases or vapor, thickness, area, temperature, difference in pressure (Siracusa 2012). According to (Xu *et al.*, 2016) an optimal WVTR that has a range equal to or greater than 2028.3 g/m² in 24 hours, are those that provide an optimal humid environment at the local level to promote wound healing.

Permeation Theory

Permeability is defined according to (Gaidos *et al.*, 2000) as “The quantification of permeate transmission, gas or vapor through a resisting material”. The second step of the permeability phenomenon, “The Diffusion”, depends on; size, shape, polarity and crystallinity of the membrane (Siracusa 2012). The theory that explain the mechanism of permeation is the Henry and Fick’s Law, that explained that “The diffusion takes place only in one direction, through the film and not along or across it” (Fig. 14) (Lee *et al.*, 2008), the formula (Eq. 3):

$$J = -D * \Delta c$$

Equation 3. Fick’s first law. The permeate (gas or vapor) flux indicated by J expressed in mol cm⁻²s⁻¹, the diffusion coefficient or diffusivity indicated by D and expressed in cm²/s and the concentration difference indicate by Δc expressed in mol/cm³.

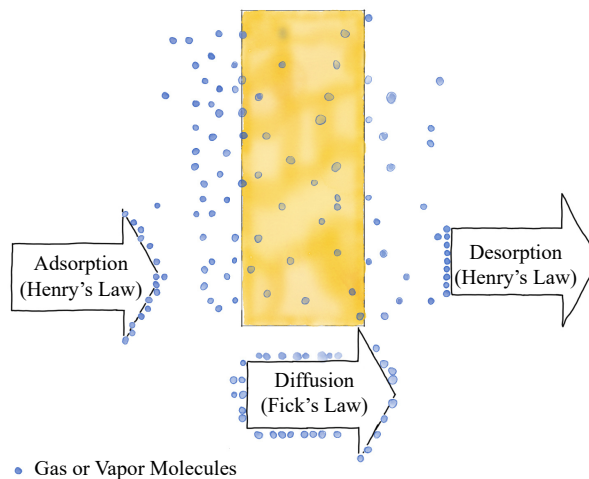


Figure 13. Diagram of Vapor or gas permeation on membrane

Drug Entrapment

Drug loading is one of the most important applications of hydrogels, according to (Lin and Metter 2006), active agents can be incorporated into hydrogels matrices by two ways:

- Post-Loading Method; Generally, the hydrogel, in the dry state meets a solution containing the drug, the concentration of the solution is determinant, a high concentration of the drug in solution increases its viscosity and delays the drug diffusion within the hydrogel.
- *In situ* loading Method; A polymer precursor solution is mixed with drug or drug-polymer conjugates with or without a crosslinker and allowed to polymerize, trapping the drug within the matrix.

A diagram (Fig. 15) explains the two ways of drug loading we explained before:

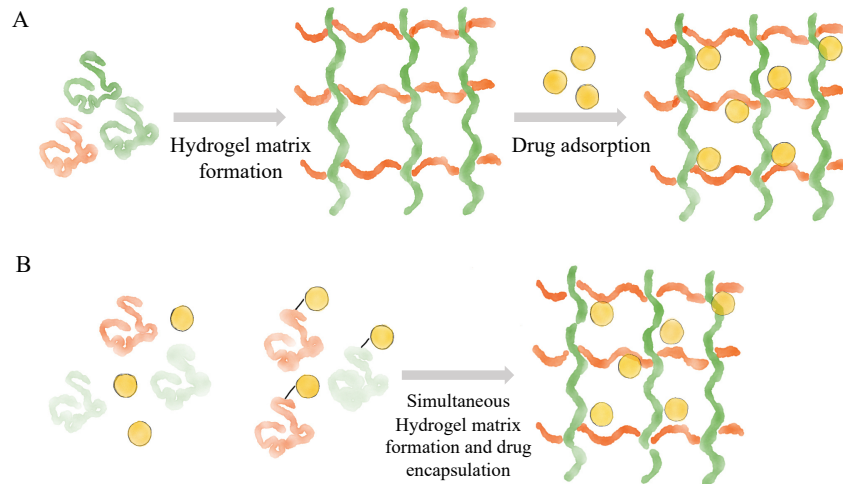


Figure 14. Representation of Drug entrapment. (A) post loading (B) *In situ* loading into the Hydrogel.

Drug loading is dependent on many variables, such as; the molecular weight and charge density of both (the drug and hydrogel), degree of cross-linking, nature of the solvent and mixing conditions. Drug loading (DL) range per unit mass of a polymer can be estimated from the following relationship:

$$\left(\frac{V_s}{W_p}\right) \times C_o = D.L. Limit$$

Equation 4. Drug Loading Formula. Where V_s is the adsorbing solvent, W_p is the dried polymer weight, C_o is the drug concentration in a solution (Kim *et al* 1992)

Nanotechnology

This science was introduced by Nobel prize winner Richard P. Feynman in 1965, as a result of multiple advances in science to manipulate matter on an extremely small scale. Nanotechnology, defined by its main pioneer (Feynman 1960) is “The development of materials in the order of nanometers (less than 100 nm) to create materials with new properties and functions” and can be defined in two types of approaches according to the synthesis of the structure: the “Top-Down” approach that is defined as “The largest structures are reduced in nano-scale size, while maintaining their original properties, and the “Bottom-Up” approach, also called “Molecular Nanotechnology” developed by (Drexler *et al.*, 1991), in which “Materials are manipulated from atomically or molecular components by a process of assembly or self-assembly” a summary scheme can be observed in (Fig. 16).

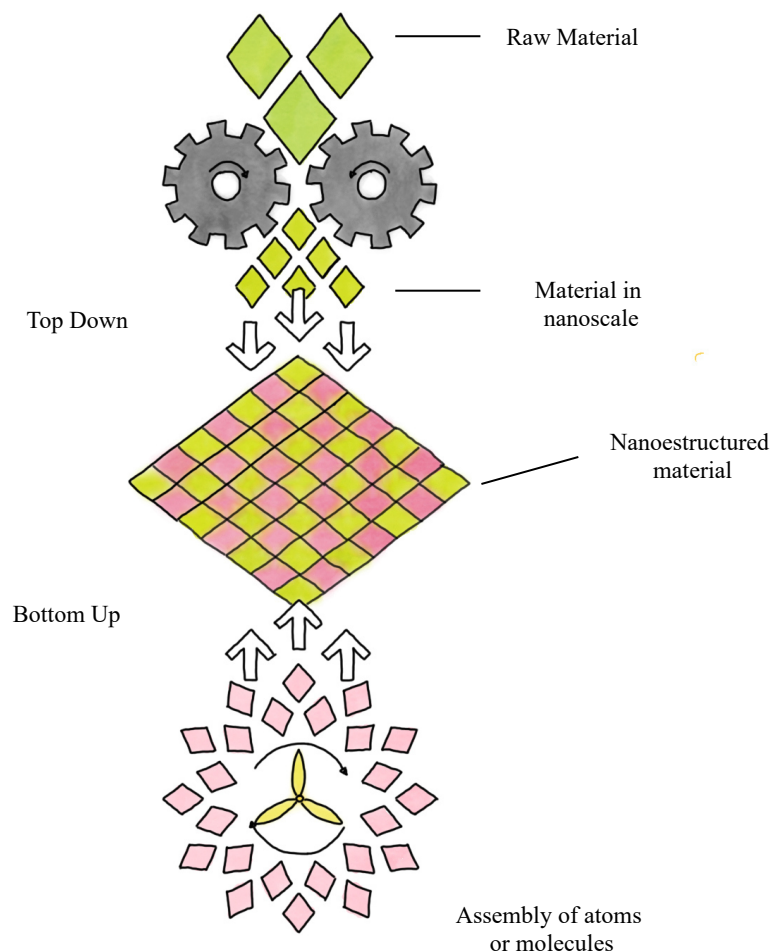


Figure 15. Different approaches in nanotechnology

Type of Nanosynthesis

There are different methods for the synthesis of nanocapsules (NCs) such as: Emulsion-diffusion, double emulsification, coacervation method, layer by layer and nanoprecipitation method (Maynard and Baxter 2007) to mention some, while the selection criteria for each method is the desired particle size to obtain (Jagadeesh *et al.*, 2016).

Nanoprecipitation

This technique was described by (Fessi *et al.*, 1989) and since its development, it is the standard technique for encapsulation different active agents, mainly hydrophobic in either NCs or nanospheres (Lasalle and Ferreira 2007), it is also called “Solvent displacement” or “Interfacial deposition”, and this technique has many advantages such as: simplicity, scalability, reproducibility and toxic solvents can be avoided (Lasalle and Ferreira 2007).

Mechanisms of Nanoprecipitation

In the investigation of (Quintanar-Guerrero *et al.*, 1998), explained the formation of nanoparticles as a result of the differences in surface tension, a liquid with high surface tension (aqueous phase) attracts more strongly the surrounding liquid with low surface tension (organic phase), this difference between tension causes interfacial tension, the organic solvent “diffuses” from low voltage regions, which causes a gradual precipitation of the polymer and the formation of NCs (Fig. 17) (Mora-Huertas *et al.*, 2010).

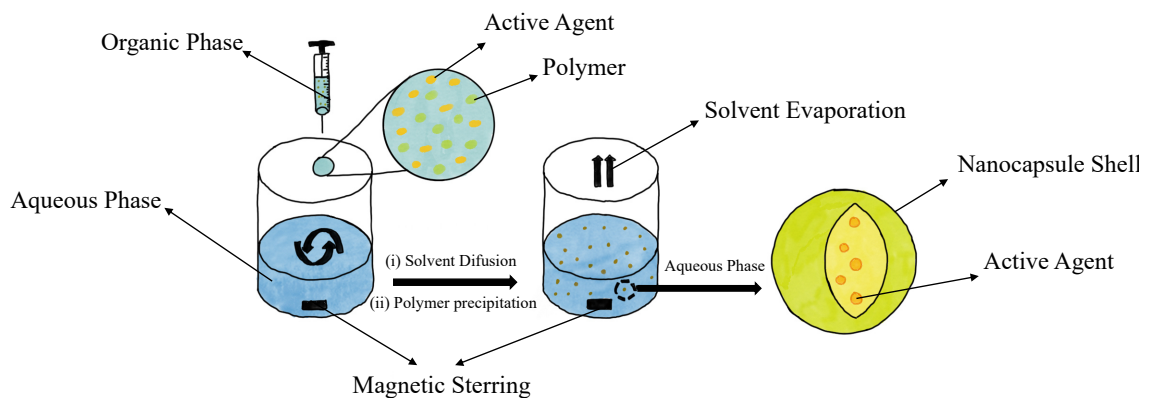


Figure 16. Nanoprecipitate process

Aqueous Phase

This phase is usually water with other excipients such as hydrophilic surfactants, these are added to avoid particle aggregation (Miladi *et al.*, 2016) also some polymers can also be added.

Organic Phase

It consists of an organic solvent that is miscible with water, such as ethanol or acetone, this phase contains the polymer and the hydrophobic agent, other compound can be added such as mineral or vegetable oils, which allow to obtain nanospheres (Miladi *et al.*, 2016).

Most used Polymers

Numerous polymers can be used by this technique, but they must meet certain criteria to be used in in vivo applications, such as being biodegradable and biocompatible (Miladi *et al.*, 2016). The most used polymers by this technique are referenced in the Table 4.

Table 4. Examples of polymer most used in the nanoprecipitation technique

Polymers	Reference
PLGA	(Bazvlinska <i>et al</i> 2014)
	(Shah <i>et al.</i> , 2014)
PLA	(Siqueira-Moura <i>et al.</i> , 213)
	(Barwal <i>et al.</i> , 2013)
PEG	(Pavot <i>et al.</i> , 2013)
	(Suen and Chau 2013)
PBLG	(Nafee <i>et al.</i> , 2013)
	(de Miguel <i>et al.</i> , 2014)
PCL	(Noronha <i>et al.</i> , 2013)
	(Neves <i>et al.</i> , 2013)
	(Mazzarino <i>et al.</i> , 2012)

Polycaprolactone

Polycaprolactone (PCL) is a biodegradable aliphatic polyester with a low melting point of around 60 °C (Mark 1999) is obtained from the polymerization of caprolactone and its name according to the International Union of Pure Applied Chemistry (IUPAC) it is 1,7-poliozepan-2-ona.

Properties of Polycaprolactone

PCL is often used as an additive for other polymers, is used as plastic that can be molded and in the manufacture of plastic parts (Labet and Thielmans, 2009), also it has received great attention for its use as a biomaterial (Ulery *et al.*, 2011) and its method of synthesis is by polymerization catalyst (Mark 1999) explained in Figure 18.

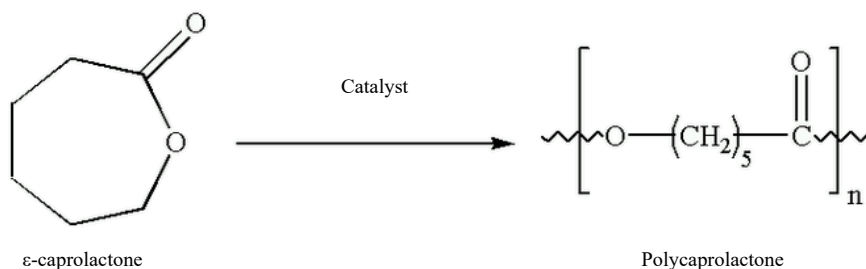


Figure 17. Synthesis of Polycaprolactone

Degradation of Polycaprolactone

At room temperature PCL is highly soluble in chloroform, dichloromethane, benzene, toluene and acetone while insoluble in alcohols, petroleum and water (Pohlmann *et al.*, 2013). The PCL can be degraded in several months to years, since the degradation rate depends on molecular weight, crystallinity level and degradation conditions (Sravanthi 2009) and many microorganisms in nature are capable of degrade the polymer (Sravanthi 2009).

Current uses of Polycaprolactone

One of the most important current uses of this polymer is as a bioplastic (Tokiwa *et al.*, 2009) also in pharmacology (Colinet *et al.*, 2009) and in the area of tissue engineering (Wang *et al.*, 2009), PCL has been used in medicine as sutures with varying degradation rates (Sava *et al.*, 2004).

Characterization of the Nanocapsules

The properties of a material changes dramatically when their size is reduced to a nanoscale range and in order to cope with these properties, the following parameters needs to be analyzed, such as; shape, degree of aggregation and agglomeration, size distribution, surface chemistry, crystal structure and surface composition (Kumar and Kumbhat 2016).

Particle Size

The smaller the particle size, the greater the surface area, and this results in a rapid release of the active agent (Choi *et al.*, 2003), and consequently smaller particles tend to aggregate during storage, also the degradation rate it is affected by the particle size (Pal *et al.*, 2011).

Surface Load (Z Potential)

This determines the interaction of particles with the environment such as electrostatic interaction with bioactive agents. The stability of the colloidal suspension is analyzed by potential Z, which is an indirect measurement of the surface charge. High Potential Z values (whether positive or negative) are sought to ensure stability and prevent particle aggregation (Dadwal *et al.*, 2014).

Polydispersity Index (PDI)

Dynamic light scattering (DLS) is an important tool for characterizing the particle size and its distribution (PSD) or Polydispersity Index (PDI) in a solution (Maherani and Wattraint 2017). DLS measures the light scattered that passes through a colloidal solution and analyzing the intensity of the scattered light intensity. This index is dimensionless and values of 0.2 and below are most commonly acceptable for polymer-based nanoparticle materials (Clarke 2013).

Drug Release and Encapsulation Efficiency

In order to be able to determine the release of active agent, it is essential to be able to determine the encapsulation efficiency, this is defined as “The amount of active agent bound to the polymer” or in another term, the concentration of the active agent within NCs (Kreuter 1983), there’s exists different methods to quantify the active agents, but high-performance liquid phase chromatography (HPLC) it’s the most used (Magenheim *et al.*, 1993).

Oxidative Stress

Oxygen is responsible for the formation of active intermediates known as ROS (San-Miguel and Martin-Gil 2009). Among these species, free radicals (FR) such as: superoxide ion (O_2^-), hydroxyl (OH), alkoxy (ROO) and nitrogen oxide (San-Miguel and Martin-Gil 2009).

Free Radicals in Chronic Wounds

The FR according to (San-Miguel and Martin-Gil, 2009) are “Chemical species that contain in their structure one or more missing electron, which makes them highly unstable compound due to the need to take or transfer an electron from adjacent molecular structure in order to stabilize”, the radicals with the highest reactivity are:

- Radical superoxide (O_2^-): lacks reactivity to attack macromolecules directly, although it can act as a weak oxidant.
- Hydrogen peroxide (H_2O_2): it is not an FR but is considered the main intermediate in the metabolisms or ROS
- Hydroxyl radical (OH): its missing electron can react with almost any molecule.

The most reactive ROS in the body is the hydroxyl radical (Fig. 19), and it is also responsible for the propagation of oxidative damage between subcellular fractions.

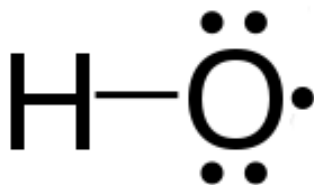


Figure 18. Hydroxyl Radical

Different biochemical processes can generate ROS (San-Miguel and Martin-Gil 2009) and can be classified into:

- Endogenous processes: FR will be generated through the mitochondrial electron transport chain or by phagocytic cells.
- Exogenous processes: by catalytic activation of various enzymes or cellular metabolism

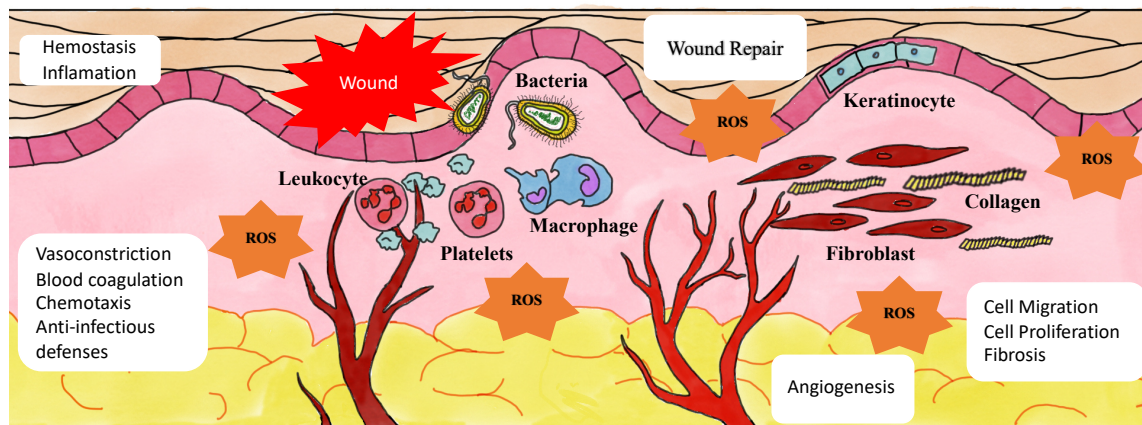


Figure 19. Phases of a normal wound repair. The relationship between wound healing and ROS. In the inflammatory and homeostatic phase, large amount of superoxide are generated from molecular oxygen mostly by NADPH oxidase expressed in the immune system. Redox signaling is also critical for modulating key events that occur during the phases of migration and cell proliferation, fibrosis and remodeling.

Molecular oxygen plays a crucial role in many processes, however, the O_2 that exists as a biradical molecule is also toxic, especially when converted to superoxide radicals, which are considered the main ROS in biological systems (Schafer and Werner 2008). In an aqueous solution O_2 spontaneously decreases to hydrogen peroxide (H_2O_2), while in the presence of metals, such as copper or iron, H_2O_2 and O_2 generate hydroxyl radicals ($OH\cdot$) (Novo and Parola 2008).

While these ROS are products of a normal aerobic metabolism and their production increases during infection processes (Moseley *et al.*, 2004), the overproduction of these ROS is the largest factor that allows cornification wounds (Nyanhongo *et al.*, 2013). This is because these FR are kept oxidizing new biomolecules in wounds and act as a promoter of pro inflammatory responses (Guo and DiPietro 2010). Currently, great progress has been made in the control of wound exudates, protecting the wound from physical damage (Widgerow 2011) control of the inflammation, proteases and FR is a great challenge.

Antioxidants

The term is defined as “Any substance that, being present at low concentrations in relation to those of the oxidizable substrate, significantly delays or inhibits the oxidation of said substrate” (Coronado *et al.*, 2015). These agents are found in all aerobic cells and their purpose is the decrease of ROS (Coronado *et al.*, 2015). The human antioxidant system is divided into two major groups: Enzymatic antioxidant and non-enzymatic oxidants (Carocho and Ferreira 2013), regarding the latter mentioned, there are quite a number of them such as: peptides (glutathione), nitrogen compounds (uric acid), enzyme cofactors (Q10) and vitamins.

Vitamins

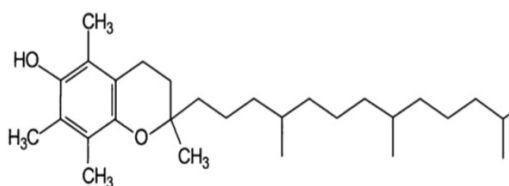
The discovery of vitamins was made by Hopkins 1912, currently they can be defined as “Group of organic compounds required in the daily diet in small quantities for the maintenance of good health and metabolic integrity” (Bender 2003) and have been classified in two groups:

Group A: they are fat-soluble vitamin, being A, D, E and K

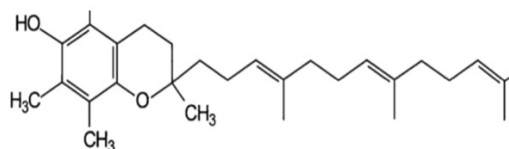
Group B: they are water soluble vitamins, B and C.

Vitamin E

Vitamin E was discovered by Evans and Bishop 1922 and is composed of four tocopherols and four tocotrienols, designated as α , β , γ and δ (Fig. 21) (Bender 2003) being α -tocopherol (α -Toc) the most active form.



α -Tocopherol



α -Tocotrienol

Figure 20. Chemical structures of α -tocopherol y α -tocotrienol

Functions of α -tocopherol

The best known function of vitamin E is to be an antioxidant soluble in lipoproteins and plasma cell membranes (Bender 2003), recent studies indicate that it is involved in inhibition of protein Kinase C (PKC), cell proliferation and activation (Hobson 2016). The chroman head group confers the antioxidant activity to tocopherols (Carocho and Ferreira 2013) and this halts lipid peroxidation by donating its phenolic hydrogen to the peroxy radicals forming tocopheroxyl radicals that, despite also being radicals, are unreactive and unable to continue the oxidative chain reaction.

α -tocopherol Degradation

The absorption of vitamin E is relatively low, since only 20 to 40 % of an intake is absorbed in the small intestine (Rigotti 2007) and is carried out by triglycerides and inhibited by polyunsaturated fatty acids, being secreted by the liver (Rigotti 2007).

Current uses of α -tocopherol

The use of vitamin E in nutrition is rare, due to its low absorption rate in the digestive system, but its antioxidant effects are mostly used in the area of cosmetology as a photoprotector (Thiele *et al.*, 2005).

Another use that has been considered for α -tocopherol is as a drug presented in nanospheres and NCs (Mu and Feng, 2002) as evidenced by a recent study, where nanospheres of polylactic-co-glycolic acid (PLGA) were made with α -tocopherol as its active agent (Goankar *et al.*, 2017) for its potential use as an anticarcinogenic drug to eliminate excess FR formation present in the body during the disease process.

JUSTIFICATION

Chronic wounds are an important cause of morbidity and deterioration of the quality of life that affects approximately 8.6 million patients in the US, since in the hospital setting, the appearance of ulcers is a minor problem until they evolve to a stage II, which lead to the formation of larger ulcers, that they are more likely to suffer an infection and that subsequently cause necrosis of the affected tissue until they become an important risk factor for the patients' health. Diseases such as diabetes have a high correlation with chronic ulcers, and in Mexico, diabetes affects 9.2 % of the population, of which 7.2 of these patients have ulcers that can complicate and increase the mortality of affected people. This type of injury is very disabling and expensive and current treatments do not cover all needs and can be expensive as they often need to be reconstructed with autologous skin grafts.

Currently, due to their applications, biomaterials are considered one of the best alternatives for this type of problem and currently the research of the global biomaterial market has an income of 18.9 billion dollars and by 2021 it is thought that it will grow to 53.7 billion dollars.

Therefore, this project proposes the development and characterization of photo responsive hydrogels made with biopolymers (Alginate and Gelatin) and Polycaprolactone nanocapsules loaded with α -tocopherol that promotes antioxidant activity with a potential use in chronic wounds.

HYPOTHESIS

Photo responsive hydrogels made with Alginate and Gelatin will serve as an absorbent, resistant and permeable structure and Polycaprolactone nanocapsules loaded with α -tocopherol after nanoprecipitation will maintain their antioxidant activity

OBJECTIVES

General Objective

Develop and Physicochemical characterize of Photo crosslinked hydrogels of Alginate/Gelatin and Polycaprolactone nanocapsules loaded with α -tocopherol

Specific Objective

1. Synthesize and physiochemically characterize matrices of Alginate and Gelatin hydrogels at different concentrations by Thermal crosslinking
2. Synthesize and physiochemically characterize matrices of Alginate/Gelatin hydrogels by Photo crosslinking
3. Synthesize and physiochemically characterize Polycaprolactone nanocapsules with different concentrations of α -tocopherol
4. Synthesize and physiochemically characterize the Polycaprolactone nanocapsules with different concentrations of Polycaprolactone
5. Synthesize and physiochemically characterize the Polycaprolactone nanocapsules with different solvents (Acetone and Methanol) concentrations
6. Evaluate the encapsulation efficiency of the α -tocopherol in the Polycaprolactone nanocapsules by HPLC

METHODOLOGY

Thermal Crosslinking of Hydrogels (Alginate or gelatin)

The method on which the synthesis of the biomaterials was based on, was reported by (Saarai *et al.*, 2102), where we modified the polymer concentrations and the crosslinking agent at different ratios to verify which component will improve the physicochemical characteristics. For the synthesis of the hydrogel, an aqueous solution of the polymer was prepared varying from 0.5 to 5 % weight/volume (w/v), where the polymers were dissolved in sterile distilled water at 40 °C while continuous stirring at 200 RPM until an homogenous solution was obtained, then the other components were added (Tab 5), when the hydrogel start to form, the stirring was reduced to 100 RPM and the temperature was maintained for 5 minutes.

Table 5. Alginate and Gelatin hydrogel formulations

Polymers (% w/v)	A1	A2	A3	G1	G2	G3
Gelatin	--	--	--	0.5	2.5	5.0
Alginate	0.5	2.5	5.0	--	--	--
Polyethylene glycol (PEG)	10.0	10.0	10.0	10.0	10.0	10.0
Glycerol	10.0	10.0	10.0	10.0	10.0	10.0
NaCl	1.0	1.0	1.0	1.0	1.0	1.0
Distilled Water (ml)	20.0	20.0	20.0	20.0	20.0	20.0

Where A mean Alginate and G gelatin, where when higher its adjacent number, higher the polymer concentration.

When having the hydrogels formed, they were kept at room temperature in sterile bottles to perform the following tests.

Physical Characterization of Hydrogels

Swelling

2 grams (g) of each dried hydrogels formulation were weighed, put into 250 mL bottles with 50 mL of sterile deionized water, was left for 24 hours and weighed in different times according to K8150, which is the standard method for determining water retention in hydrogels, where dry hydrogel (W_d) is weighed and then submerged at room temperature, after swelling (W_s) was dried/filtered in paper towels for 1 minute to remove as much water as it not fixed in the hydrogel (Katayama *et al.*, 2006), as explained in (Fig. 22).

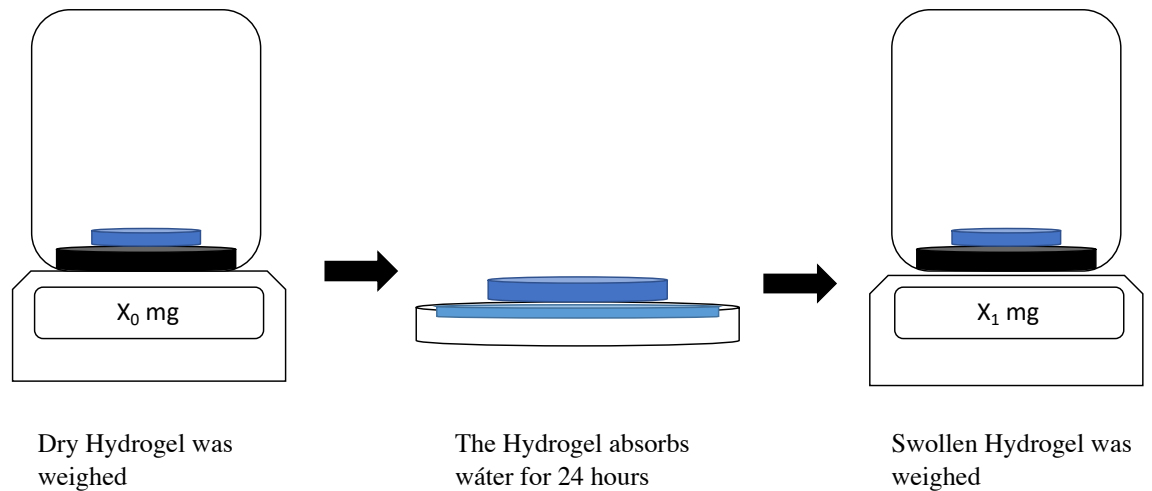


Figure 21. Swelling test representation

The percentage of swelling was calculated with the following formula (Eq. 5):

$$Swelling \% = \frac{W_s - W_d}{W_d} \times 100$$

Equation 5. Percentage of swelling formula. Where W_s is the weight of hydrogel in a swelling state (Weight Swollen) and W_d is the weight of hydrogel in a dry state (Weight Dry)

Solubility

A sample of each treatment of 2 g of hydrogel was placed in 250 mL bottles with 50 mL of sterile deionized water and put in an water bath, thermo Precision 2870, for 24 hours at 37 °C with constant stirring of 100 RPM (Nagasawa *et al.*, 2004) where W_d is weighed and then submerged in sterile deionized water for 24 hours at room temperature, after W_s was dried in paper towel for 1 minute to remove as much water as is not fixed in the hydrogel,

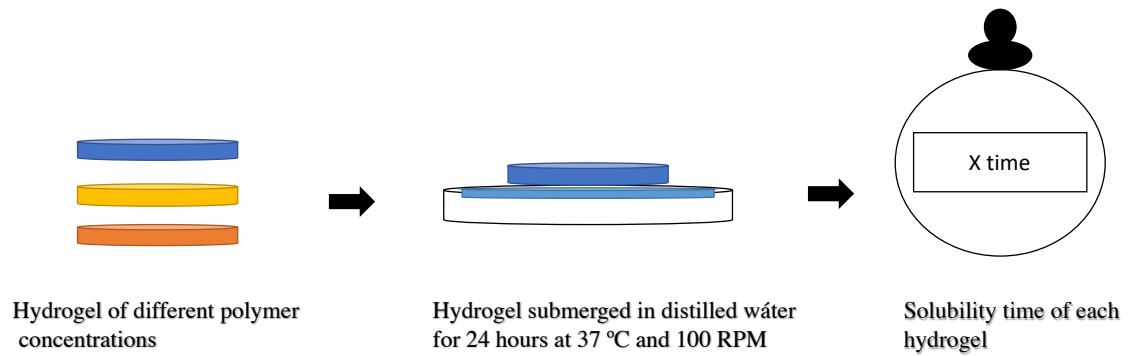


Figure 22. Solubility Test representation

The fraction of insoluble gel was measured with the following formula (Eq. 6):

$$\text{Solubility \%} = \frac{W_d}{W_i} \times 100$$

Equation 6. Percentage of solubility formula. Where W_i is the initial weight of the dry sample and W_d is the weight of the insoluble part of the hydrogel after being extracted from the water.

Rheological Behavior

The samples were placed on the plate of the rheometer using a conical geometry. The results were plotted where the Y-axis was the cutting force (τ), given in Pascal units per second ($Pa.s$) and the X-axis is the shear rate ($\dot{\gamma}$) represented with the units ($1/s$). Rheostress 1 (Haake) was used to obtain the reograms and the cone-plate geometries (Fig. 24), where the cutting speed was varied from 0.1 to 400 $1/s$.

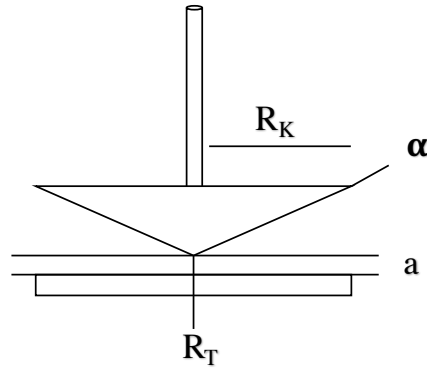


Figure 24. Cone-plate sensor representation. Where R_K represents the torque, α represents the impact angle of the geometry, a represents the gap and R_T represents the measure point.

Index of Consistency

The force required for the material to flow, we used the mathematical model of “Power Law” (ref). The viscosity (η) represented by the units of $Pa.s$ versus the $\dot{\gamma}$, were plotted and adjusted to a logarithmic scale with the cutting speed, using the linear regression formula (Eq. 7):

$$Y = mx + b$$

Equation 7. Linear regression formula.

Chemical Characterization

pH

The pH readings of the biomaterials were performed during the thermal crosslinking and the photo crosslinking, with a previous calibrated potentiometer (Beckam 390).

When obtaining the results of the previous test, it was decided to reformulate the polymeric concentrations (Tab. 6) to have the parameters that are required for the application to be given to the biomaterial, polymeric concentrations ranged from 1.5 to 5 % w/v and where parameters were studied which modified the use of a concentration of 2.2 mMol photoreceptor (Irgacure 2959 TM).

Table 6. Experimental design of Thermal and Photo crosslinked hydrogels

Polymers (% w/v)	AG1 WoPi	AG WoPi	GA1 WoPi	AG1 WPi	AG WPi	GA1 WPi
Gelatin	1.5	2.5	3.5	1.5	2.5	3.5
Alginate	3.5	2.5	1.5	3.5	2.5	1.5
PEG	10.0	10.0	10.0	10.0	10.0	10.0
Glycerol	10.0	10.0	10.0	10.0	10.0	10.0
NaCl	1.0	1.0	1.0	1.0	1.0	1.0
Distilled Water (mL)	20.0	20.0	20.0	20.0	20.0	20.0
Irgacure 295 (mMol)	--	--	--	2.2	2.2	2.2

Where A mean Alginate and G gelatin, where when higher its adjacent number, higher the polymer concentration, while *WoPi* means Without Photoinitiators and *WPi* means With Photoinitiators

The hydrogels obtained from this new formulation were subjected to the same exclusion test as the previous one, only that new test was performed which were now explained.

Contact Angle

It was analyzed with the equipment Drop shape analyzer DSA 25, Krüss, where 500 microliters (μ L) of distilled water were deposited on the surface of each hydrogel and the angle that each drop produced on each formulation was analyzed, the difference of each angle was reported.

Fourier Infrared Transform Spectroscopy (FTIR)

The readings were taken using the equipment (Nicolet iS10) and distilled water was used as background, then the biomaterial of each treatment was analyzed separately to see the functional groups presents in the material.

Water Vapor Permeability

The permeability to water-vapor (% *WVP*) of the biomaterial was determined using a hygroscopic material, in this case Calcium Chloride (CaCl_2). 2 g of the CaCl_2 were first weighed into capsules and 2.5 cm of diameter circles of hydrogel were cut and mounted on the capsule, so that each capsule covered and sealed with it. They were then placed in a desiccator containing a saturated sodium chloride solution (NaCl) with a relative humidity of 90 % and an ambient temperature for 24 hours (Chambi and Grosso, 2011),

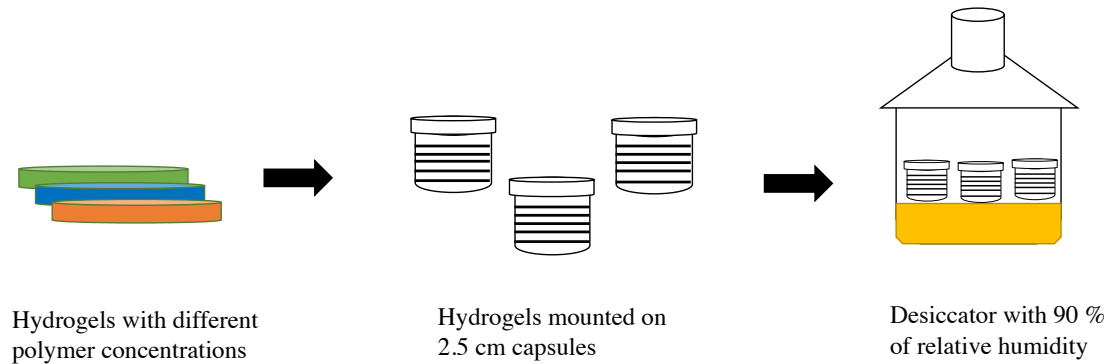


Figure 24. Water Vapor Permeability test representation

The WVTR was calculated from linear regression of the slope of weight gained versus time, and then by dividing the slope by expose area, using the next formula (Eq. 8):

$$WVTR = \text{Slope} * \text{Time (Hours)} / m^2$$

Equation 8. Water Vapor Transmission Rate formula.

Synthesis of Nanocapsules

The NCs were synthesized by the nanoprecipitation method, which was used in the research of (Khayata *et al.*, 2012) with some variations in the synthesis process, such as the polymer and α -tocopherol concentration and the ratios of solvents.

Where PCL was sonicated for 10 minutes in 10 mL of the solvent acetone, after this time, a homogenous solution was obtained, then the α -tocopherol concentration was added to be dissolved at room temperature, this being the organic phase (OP).

The OP was injected at constant drip by gravity to the aqueous phase (AP) while in constant agitation (200 RPM), then the solvent was evaporated using a rotavapor (at 27 °C and 110 RPM for 10 minutes).

Table 7. Formulation of Nanocapsules

		Components	Concentration				
1	Organic Phase	Acetone (ml)	10				
		PCL (mg)	20				
		α -tocopherol (mg)	0	5	10	15	20
2	Organic Phase	Acetone (ml)	10				
		PCL (mg)	10				
		α -tocopherol (mg)	0	5	10		
3	Organic Phase	Acetone (ml)	10	10	12	7	5
		Methanol (mL)	0	0	0	3	5
		PCL (mg)	10				
		α -tocopherol (mg)	5				

All the formulations above, had an aqueous phase of 20 mL of Distilled water with a concentration of 0.5% of PVA.

Physical Characterization

The diameter, the polydispersity (PDI) and the Z potential (ζ) were analyzed by nanosizer, where 500 μL of the nanocapsules suspension and 1 mL of distilled water were added to be measured in triplicate for each formulation.

Chemical Characterization

Antioxidant Activity

The antioxidant activity was analyzed by the method of 2,2-Diphenyl-1-Picrylhydrazyl (DPPH) ($\text{C}_{18}\text{H}_{12}\text{N}_5\text{O}_6$), this being an effective method to measure the antioxidant activity (Muid *et al.*, 2013). A solution of 0.3 mMol of DPPH in 99 % of ethanol was prepared. The nanocapsule suspension was centrifuged for 1 hour at 13,300 RPM to separate the supernatant from the precipitate, then the precipitate was sonicated for 30 minutes to extract the α -tocopherol from the nanocapsules, then in a well from a 96-well plate, 280 μL of the DPPH solution was mixed with 20 μL of both phases (supernatant and precipitate) and allowed to react for 30 minutes in the dark and read at 520 nm in a microplate reader (EZ Read).

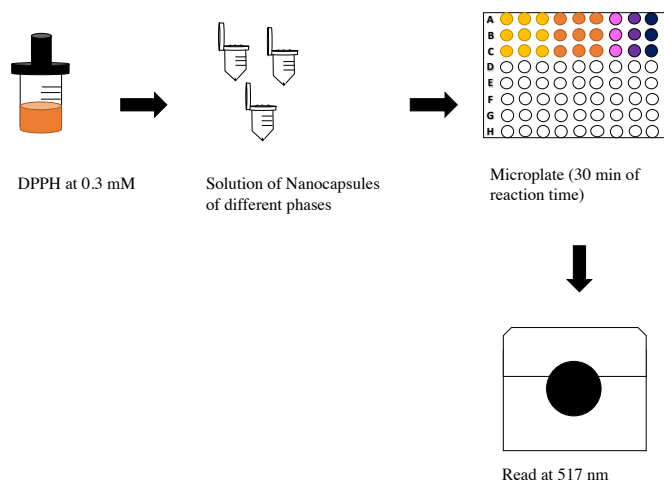


Figure 25. Antioxidant Activity by DPPH test

Antioxidant activity was calculated using the following formula (Eq. 9):

$$\text{Antioxidant Activity \%} = \frac{\text{Abs Control} - \text{Abs Sample}}{\text{Abs Control}} \times 100$$

Equation 9. Antioxidant Activity formula.

α -Tocopherol Quantification

Direct quantification (HPLC)

Measurement was performed by high pressure liquid chromatography (HPLC) using the HP1100 Chromatograph with a UV wavelength detector with variable wavelength, a Phenomenex Luna PFP column (2.0 x 150 mm, 5 μ) at 30 °C was used with a mobile phase of Methanol:Water (93:7) with a flow of 0.3 mL/min. The detection was performed at a wavelength of 295 nm.

The method validation was carried out under the criteria of the ICH, the parameter evaluated were linearity, limit of detection (LDD), limit of quantification (LDQ) and precision. A calibration curve was performed with five levels of α -tocopherol concentration per level (4, 8, 16, 32 and 64 μ g/mL)

Indirect Quantification (DPPH)

A calibration curve was performed (R^2 of 0.998) with methanol with up to 160 parts per million (ppm) of α -tocopherol, where respective dilutions were made to the samples to fit within the curve, the absorbance obtained were used in the next formula:

$$Y = mx + b$$

Equation 7 a. Formula de la recta

$$X = \frac{y - b}{m}$$

Equation 7 b. Formula despejada para X

Stability of α -tocopherol after UV exposure

Quantification

A solution of NCs were exposed to different times of UV light (0, 15, 20 and 25 minutes), then by sonication the α -tocopherol was extracted and analyzed by HPLC with the aforementioned characteristics.

Antioxidant Activity

In 6 cm petri dishes, 2 mL of solution of nanocapsules with 5 mg of α -tocopherol were deposited and were exposed to UV light at different times (0, 15, 20 and 25 minutes), and then analyzed by DPPH.

RESULTS

Thermal crosslinked Hydrogels (Alginate or Gelatin)

Physical Characterization

Swelling Behavior

Alginate Hydrogels

In (Fig. 27) the swelling behavior of Alginate hydrogels is observed, the highest concentration being the only one that could be measurable (A3), since due to its consistency it was not possible to take samples of the other concentrations (A1 and A3), while A3 had a maximum swelling time at 8 hours (143 ± 7 %) and then began to solubilize.

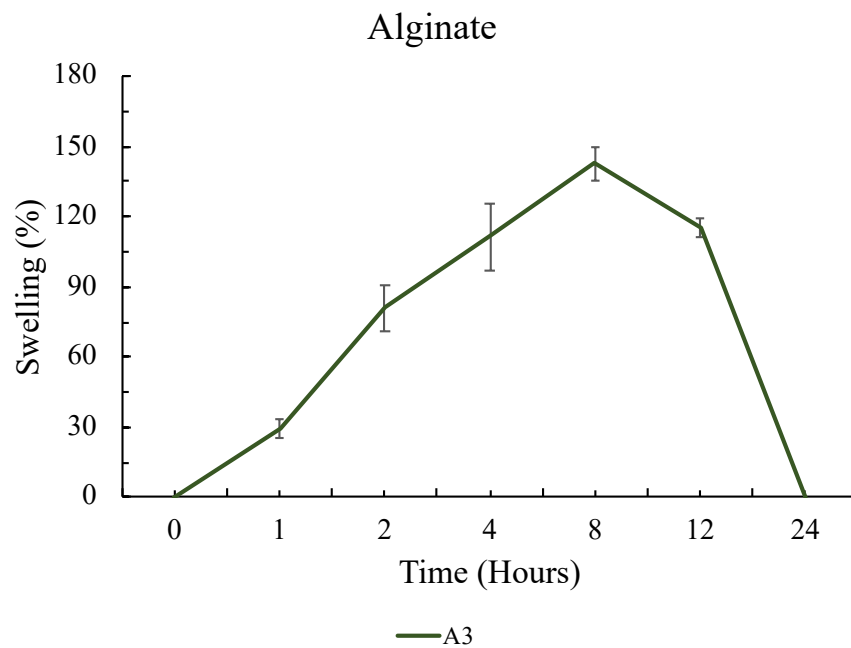


Figure 26. Swelling Behavior of Alginate Hydrogels

Gelatin Hydrogels

In (Fig. 28) the swelling behavior of hydrogels of Gelatin is observed, where only G2 and G3 could be measured, where the G2 hydrogel maximum swelling time was at 4 hours ($140 \pm 8 \%$) and G3 was at 8 hours ($202 \pm 2 \%$) then they began to solubilize.

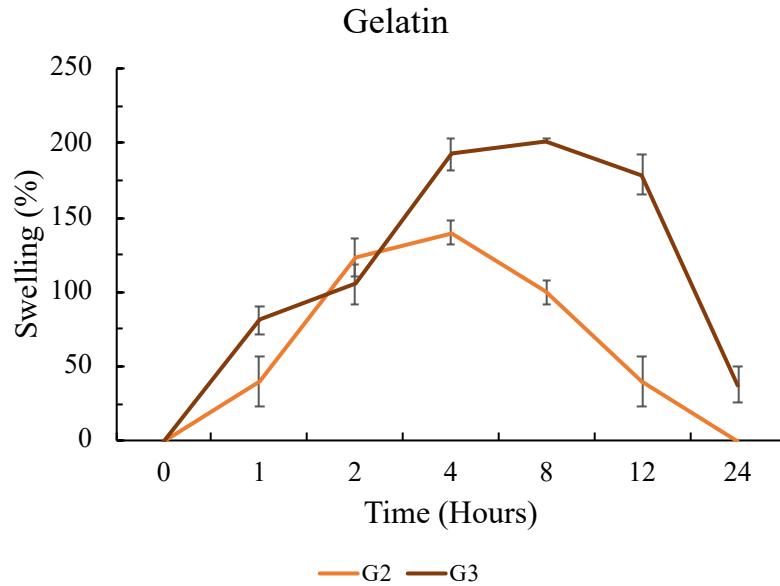


Figure 27. Swelling Behavior of Alginate Hydrogels

As shown in our result and in appendix B, it is possible to see that there is a significant difference in the swelling percentage, where it is appreciated that the hydrogels with the highest polymer concentration (A3 and G3) have a maximum swelling time at 8 hours, being G3 the one with the highest percentage (202 ± 2).

Solubility Behavior

Alginate Hydrogels

The solubility behavior of Alginate hydrogels (Fig. 29), where only the sample (A3) could be measured, due to its consistency it was not possible to take a sample of the other hydrogels (A1 and A2), note that A3 was completely solubilize until 12 hours, having a maximum swelling time at 4 hours (-122.33 ± 3.40 %) before starting to solubilize.

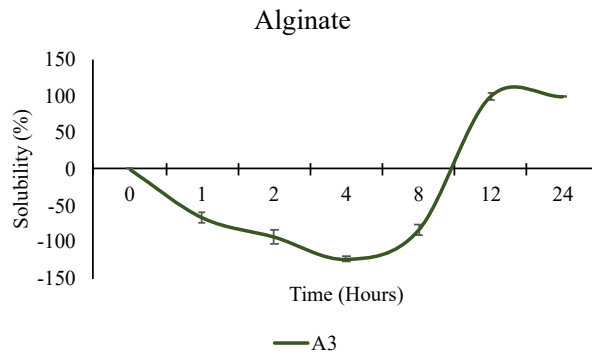


Figure 28. Solubility Behavior of Alginate Hydrogels

Gelatin Hydrogels

In (Fig. 30) can be seen the solubility behavior of the Gelatin hydrogels, where the sample (G1) could not be measured by its consistency. It can be observed in the G2 hydrogel, its maximum swelling time was at 2 hours (-30 ± 16.09 %) and for the G3 hydrogels it was 4 hours (-109 ± 16.21 %) before beginning to solubilize, being its total solubility for the G2 sample at 12 hours and for G3 at 24 hours.

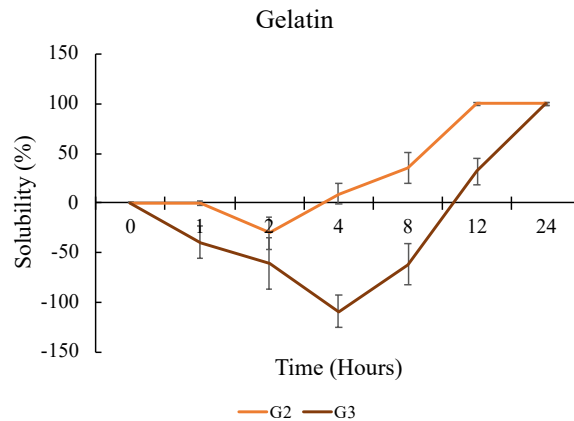


Figure 29. Solubility Behavior of Gelatin Hydrogels

As shown in our results (Appendix C) the hydrogels that solubilize faster were the higher alginate content, but they absorb more water content in the conditions that were put, while gelatin hydrogels solubilize until 24 hours, but with less water content.

Rheological Analysis of Thermal crosslinked Hydrogels (Alginate or Gelatin)

Rheological Behavior

Alginate Hydrogels

For the hydrogels formed by Alginate (Fig. 31), only at concentrations higher than or similar to 1 g, showed a pseudoplastic behavior (A3), while at concentration less than 1 g, they presented a Newtonian behavior (A1 and A2).

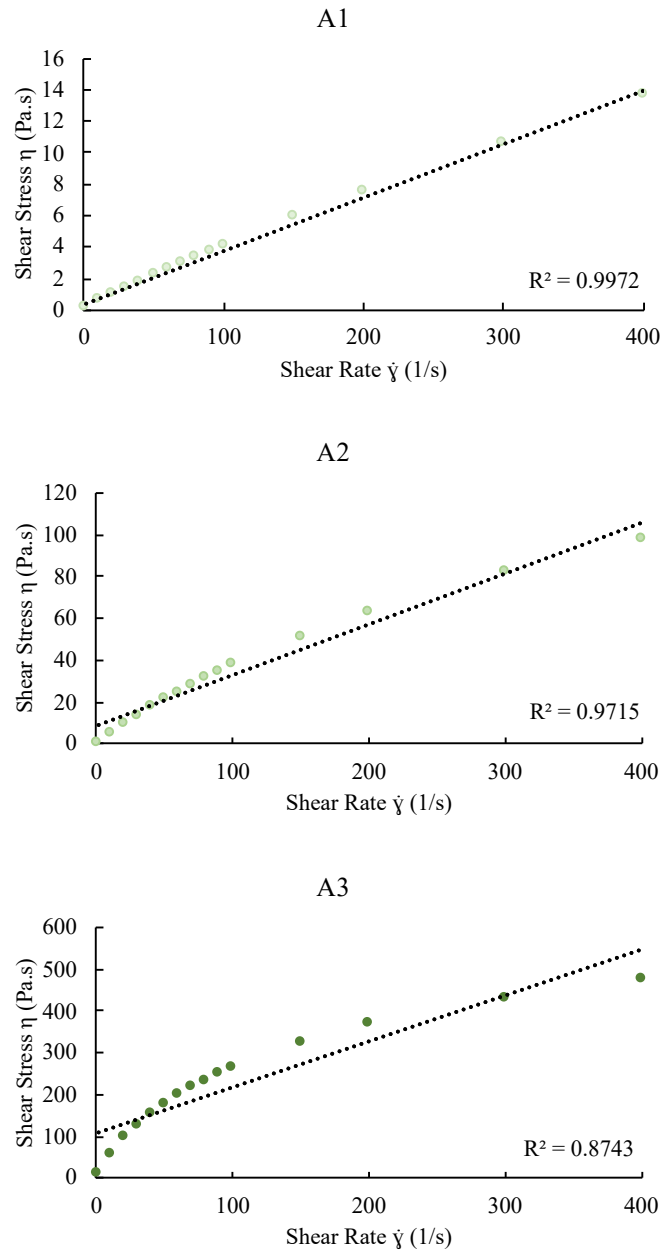


Figure 30. Rheological Behavior of Alginate Hydrogels.

Gelatin Hydrogels

Hydrogels formed only with Gelatin (Fig. 32) where concentrations less than 500 mg showed a Newtonian behavior (G1), while concentrations greater than 500 mg showed a pseudoplastic behavior (G2 and G3).

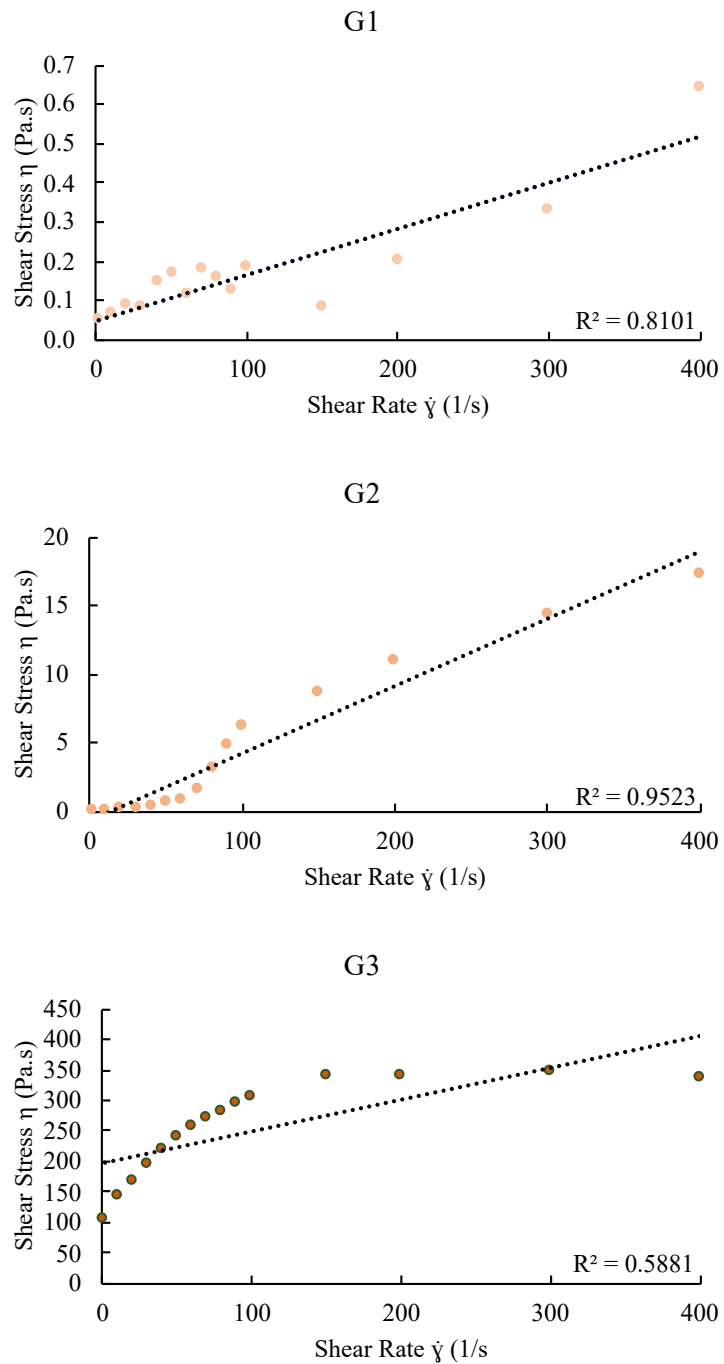


Figure 31. Rheological Behavior of Alginate Hydrogels.

As our result above showed, hydrogels from a concentration higher than 500 mg, start to have a pseudoplastic behavior, were, hydrogels with a concentration higher or similar to 1 g, start to behave like a pseudoplastic fluid.

Thermal and Photo crosslinked Hydrogels (Alginate and Gelatin)

Physical Characterization

Swelling Behavior

Thermal crosslinked Hydrogels

The swelling behavior (Fig. 33) of thermo crosslinked hydrogels (WoPi), showed that when they had a higher concentration of Alginate (AG1) they swelled less, having a maximum swelling time at 8 hours ($152 \pm 7\%$), while when they had similar concentration of polymer (AG WoPi) and higher concentration of Gelatin (GA1 WoPi) they had a lower maximum swelling time (4 horas), but higher percentages of swelling ($187 \pm 26\%$ y $170 \pm 8\%$, AG y GA1 respectively).

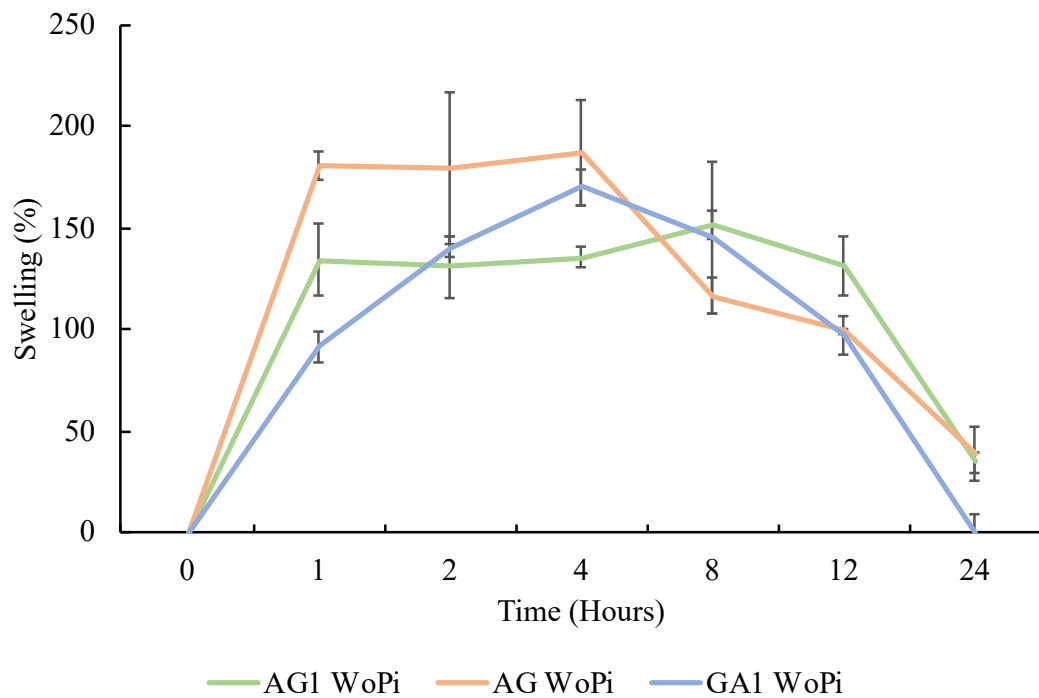


Figure 32. Swelling Behavior of Thermal crosslinked

Photo crosslinked Hydrogels

The swelling behavior (Fig. 34) of Photo crosslinked hydrogels (WPI) showed that all the hydrogels had a maximum swelling time at 4 hours, the highest being AG hydrogels (180 ± 24 %), and after this period of 4 hours, they began to solubilize.

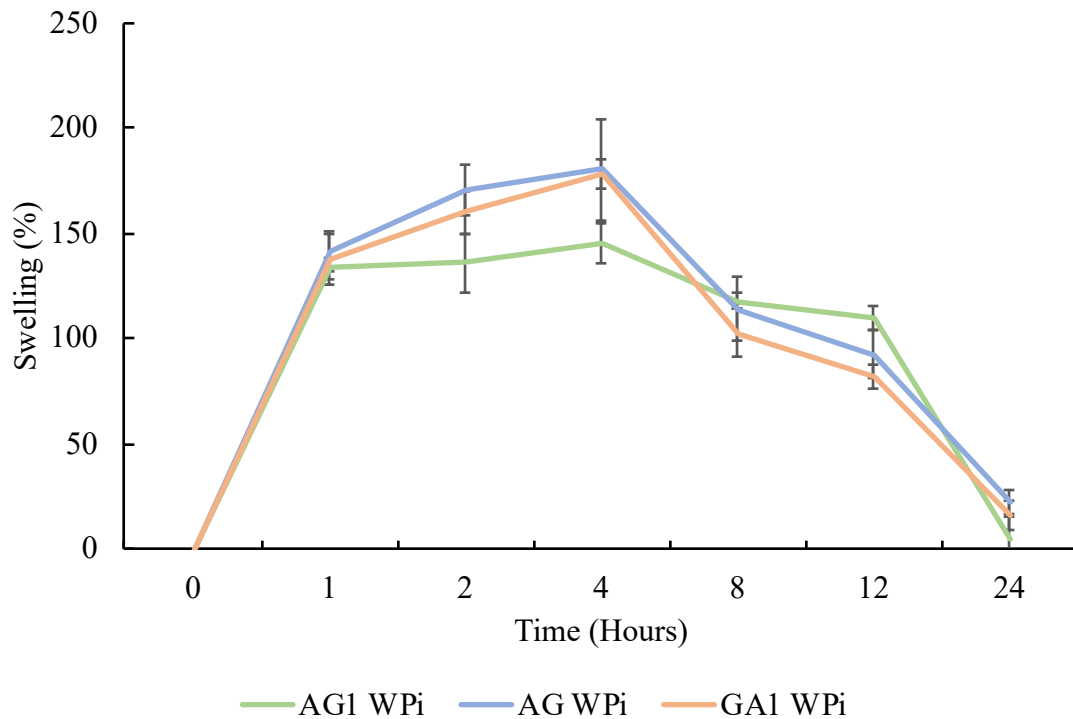


Figure 33. Swelling Behavior of Photo crosslinked Hydrogels

As shown in our result (Appendix D), hydrogels that were photo crosslinked, shown a more controlled behavior under this solvent, without showing a significant difference between them, while the thermal crosslinked hydrogels, showed difference in the AG WoPi hydrogels.

Solubility Behavior

Thermal crosslinked

The solubility behavior (Fig. 35) of thermo crosslinked hydrogels (WoPi), showed that hydrogels with a higher Alginate concentration, before starting to solubilize, swell until 8 hours (-73 ± 14), these being the ones that withstood the conditions in which, while the hydrogels (AG1 and GA1) were completely solubilized at 24 hours, the hydrogels AG were solubilized until 48 hours.

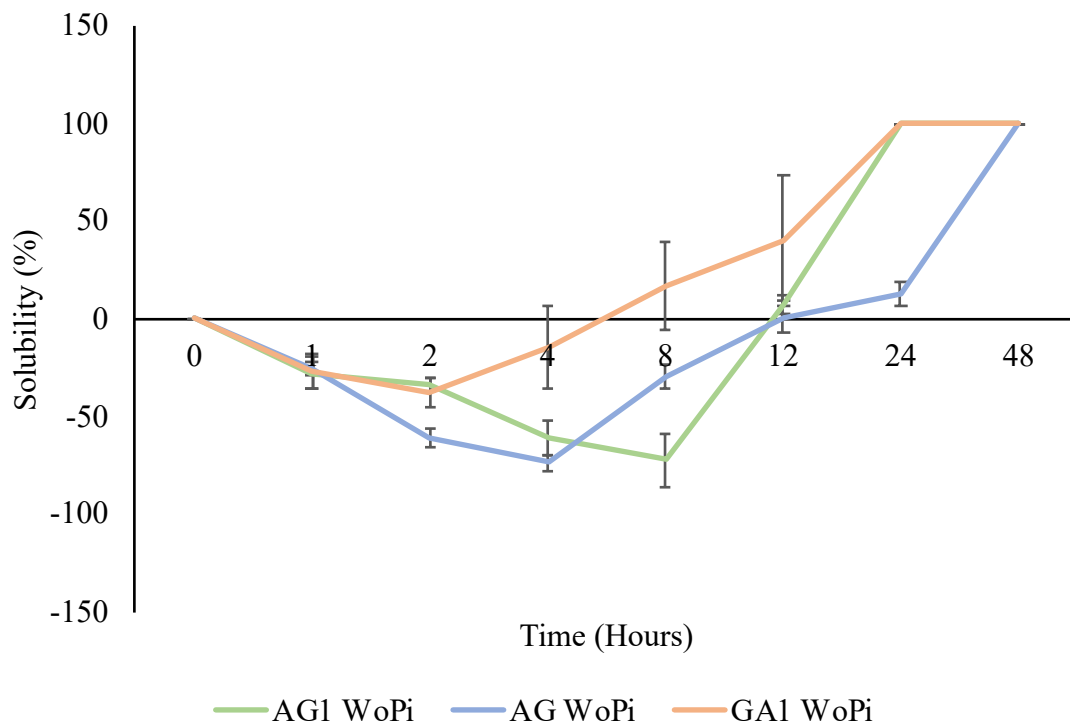


Figure 34. Solubility of Thermal crosslinked Hydrogels

Photo crosslinked Hydrogels

The solubility behavior (Fig. 36) of the Photo crosslinked hydrogels (WPI), showed that hydrogels with a higher concentration of Alginate (AG1) resisted solubilization (12 hours) longer with a solubility percentage of $-68 \pm 10\%$ before it begins to solubilize and it is the only treatment that did not solubilize completely after 48 hours

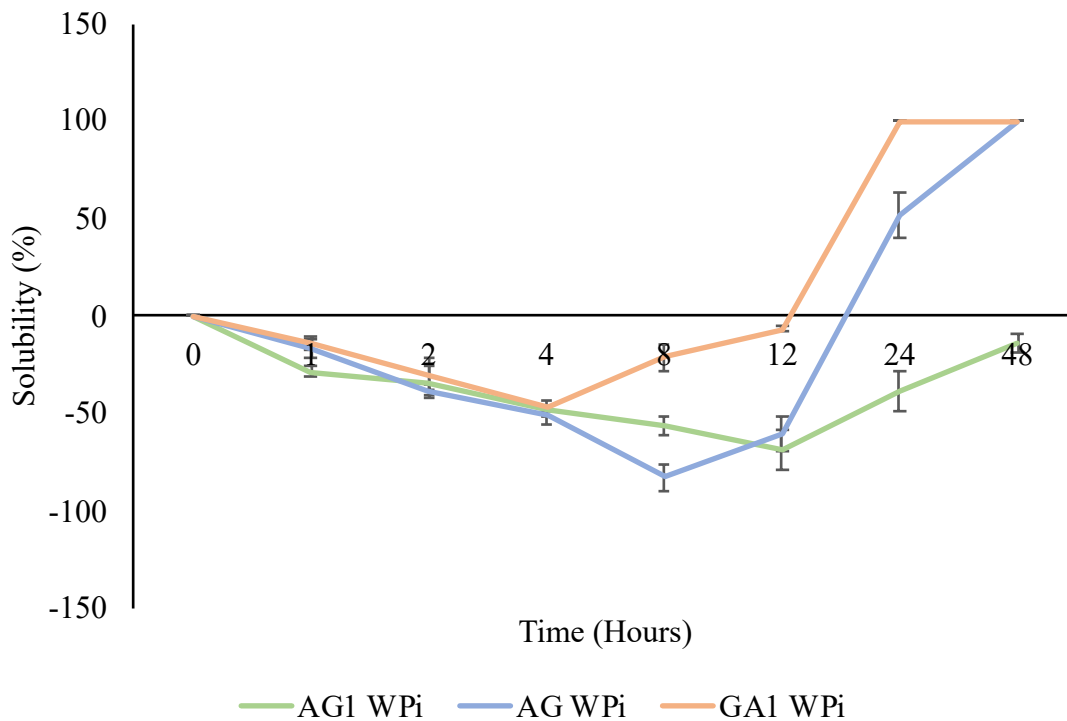


Figure 35. Solubility of Photo crosslinked Hydrogels

As shown in our results (Appendix E), Thermal crosslinked hydrogels, solubilize at 24 hours, but the same polymer concentration hydrogel (AG) completely solubilize until 48 hours, while the photo crosslinked hydrogels tend to have a 100 % solubilization percentage, while the AG show a similar behavior as the thermal crosslinked hydrogels.

Rheological Analysis of (Thermal and Photo) Hydrogels

Rheological Behavior of Thermal crosslinked Hydrogels

The thermo crosslinked hydrogels (Fig. 37), showed a pseudoplastic behavior, while the GA1 WoPi hydrogels, were the ones that resisted the flow without significant difference to the AG WoPi hydrogels, while AG1 were the ones that needed less force to start flowing.

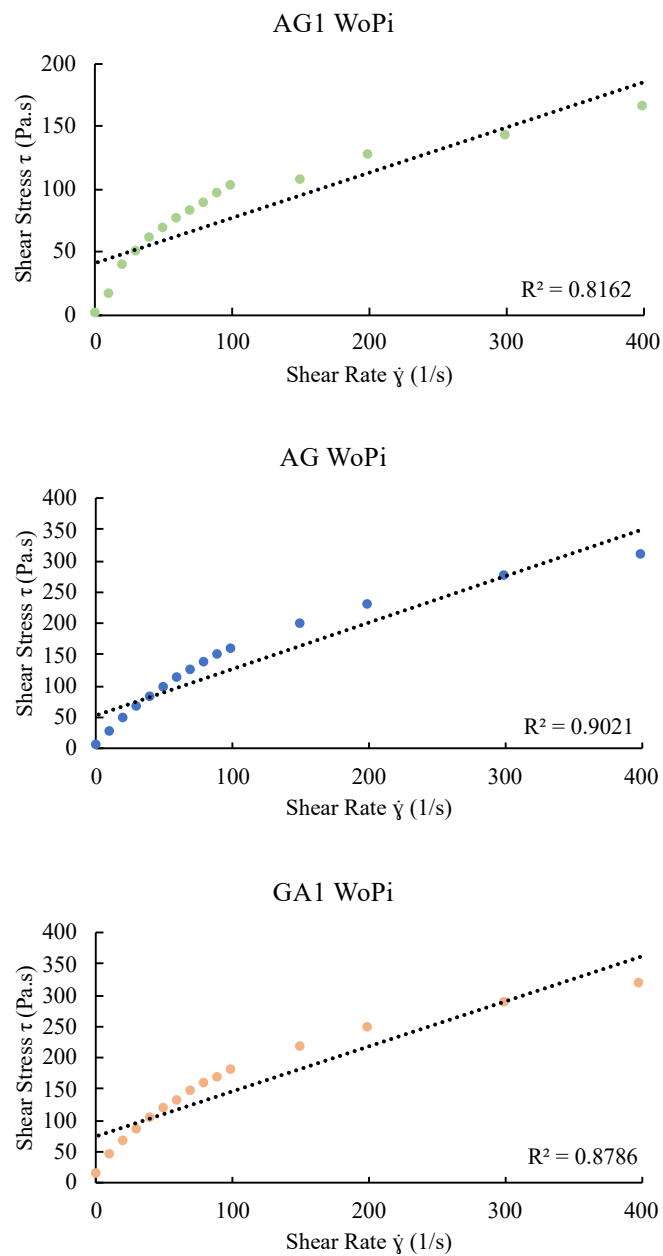


Figure 36. Rheological Behavior of Thermal crosslinked Hydrogels

Rheological Behavior of Photo crosslinked Hydrogels

The Photo crosslinked hydrogels (Fig. 38), presented a pseudoplastics behavior, while those with the highest Alginate concentration (AG1Wpi) and similar polymer concentration (AG Wpi) were the ones that resisted flow the most, while those with the highest concentration of Gelatin (GA1 Wpi) were the ones with the lowest strength needed to start flowing.

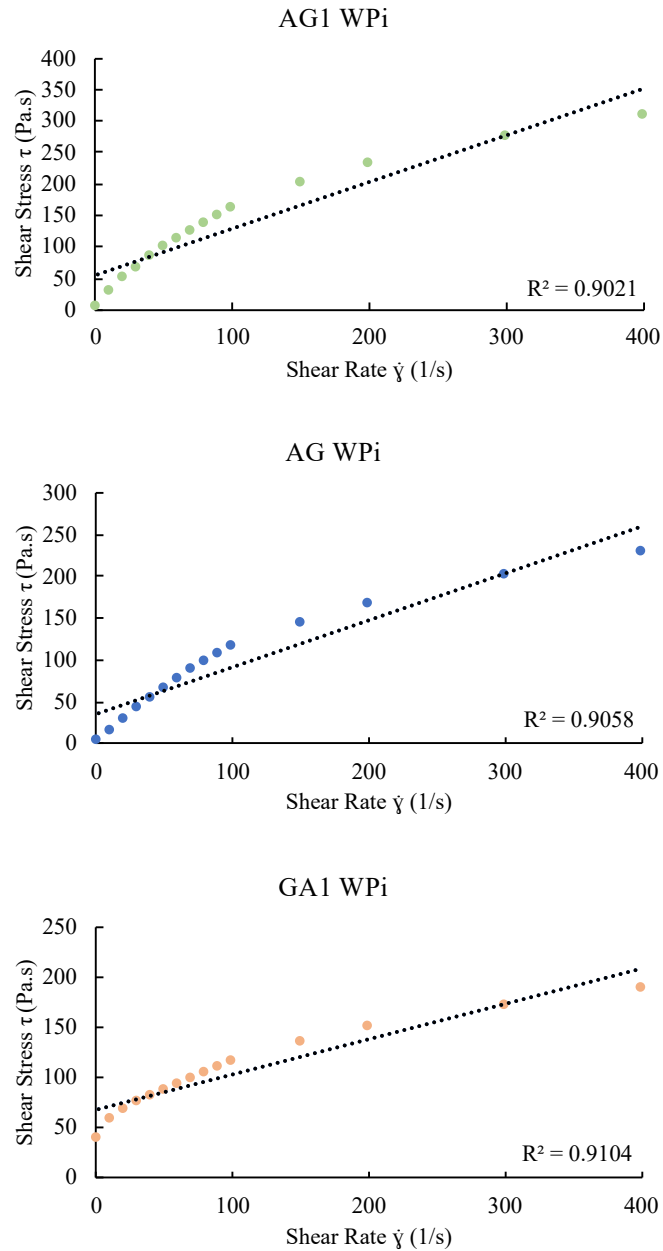


Figure 37. Rheological Behavior of Photo crosslinked Hydrogels

Consistency Index

Thermal crosslinked Hydrogels

The hydrogels that were Thermo crosslinked, had a consistency index (K) (Fig. 39) that varied between 0.91537 (AG WoPi) to 13.0346 (AG1 WoPi), being the latter the most resistant.

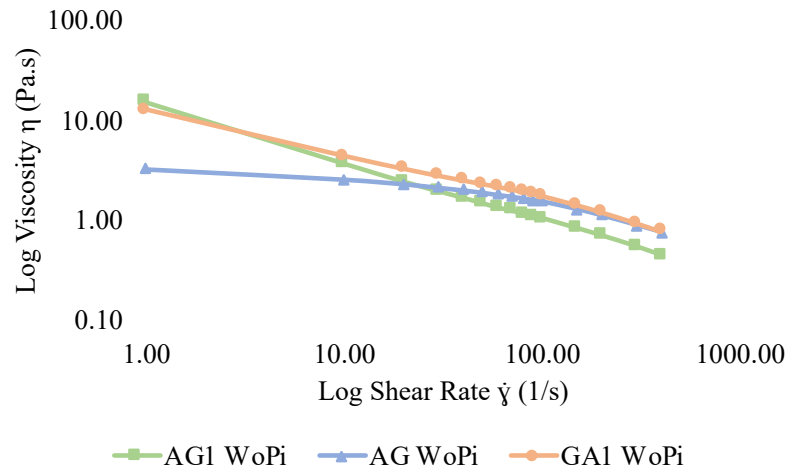


Figure 38. Consistency Index of Thermal crosslinked Hydrogels

Photo crosslinked Hydrogels

The hydrogels that were Photo crosslinked (Fig. 40), had a consistency index (K) that varied between 2.4271 (AG WPI) to 32.2775 (AG1 WPI), being the firmest.

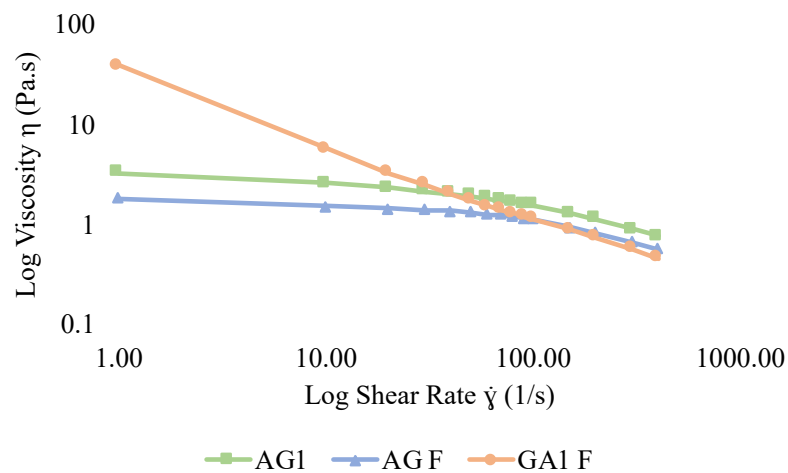


Figure 39. Consistency Index of Crosslinked Hydrogels

Fourier Transform Infrared Spectroscopy (FTIR)

FTIR Photo crosslinked

When the samples were analyzed (Fig. 41), the intensity of the functional groups were almost generally, the AG1 hydrogels that had a greater intensity in the most representative peaks of each polymer that was present in them.

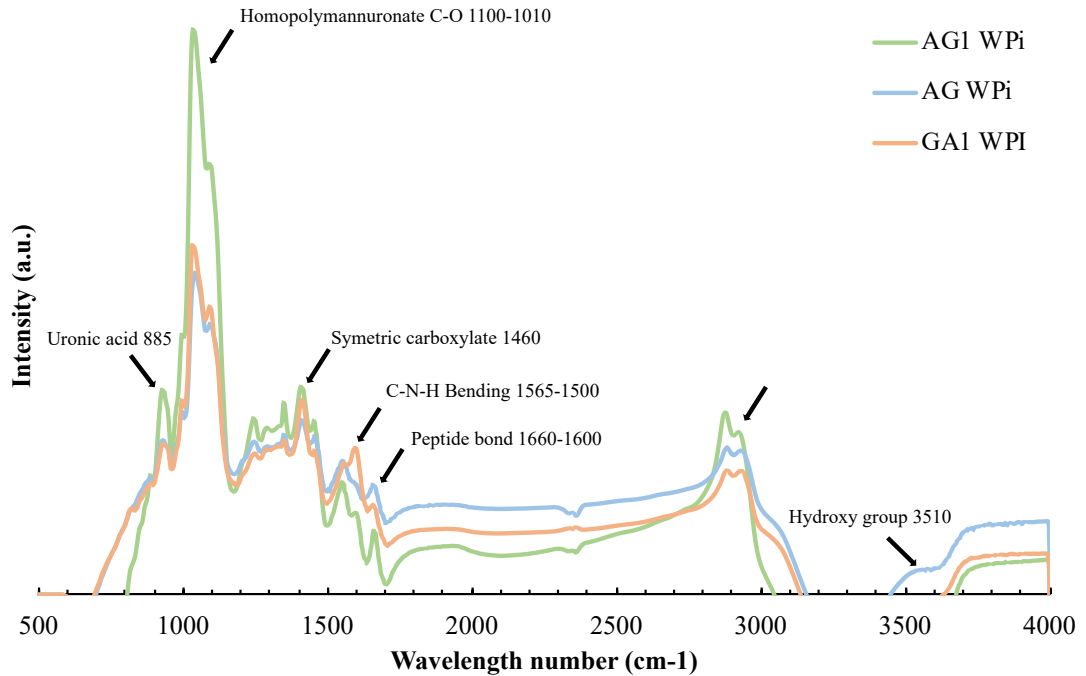


Figure 40. FTIR of Photo crosslinked Hydrogels

Porosity by SEM

In (Fig. 41) the SEM of the hydrogels can be appreciated, and the porosity of the AG (WoPi) with $11.12 \pm 1.89 \mu\text{m}$ and for AG (WPi) was $7.84 \pm 1.10 \mu\text{m}$, we confirm that when the hydrogels were photo crosslinked, its porosity decreases.

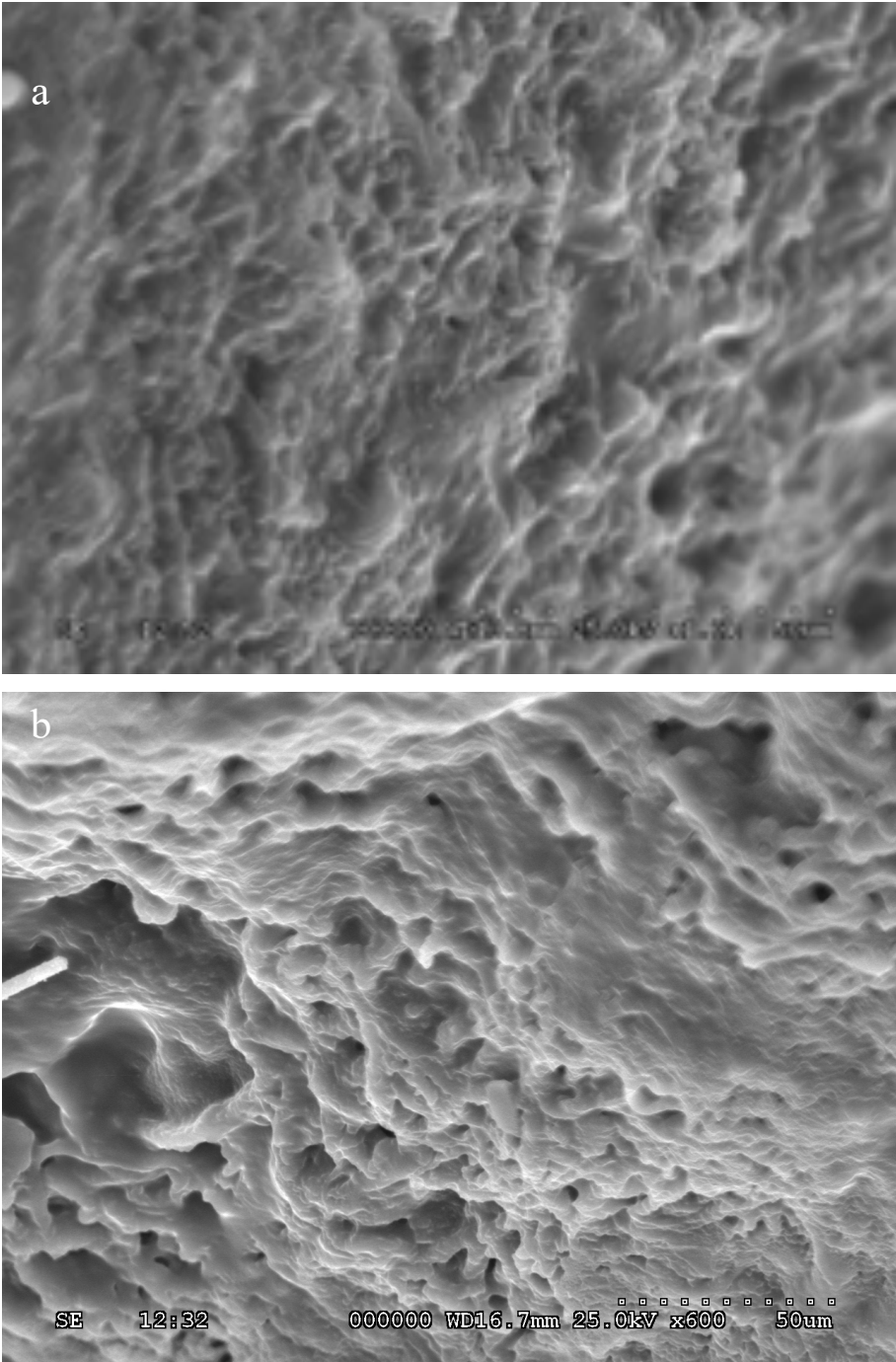


Figure 41. SEM images. Where (a) AG (WoPi) and (b) AG (WPi)

Chemical Characterization

pH

Thermal and Photo crosslinked Hydrogels

When the pH of the Thermo and Photo-crosslinked hydrogels was analyzed, the pH ranged from 5.3 to 5.4, without presenting any significant difference.

Water Vapor Permeability

Thermal crosslinked

In (Fig. 42) it can be seen the WVPR ($\text{g.H}_2\text{O.h/m}^2$) of Thermal crosslinked hydrogels, where the hydrogels of the same polymer concentration (AG WoPi) was the one with the highest WVPR at 24 hours ($14.59 \pm 8.08 \text{ g.H}_2\text{O.h/m}^2$), while the lowest was the one with the highest concentration of Alginate (AG1 WoPi) with $6.72 \pm 1.35 \text{ g.H}_2\text{O.h/m}^2$.

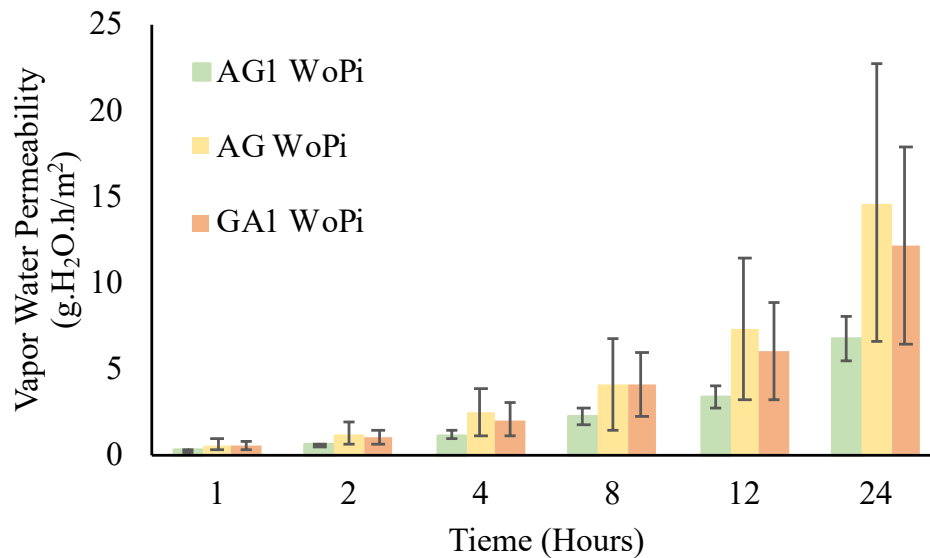


Figure 42. Permeability Behavior of Thermal crosslinked Hydrogels

Photo crosslinked Hydrogels

In Figure 43, it can be seen the WVPR of Photo crosslinked hydrogels, where hydrogels with the highest concentration of Gelatin (GA1 WoPi) were the ones that presented greater permeability at 24 hours ($12.70 \pm 1.39 \text{ g.H}_2\text{O.h/m}^2$), while the lowest was the ones with the highest concentration of Alginate (AG1 WoPi) with $6.72 \pm 1.35 \text{ g.H}_2\text{O.h/m}^2$.

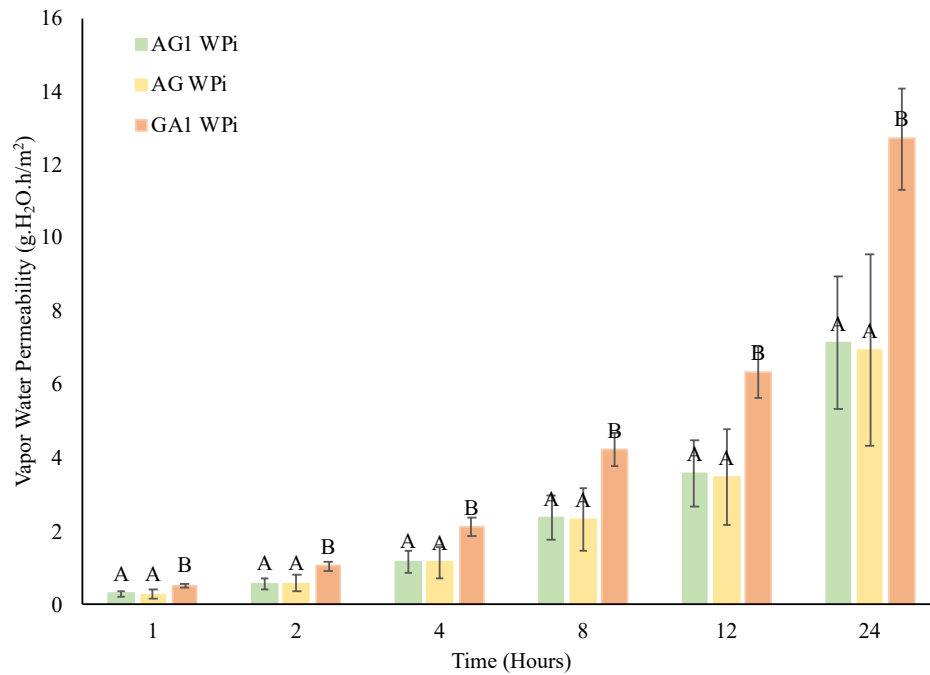


Figure 43. Permeability Behavior of Photo crosslinked Hydrogels

As shown (Appendix F) the type of crosslinking of hydrogels, does not show a significant difference between the treatments, showing that the permeation of water vapor, was present in both methods.

Contact Angle (Wettability)

Thermal crosslinked

When the Thermo crosslinked hydrogels were analyzed, it can be seen that the contact angles (CA) (Fig. 44) of the hydrogels with highest Alginate concentration (AG1) (Fig. 57 a) were the ones with the greatest angle (87.24 °), while the higher Gelatin concentration (GA1) (Fig. 44 a) presented the lowest angle (53.34 °), while those of equal polymer concentration (AG) (Fig. 44 b) presented an angle of 80.31 °.

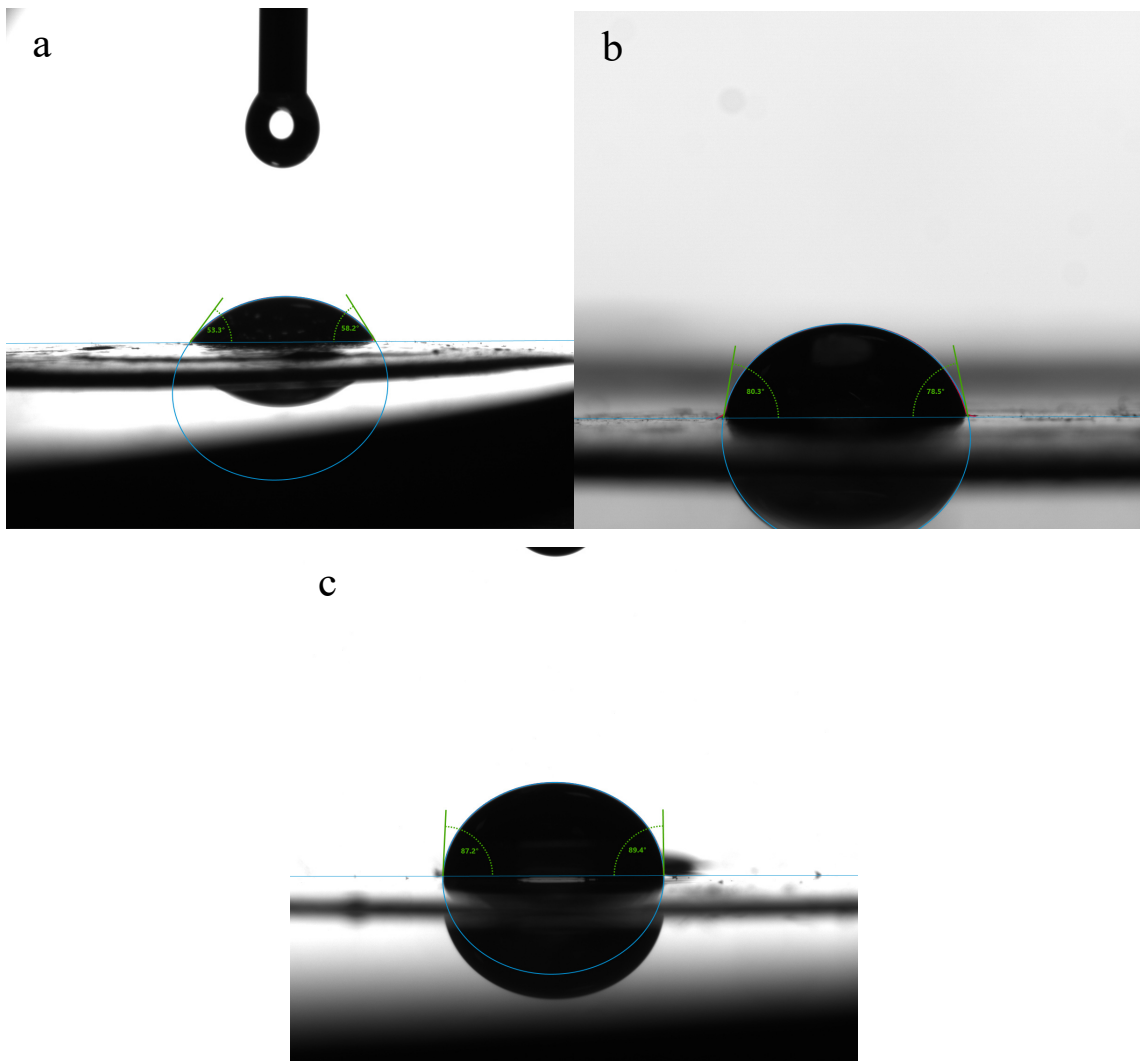


Figure 44. Contact angle of Thermal Crosslinked Hydrogels

Photo crosslinked

When the Photo crosslinked hydrogels contact angles (Fig. 58) were analyzed, it can be seen that the hydrogels with the highest concentration of Alginate (AG1) (Fig. 58 a) were the ones with the greatest angle (113.53 °), while the ones with equal polymer concentration (AG) (Fig. 58 b), they presented the lowest (91.56 °), while those with the highest concentration of Gelatin (GA1) (Fig. 58 c) presented an angle of 101.09 °.

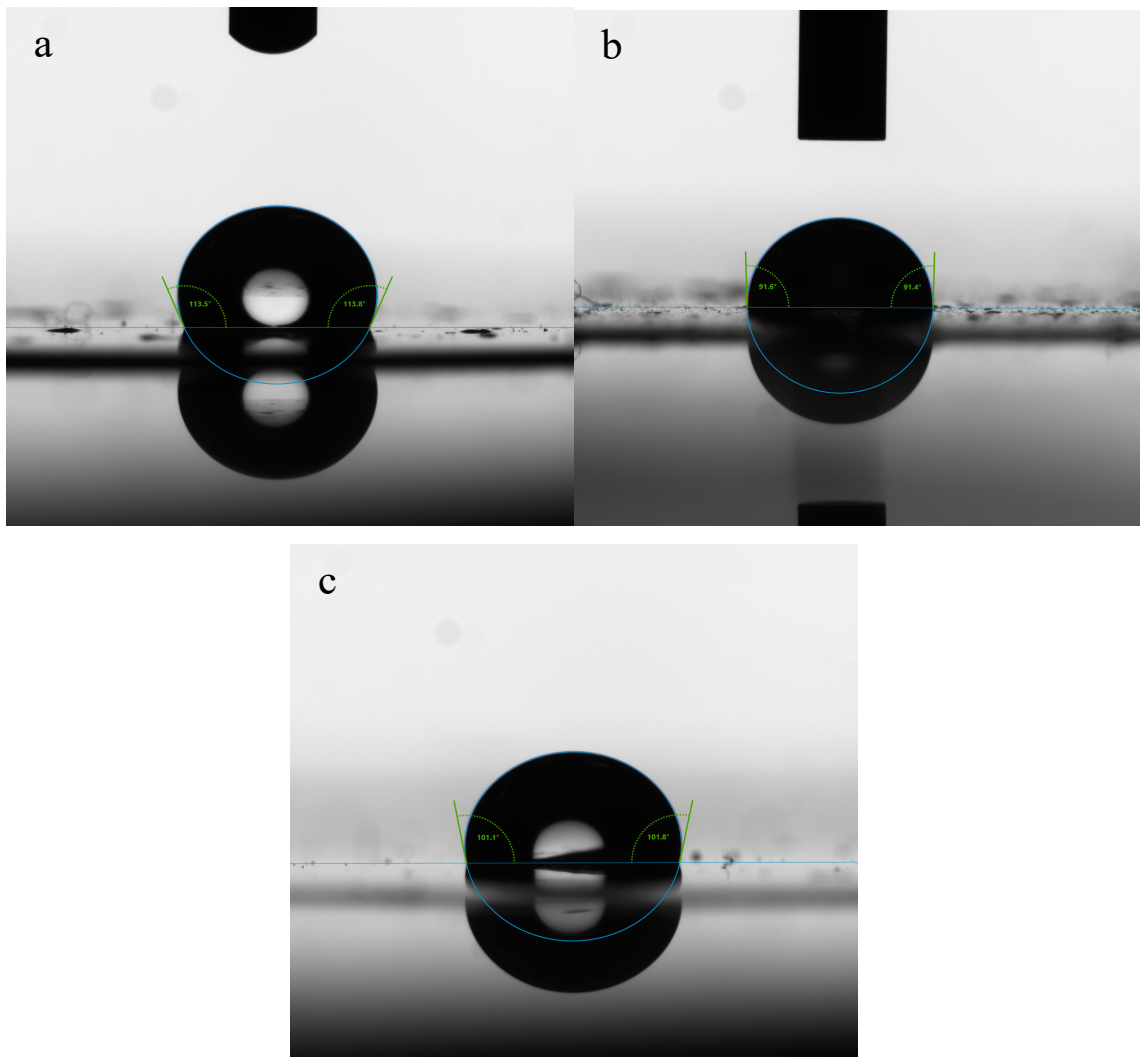


Figure 58. Contact angle of Photo crosslinked Hydrogels

As it can be seen, the CA, was higher than 90 ° in all the photo crosslinked hydrogels, but not higher than 113 °, showing a hydrophobic behavior.

Nanoprecipitation of PCL nanocapsules with 20 mg of PCL

Physical Characterization

When the diameters, the polydispersity index (PDI) and the Z-potential of the 20 mg of PCL NCs were analyzed, the largest ones were those with the highest concentration of vitamin (20 mg) and the smallest were those with lower concentration of α -Toc (5 and 10 mg), of which between the last two, did not represent a significant difference in their size or polydispersity index, as can be seen in Table 11.

Table 8. Physical characteristics of 20 mg of PCL nanocapsules

α -Toc (mg)	Diameter (nm) *	PDI *	Z Potential (mV) *
0	256.1 \pm 2.74 ^a	0.123 \pm 0.01 ^{ab}	- 4.88 \pm 0.27 ^a
5	280.4 \pm 1.51 ^b	0.093 \pm 0.02 ^a	- 3.73 \pm 0.12 ^b
10	281.0 \pm 2.27 ^b	0.137 \pm 0.01 ^{ab}	- 4.92 \pm 0.13 ^a
15	297.4 \pm 0.57 ^c	0.150 \pm 0.02 ^b	- 3.42 \pm 0.06 ^{bc}
20	295.8 \pm 2.36 ^c	0.161 \pm 0.01 ^b	- 3.19 \pm 0.24 ^c

An ANOVA was performed, where * is equal to $p < 0.05$. A post-hoc (Tukey) was carried out, where the lower-case indices (left) (e.g. ^a) represent the vertical groups between treatments.

Chemical Characterization

Antioxidant Activity by DPPPH

When performing a DPPH of the NCs suspensions, it can be observed that the antioxidant activity (%AA) (Fig. 59) was higher in the supernatant (SN) compared to the pellet (NP) in almost all cases (not in the 5 mg NCs suspension), being in both cases, the highest concentration of vitamin (15 and 20 mg) had the highest antioxidant activity and showed no significant difference.

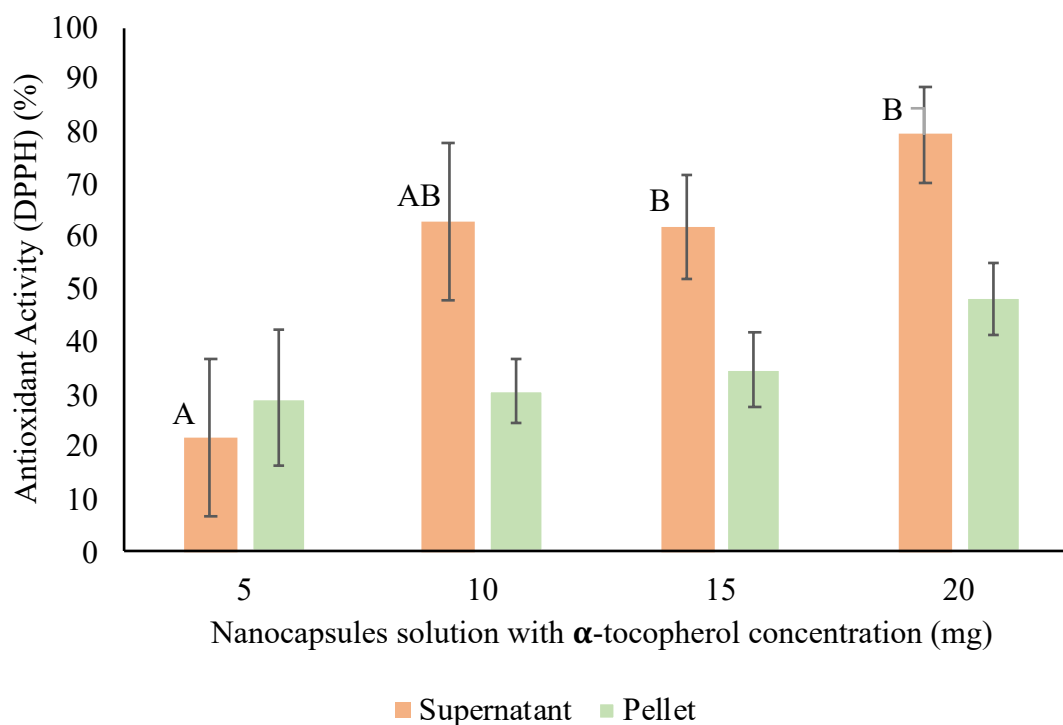


Figure 46. Antioxidant Activity by DPPH of the supernatant and the precipitate of the nanocapsules suspension of 20 mg of PCL.

Quantification of α -tocopherol by HPLC

Nanocapsules obtained varying PCL concentration

According to the results of quantification of α -Toc obtained by HPCL of the NCs formed with 20 mg of PCL it % EE varied between 16 to 30 %, and showed that the NCs with the highest encapsulation efficiency were those of 5 and 15 mg, with 27 and 30 of % EE respectively.

Nanoprecipitation of PCL with 10 mg of PCL

Physical Characterization

When the diameters and the polydispersity index (PDI) of the 10 mg of PCL NCs were analyzed (Tab. 13), the sizes ranged from 285 to 366 nm, being the lower size, the NCs with the lower vitamin concentration (5 mg).

Table 9. Physical characteristics of 10 mg of PCL nanocapsules

α -tocopherol (mg)	Diameter (nm)*	Polydispersity Index *
0	285.97 \pm 2.18 ^a	0.08 \pm 0.02 ^a
5	340.20 \pm 4.75 ^b	0.12 \pm 0.01 ^a
10	366.80 \pm 4.75 ^c	0.20 \pm 0.01 ^b

An ANOVA was performed, where * is equal to $p < 0.05$. A post-hoc (Tukey) was carried out, where the lower-case indices (right) (e.g. ^a) represent the vertical groups between treatments.

Nanoprecipitation using different solvent concentrations

Physical Characterization

The sizes and polydispersity index of the NCs, ranged from 238.60 to 304.90 nm, being the smaller ones those from the treatments L5 (238.60 \pm 1.93 nm), while its PDI did not shown a significant difference between treatments.

Table 10. Physical characteristics of nanocapsules with different solvents

Sample	Diameter (nm) *	Polydispersity index
L1	304.90 \pm 2.03 ^d	0.084 \pm 0.066
L3	283.93 \pm 1.51 ^c	0.088 \pm 0.011
L4	277.83 \pm 2.56 ^b	0.095 \pm 0.055
L5	238.60 \pm 1.93 ^a	0.077 \pm 0.037

An ANOVA was performed, where * is equal to $p < 0.05$. A post-hoc (Tukey) was carried out, where the lower-case indices (right) (e.g. ^a) represent the vertical groups between treatments.

Chemical Characterization

Antioxidant Activity by DPPH

When performing a DPPH to the NCs suspensions, was observed that the (% AA) (Tab. 15) was higher in the NP compared to the supernatant SN, being the highest in the L5 and without significant difference with the treatments L1, L4 and L6.

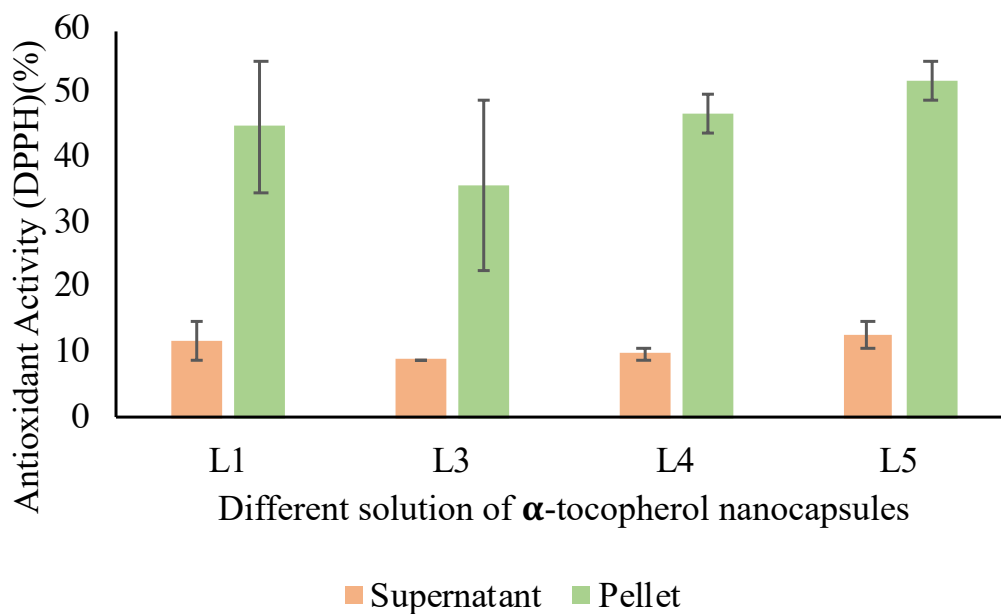


Figure 47. Antioxidant activity of supernatant and pellet of nanocapsules with different solvents.

Quantification of α -tocopherol Nanocapsules obtained Acetone:Metanol (1:1)

Direct (HPLC)

Upon obtaining the quantification results by HPLC of the NCs of 10 mg of PCL synthesized with Acetone:Methanol in a 1:1 ratio, when all concentration were added (Tab. 16) a total of 4.47 ± 0.45 mg is obtained, this being a total encapsulation efficiency (% EE) of 90 ± 9 %.

Table 11. Quantification of α -tocopherol by HPLC of nanocapsules with different solvents

Sample	Phase	mg
L5	Supernatant 1	0.26 ± 0.04
	Extraction 1	0.32 ± 0.03
	Supernatant 2	4.02 ± 0.12
	Extraction 2	0.03 ± 0.00

Indirect (DPPH)

When the concentration of active whitening the NCs of the samples was analyzed by DPPH, a concentration of 4.11 ± 0.29 mg could be found, this representing an % EE of 82.13 ± 5.75

Stability of α -tocopherol after UV light exposure

HPLC

When the samples are analyzed by DPPH, it can be observed (Tab. 12), that when exposed to UV light for 15 min or more, the concentration decrease more than 13%, but when performing a statistical analysis, it was not shown significant difference.

Table 12. Antioxidant activity of nanocapsules after being exposed to UV light

Sample	mg
Control	4.47 ± 0.45
15 min	3.87 ± 0.30
20 min	3.88 ± 0.30

Antioxidant Activity

After the samples that were exposed to the above-mentioned UV times, were analyzed by DPPH, the results showed that there was no significant difference in their antioxidant activity after 15 and 20 minutes of UV exposure against the control (0 minutes), but its antioxidant activity decreases more than 10 % after being exposed for more than 20 minutes, showing significant difference.

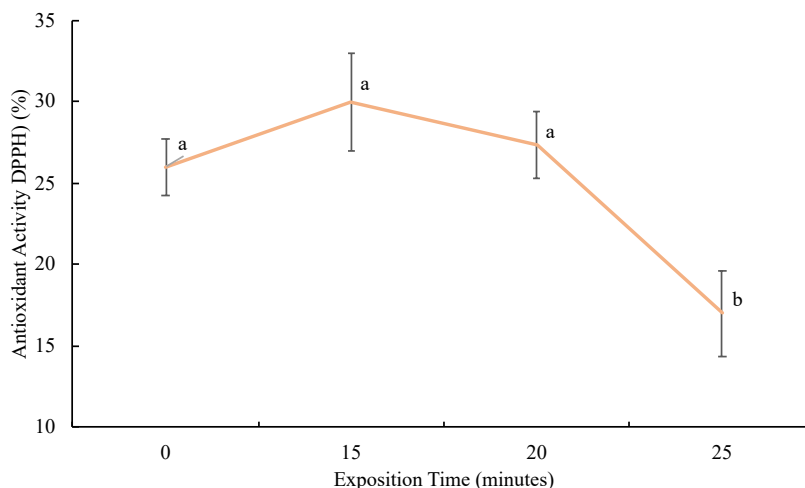


Figure 48. Antioxidant Activity by DPPH of nanocapsules suspension after being exposed to different times of UV light exposure.

DISCUSSION

Alginate or Gelatin Hydrogels

Physical Characterization

Swelling

Our results showed that hydrogels with the highest concentration of Gelatin (G3) and in the same proportion of Alginate (A3) were the ones that presented a greater percentage of swelling in the first hour of contact with distilled water ($81 \pm 9 \%$), likewise the hydrogels with the highest polymer concentration (G3 and A3) had a significant difference in their maximum swelling time (8 hours), being the G3 hydrogel the one with the highest swelling ($202 \pm 2 \%$). Recent studies demonstrated some of the characteristics that hydrogels depend on to swell such as: the nature of monomers (Baker *et al.*, 1992), the ionic force (Zhai *et al.*, 2004), pH of the medium (Baker *et al.*, 1995), temperature (Ogawa *et al.*, 2004). The major swellings in the gelatin hydrogels may be due to the fact that gelatin has more functional group with high affinity to water, and therefore this allows it to absorb more water, on the other hand we can assume that alginate, has a lower concentration of M-Blocks, since according to the literature, the higher the content of these block, the higher the water absorption (Jorgensen *et al.*, 2007) because the ion exchange is easier.

Solubility

Our results showed that the solubility of hydrogels with the higher concentration of Alginate (A3) and 500 mg of Gelatin (G2) solubilize at 12 hours but absorbed more water regardless of the environmental conditions while G3, solubilize until 24 hours of exposure. These results were expected, since gelatin present a high affinity to water as Djagny *et al.*, (2001) mentioned, a behavior was not expected, were the solubilization time of alginate hydrogels, since current literature says that alginate, in distilled water has a low rate of solubilization (Szekaslska *et al.*, 2016), although other studies emphasizes that the higher the G-Block content present in the alginate backbone, greater water affinity alginate will have (Niekraszewicz B. and Niekraszewicz A. 2009).

Rheological Analysis

Our results on their rheological behavior shown, that hydrogels with more polymer concentration, presented a Pseudoplastic behavior (A3 and G3), while those of lower concentration, showed similar behavior as water (Newtonian). This was expected, since according to literature, Alginate forms more networks compared to those formed only by gelatin, different authors mentioned that alginate increases the consistency index when its type of crosslinking was made by divalent cations such as Ca^{2+} (Funami *et al.*, 2009).

Thermal and Photo crosslinked Hydrogels

Physical Characterization

Swelling

Our results of hydrogels swelling that were crosslinked by a Thermal or Photo manner shown that those that swelled the most were the hydrogels that were Thermal-crosslinked, with a maximum swelling time at 4 hours and among these treatments that present a similar polymer concentration (AG WoPi) were those that presented the highest swelling, while at all times, all samples (Except AG1 WPi) was no significant different. As mentioned before, studies indicate that the greater the presence of G-Blocks, the greater the swelling capacity (ref), where we can observed, regardless of the type of crosslinking, there is no significant difference with those of equal polymer concentration that were photo crosslinked (AG).

Solubility

Our results of the solubility of hydrogels that were crosslinked by a Thermal or Photo manner shown that those that swelled the most were the hydrogels that were Thermal-crosslinked, with a maximum swelling time at 4 hours and among these treatments that present a similar polymer concentration (AG WoPi) were those that presented a greater swelling, while at all times, all samples (Except AG1 WPi hydrogel), there was no significant difference between their percentage of swelling. Recent studies mention that the type of interaction that Gelatin and Alginate creates, is through the formation of bio (polyelectrolyte) complexes(ref), while the photo crosslinked generate radicals that form covalent bond with the polymer in the solution, some studies mentions that their solubility rate will decreases (ref).

Rheological Analysis

While the individual data of each form of cross-linking are presented in the Table 22, showing that all hydrogels, regardless of their cross-linking method (Thermal or Photo) all presented a Pseudoplastic behavior, and the Photo crosslinked hydrogel had a higher consistency index were those that were Photo-crosslinked in all formulas. The hydrogels that present high concentration of G-Blocks, create more stiffer gels (Braccini and Perez 2001).

Chemical Characterization

pH

When comparing the pH of the hydrogels that were crosslinked by Thermo and Photo manner, they presented a significant difference, showing that the photo crosslinked hydrogel GA1 WPI, presented a higher pH compares to all the other treatments (5.43 ± 0.01). According to Boer et al., (2016), the pH of a healthy skin in humans, is whitening the range of 4 to 6 pH. Rizwan et al., (2017), mentions that the optimal pH for biomaterials it between 5.1 and 5.5, since these promote antibacterial and antifungal activities, so our hydrogels regardless of crosslinking method, they entered these ranges.

Water Vapor permeability

With our results, was no significant difference between the method of crosslinking, this could be due to the high standard deviation that a sample showed, but it can be observed a behavior of permeability that all hydrogels had, while the time was passing, it permeation was higher, being at 24 hours the highest for all of them.

Wettability

Thermo crosslinked hydrogels showed an angle of less than 90° , being classified as a hydrophilic or with high affinity to water, while those that were photo crosslinked, had less affinity without becoming hydrophobic, having degrees greater than 90° , but less than 115° , according to (Raffaini and Ganazolli 2007) biocompatibility is highly correlated with wettability, since characteristics such as surface chemistry, surface energy and topography, affect this criteria, and in the research carried out by (Fauchez et al., 2004) mentions that angles greater than 80° and less than 110° are ideal for cell adhesion, while Menzies and Jones (2010) reached to the conclusion that contact angle cannot be correlated with the biocompatibility of a material.

Effect of the concentration of PCL, α -tocopherol and different solvents in the synthesis of nanocapsules

PCL concentration

Physical Characterization

As shown in our results, when PCL concentration were used in the process of nano synthesis, NCs tend to reduce its diameter and its PDI, this being a characteristic that we were looking for, studies such as (Silva *et al.*, 2014) mentioned while augmenting the PCL concentration on the process of nanoprecipitation from 0.1 to 0.100, its mean diameter were higher than 300 nm while its PDI rises slightly.

Chemical

When we obtained higher Antioxidant activity at the supernatant, we thought that got a low encapsulation efficiency, when the α -tocopherol concentration were analyzed by HPLC we could conclude that the amount of α -tocopherol within the nanocapsules were lower than 35 %,

α -Tocopherol concentration

Physical

When comparing the effect on the sizes or the PDI of the nanocapsules, we conclude that its diameter its highly affected, this as (ref),

Solvent Concentration

Physical

When comparing the diameter and the PDI within the different methods of synthesis of NCs, it was showed the solvent have a high impact on the diameter of the produced NCs, where we could observed that the NCs made with Acetone:Methanol at a ratio 1:1 were the smaller ones, this could be due for the (ref)

Chemical

When comparing the antioxidant activity of the supernatant and the pellet of the nanocapsules, synthesized with only acetone vs. different solvent concentration, it was shown a significant difference, where the only acetone NCs showed higher activity in their supernatant, than in the pellets, compared to the different solvent nanocapsules, the activity was higher in the precipitate, this led us to conclude that using this variation the encapsulation efficiency was higher using these variations, to assure this assumption, the HPLC analysis showed an encapsulation efficiency of 90 %.

Protection against UV exposure

One of the major problems while using α -tocopherol is the instability of the molecule in the presence of light (ref) this led us to try the experimental stability times, where after the NCs were exposed, the content of α -tocopherol was analyzed, and we could conclude that there was no difference with the control which was not exposed to UV light, led us to conclude that the PCL coating is functional for the α -tocopherol, but, when its antioxidant activity was analyzed, it showed that after 20 minutes, it reduced 10 %.

CONCLUSIONS

For this work, we can generate one conclusion of every phase: Hydrogels and Nanocapsules.

On the part of the hydrogels; more than 500 mg of Gelatin is needed to obtain a pseudoplastic behavior, while 1 gram of Alginate is needed to obtain it. Hydrogels with a higher concentration of Gelatin absorb more than 40% of water, but, under controlled conditions such as: temperature (37 ° C) and constant agitation (100 rpm), they absorb 12% less than those of Alginate, making them less resistant under controlled conditions.

All hydrogels, regardless of the cross-linking method (Thermal or Photo) or their polymer proportions, shown a pseudoplastic behavior, a gain of water weight (swelling) of more than 100% of its initial weight, completely solubilized after 24 hours in aqueous media, pH ranged between 5.3 and 5.5 and there was no significant difference in water vapor permeability.

Where they presented a difference, it was in their consistency index, where it is shown that the hydrogels that were Photo crosslinked were more resistant (+ 90%) than the thermals. While the porosity of the photo crosslinked hydrogels decreased more than 40%. Finally, to the wettability of the surface of the hydrogels, we can see that the angle increases more than 10% in all photo-cross-linked hydrogels making the surface more hydrophobic.

On the part of the nanocapsules; by reducing the PCL concentration, the diameter of the NCs decreased more than 20 %, while their PDI did not shown a significant difference, by reducing the concentration of α -tocopherol, the diameter of the nanocapsules decrease more than 15 %, while its PDI did not shown a significant difference. When the solvent ratios changed from Acetone to Acetone:Methanol (1:1) the diameter decreased more than 25 %, while its PDI did not show a significant difference.

When analyzing the antioxidant activity of the NCs that were synthesized with only Acetone, more activity was observed in the supernatant, than those that were synthesized using Acetone:Methanol (1:1), where more activity was presented in the precipitate of the nanocapsules.

The encapsulation efficiency of the NCs that were synthesized only with acetone, when compared with those that were synthesized with Acetone:Methanol (1:1) can be seen that the efficiency increase more than 90 %. When measuring the encapsulation efficiency by DPPH, it was observed that an efficiency similar to that obtained by HPLC was obtained.

When analyzing the stability of the α -tocopherol inside the PCL nanocapsules, it was observed that no significant difference existed by HPLC, but when its antioxidant activity was analyzed, after more than 20 minutes of UV exposure, it decreases more than 10 %.

As a general conclusion (and partly a perspective), these biomaterials can be considered for their near future as a complex system for a potential use in wound healing.

PERSPECTIVES

For this work it is recommended to perform mechanical tests on hydrogels, such as Young's Modulus (break point), oscillatory tests by rheology and a contact angle for a set period of time (more than 8 hours).

For nanocapsules, a morphological characterization by SEM is recommended, to perform confirmatory tests of functional groups such as FT-IR, and a shelf life test of them, both their antioxidant activity and their encapsulation efficiency.

As prospects for the potential use of these biomaterials as a system, it is suggested to perform biological tests such as cytotoxicity, cell proliferation and hemolytic tests. Re-perform a complete physicochemical characterization of the system and perform nanocapsules release tests of the hydrogel.

BIBLIOGRAPHY

1. Ahmed, E. M. (2015). Hydrogel: Preparation, characterization, and applications: A review. *Journal of advanced research*, 6(2), 105-121. DOI: 10.1016/j.jare.2013.07.006.
2. Bajpai, A. K., Shukla, S. K., Bhanu, S., & Kankane, S. (2008). Responsive polymers in controlled drug delivery. *Progress in Polymer Science*, 33(11), 1088-1118.
3. Baker, J. P., Blanch, H. W., & Prausnitz, J. M. (1995). Swelling properties of acrylamide-based ampholytic hydrogels: comparison of experiment with theory. *Polymer*, 36(5), 1061-1069.
4. Baker, J. P., Stephens, D. R., Blanch, H. W., & Prausnitz, J. M. (1992). Swelling equilibria for acrylamide-based polyampholyte hydrogels. *Macromolecules*, 25(7), 1955-1958.
5. Barbucci, R., & Pasqui, D. (2013). Hydrogels: Characteristics and properties. *Scaffolds for Tissue Engineering: Biological Design, Materials and Fabrication*.
6. Barwal, I., Sood, A., Sharma, M., Singh, B., & Yadav, S. C. (2013). Development of stevioside Pluronic-F-68 copolymer based PLA-nanoparticles as an antidiabetic nanomedicine. *Colloids and Surfaces B: Biointerfaces*, 101, 510-516.
7. Bazylińska, U., Lewińska, A., Lamch, Ł., & Wilk, K. A. (2014). Polymeric nanocapsules and nanospheres for encapsulation and long sustained release of hydrophobic cyanine-type photosensitizer. *Colloids and Surfaces A: Physicochemical and Engineering Aspects*, 442, 42-49.
8. Bender, D. A. (2003). *Nutritional biochemistry of the vitamins*. Cambridge university press.
9. Bennett, G., Dealey, C., & Posnett, J. (2004). The cost of pressure ulcers in the UK. *Age and ageing*, 33(3), 230-235.

10. Berger, J., Reist, M., Mayer, J. M., Felt, O., Peppas, N. A., & Gurny, R. (2004). Structure and interactions in covalently and ionically crosslinked chitosan hydrogels for biomedical applications. *European journal of pharmaceutics and biopharmaceutics*, 57(1), 19-34.
11. Boer, M., Duchnik, E., Maleszka, R., & Marchlewicz, M. (2016). Structural and biophysical characteristics of human skin in maintaining proper epidermal barrier function. *Advances in Dermatology and Allergology/Postępy Dermatologii i Alergologii*, 33(1), 1.
12. Bouhadir, K. H., Lee, K. Y., Alsberg, E., Damm, K. L., Anderson, K. W., & Mooney, D. J. (2001). Degradation of partially oxidized alginate and its potential application for tissue engineering. *Biotechnology progress*, 17(5), 945-950. DOI: 10.1021/bp010070p.
13. Braccini, I., & Pérez, S. (2001). Molecular basis of Ca²⁺-induced gelation in alginates and pectins: the egg-box model revisited. *Biomacromolecules*, 2(4), 1089-1096.
14. Brookfield Engineering Labs. (2017). *More Solutions to Sticky Problems: A Guide to Getting More From Your Brookfield Viscometer*.
15. C.G.Williams, A.N. Malik, T.K. Kim, P.N. Manson, J.H. Elisseff, Variable cytocompatibility of six cell lines with photoinitiators used for polymerizing hydrogels and cell encapsulation, *Biomaterials* 26 (2005) 1211–1218.
16. Cañón Abuchar, Hilda María; Adarve Balcazar, Marcela; Castaño Duque, Ana Victoria. (2005). *Prevención de las úlceras por presión en personas adultas hospitalizadas. Guías ACOFAEN. Biblioteca Las casas*.
17. Caroch, M., & Ferreira, I. C. (2013). A review on antioxidants, prooxidants and related controversy: natural and synthetic compounds, screening and analysis methodologies and future perspectives. *Food and chemical toxicology*, 51, 15-25.
18. Cascone, M. G., Maltinti, S., Barbani, N., & Laus, M. (1999). Effect of chitosan and dextran on the properties of poly (vinyl alcohol) hydrogels. *Journal of Materials science: Materials in medicine*, 10(7), 431-435.
19. Chai, Q., Jiao, Y., & Yu, X. (2017). Hydrogels for biomedical applications: their characteristics and the mechanisms behind them. *Gels*, 3(1), 6.

20. Chambi, H. N. M., & Grosso, C. R. F. (2011). Mechanical and water vapor permeability properties of biodegradable films based on methylcellulose, glucomannan, pectin and gelatin. *Food Science and Technology*, 31(3), 739-746.
21. Chau, T. T., Bruckard, W. J., Koh, P. T. L., & Nguyen, A. V. (2009). A review of factors that affect contact angle and implications for flotation practice. *Advances in colloid and interface science*, 150(2), 106-115.
22. Cherizol, R., Sain, M., & Tjong, J. (2015). Review of non-Newtonian mathematical models for rheological characteristics of viscoelastic composites. *Green and Sustainable Chemistry*, 5(01), 6.
23. Choi, S. W., Kim, W. S., & Kim, J. H. (2003). Surface modification of functional nanoparticles for controlled drug delivery. *Journal of dispersion science and technology*, 24(3-4), 475-487.
24. Clarke, S. (2013). Development of hierarchical magnetic nanocomposite materials for biomedical applications (Doctoral dissertation, Dublin City University).
25. Coimbra, P., Fernandes, D., Ferreira, P., Gil, M. H., & de Sousa, H. C. (2008). Solubility of Irgacure® 2959 photoinitiator in supercritical carbon dioxide: Experimental determination and correlation. *The Journal of Supercritical Fluids*, 45(3), 272-281.
26. Colinet, I., Dulong, V., Mocanu, G., Picton, L., & Le Cerf, D. (2009). New amphiphilic and pH-sensitive hydrogel for controlled release of a model poorly water-soluble drug. *European Journal of Pharmaceutics and Biopharmaceutics*, 73(3), 345-350. DOI: 10.1016/j.ejpb.2009.07.008.
27. Coronado, M., Vega y León, S., Gutiérrez, R., Vázquez, M., & Radilla, C. (2015). Antioxidantes: perspectiva actual para la salud humana. *Revista chilena de nutrición*, 42(2), 206-212. DOI: 10.4067/S0717-75182015000200014.
28. Currie, H. A., Patwardhan, S. V., Perry, C. C., Roach, P., & Shirtcliffe, N. J. (2007). Natural and artificial hybrid biomaterials. *Hybrid materials—synthesis, characterization and applications*. Wiley, Weinheim, 138.
29. Dadwal, M., Solan, D., & Pradesh, H. (2014). Polymeric nanoparticles as promising novel carriers for drug delivery: An overview. *Journal of Advanced Pharmacy Education & Research* Jan-Mar, 4(1).

30. das Neves, J., Amiji, M., Bahia, M. F., & Sarmiento, B. (2013). Assessing the physical–chemical properties and stability of dapivirine-loaded polymeric nanoparticles. *International journal of pharmaceutics*, 456(2), 307-314.
31. Datt, C., & Elfring, G. J. (2018). Dynamics and rheology of particles in shear-thinning fluids. *Journal of Non-Newtonian Fluid Mechanics*, 262, 107-114.
32. de Miguel, L., Noiray, M., Surpateanu, G., Iorga, B. I., & Ponchel, G. (2014). Poly (γ -benzyl-L-glutamate)-PEG-alendronate multivalent nanoparticles for bone targeting. *International journal of pharmaceutics*, 460(1-2), 73-82.
33. Djagny, K. B., Wang, Z., & Xu, S. (2001). Gelatin: a valuable protein for food and pharmaceutical industries. *Critical reviews in food science and nutrition*, 41(6), 481-492. DOI: 10.1080/20014091091904.
34. Dorkoosh, F. A., Verhoef, J. C., Borchard, G., Rafiee-Tehrani, M., Verheijden, J. H. M., & Junginger, H. E. (2002). Intestinal absorption of human insulin in pigs using delivery systems based on superporous hydrogel polymers. *International journal of pharmaceutics*, 247(1-2), 47-55.
35. Drexler, K. E., Peterson, C., & Pergamit, G. (1991). *Unbounding the future*. William Morrow, New York, 294.
36. Dutta J. Synthesis and characterization of γ -irradiated PVA/ PEG/CaCl₂ hydrogel for wound dressing. *Am J Chem* 2012;2 (2):6–11.
37. E. Novo, M. Parola, Redox mechanisms in hepatic chronic wound healing and fibrogenesis, *Fibrogenesis Tissue Repair* 1 (2008).
38. Elbert, D. L., & Hubbell, J. A. (2001). Conjugate addition reactions combined with free-radical cross-linking for the design of materials for tissue engineering. *Biomacromolecules*, 2(2), 430-441.
39. Evans, H. M., & Bishop, K. S. (1922). On the existence of a hitherto unrecognized dietary factor essential for reproduction. *Science*, 56(1458), 650-651. DOI: 10.1126/science.56.1458.650.
40. Fahmy, A., Kamoun, E. A., El-Eisawy, R., El-Fakharany, E. M., Taha, T. H., El-Damhougy, B. K., & Abdelhai, F. (2015). Poly (vinyl alcohol)-hyaluronic acid membranes for wound dressing applications: synthesis and in vitro bio-evaluations. *Journal of the Brazilian Chemical Society*, 26(7), 1466-1474.

41. Fairbanks, B. D., Schwartz, M. P., Bowman, C. N., & Anseth, K. S. (2009). Photoinitiated polymerization of PEG-diacrylate with lithium phenyl-2, 4, 6-trimethylbenzoylphosphinate: polymerization rate and cytocompatibility. *Biomaterials*, 30(35), 6702-6707.
42. Falanga, V. (2004). Preparación del lecho de la herida. *Ciencia aplicada a la práctica. EWMA. Documento de Posicionamiento GNEAUPP*, (3), 1-11.
43. Faucheux, N., Schweiss, R., Lützow, K., Werner, C., & Groth, T. (2004). Self-assembled monolayers with different terminating groups as model substrates for cell adhesion studies. *Biomaterials*, 25(14), 2721-2730.
44. Fessi, H. P. F. D., Puisieux, F., Devissaguet, J. P., Ammoury, N., & Benita, S. (1989). Nanocapsule formation by interfacial polymer deposition following solvent displacement. *International journal of pharmaceutics*, 55(1), R1-R4. DOI: 10.1016/0378-5173(89)90281-0.
45. Feynman, R. P. (1960). There's plenty of room at the bottom. *Engineering and science*, 23(5), 22-36.
46. Fouassier, J. P., & LalevÃ, J. (2012). *Photoinitiators for Polymer Synthesis: Scope, Reactivity, and Efficiency*. John Wiley & Sons.
47. Funami, T., Fang, Y., Noda, S., Ishihara, S., Nakauma, M., Draget, K. I., ... & Phillips, G. O. (2009). Rheological properties of sodium alginate in an aqueous system during gelation in relation to supermolecular structures and Ca²⁺ binding. *Food Hydrocolloids*, 23(7), 1746-1755.
48. Gajdoš, J., Galić, K., Kurtanjek, Ž., & Ciković, N. (2000). Gas permeability and DSC characteristics of polymers used in food packaging. *Polymer Testing*, 20(1), 49-57.
49. Ganji, F., Vasheghani, F. S., & VASHEGHANI, F. E. (2010). Theoretical description of hydrogel swelling: a review.
50. Gaonkar, R. H., Ganguly, S., Dewanjee, S., Sinha, S., Gupta, A., Ganguly, S., ... & Debnath, M. C. (2017). Garcinol loaded vitamin E TPGS emulsified PLGA nanoparticles: preparation, physicochemical characterization, in vitro and in vivo studies. *Scientific reports*, 7(1), 530.

51. Gasperini, L., Maniglio, D., Motta, A., & Migliaresi, C. (2014). An electrohydrodynamic bioprinter for alginate hydrogels containing living cells. *Tissue engineering part C: Methods*, 21(2), 123-132.
52. George, K. A., Wentrup-Byrne, E., Hill, D. J., & Whittaker, A. K. (2004). Investigation into the diffusion of water into HEMA-co-MOEP hydrogels. *Biomacromolecules*, 5(4), 1194-1199.
53. Gerecht, S., Burdick, J. A., Ferreira, L. S., Townsend, S. A., Langer, R., & Vunjak-Novakovic, G. (2007). Hyaluronic acid hydrogel for controlled self-renewal and differentiation of human embryonic stem cells. *Proceedings of the National Academy of Sciences*, 104(27), 11298-11303.
54. Gonzalez, A. C. D. O., Costa, T. F., Andrade, Z. D. A., & Medrado, A. R. A. P. (2016). Wound healing-A literature review. *Anais brasileiros de dermatologia*, 91(5), 614-620. DOI: 10.1590/abd1806-4841.20164741.
55. Gulrez, S. K., Al-Assaf, S., & Phillips, G. O. (2011). Hydrogels: methods of preparation, characterisation and applications. In *Progress in molecular and environmental bioengineering-from analysis and modeling to technology applications*. InTech. DOI: 10.5772/24553.
56. Guo, S. A., & DiPietro, L. A. (2010). Factors affecting wound healing. *Journal of dental research*, 89(3), 219-229.
57. Gutierrez, J. P., Rivera-Dommarco, J., Shamah-Levy, T., Villalpando-Hernández, S., Franco, A., Cuevas-Nasu, L., ... & Hernández-Ávila, M. (2012). Encuesta nacional de salud y nutrición 2012. *Resultados Nacionales*. Cuernavaca, México: Instituto Nacional de Salud Pública, 1(1.48).
58. Haesler, E. (2014). National Pressure Ulcer Advisory Panel, European Pressure Ulcer Advisory Panel and Pan Pacific Pressure Injury Alliance. *Prevention and treatment of pressure ulcers: quick reference guide*.
59. Hobson, R. (2016). Vitamin E and wound healing: an evidence-based review. *International wound journal*, 13(3), 331-335. DOI: 10.1111/iwj.12295.
60. Hooper, S.J.; Percival, S.L.; Hill, K.E.; Thomas, D.W.; Hayes, A.J.; Williams, D.W. The visualisation and speed of kill of wound isolates on a silver alginate dressing. *Int. Wound J.* 2012, 9, 633–642.

61. Hopkins, F. G. (1912). Feeding experiments illustrating the importance of accessory factors in normal dietaries. *The Journal of Physiology*, 44(5-6), 425-460. DOI: 10.1113/jphysiol.1912.sp001524.
62. Hu, W., Wang, Z., Xiao, Y., Zhang, S., & Wang, J. (2019). Advances in crosslinking strategies of biomedical hydrogels. *Biomaterials science*, 7(3), 843-855.
63. J.B. Leach, C.E. Schmidt, Characterization of protein release from photocrosslinkable hyaluronic acid-polyethylene glycol hydrogel tissue engineering scaffolds, *Biomaterials* 26 (2005) 125–135.
64. Jagadeesh P., Dasthagiri G., Nethravani G., (2016). Review of nanocapsules. *World journal of pharmacy and pharmaceutical sciences*, 5(2), 1365-1380 PP.
65. Jørgensen, T. E., Sletmoen, M., Draget, K. I., & Stokke, B. T. (2007). Influence of oligoguluronates on alginate gelation, kinetics, and polymer organization. *Biomacromolecules*, 8(8), 2388-2397.
66. Karim, A. A., & Bhat, R. (2008). Gelatin alternatives for the food industry: recent developments, challenges and prospects. *Trends in food science & technology*, 19(12), 644-656. DOI: 10.1016/j.tifs.2008.08.001.
67. Katayama, T., Nakauma, M., Todoriki, S., Phillips, G. O., & Tada, M. (2006). Radiation-induced polymerization of gum arabic (*Acacia senegal*) in aqueous solution. *Food hydrocolloids*, 20(7), 983-989. DOI: 10.1016/j.foodhyd.2005.11.004.
68. Khalid, M. N., Agnely, F., Yagoubi, N., Grossiord, J. L., & Couarraze, G. (2002). Water state characterization, swelling behavior, thermal and mechanical properties of chitosan based networks. *European Journal of Pharmaceutical Sciences*, 15(5), 425-432.
69. Khayata, N., Abdelwahed, W., Chehna, M. F., Charcosset, C., & Fessi, H. (2012). Preparation of vitamin E loaded nanocapsules by the nanoprecipitation method: From laboratory scale to large scale using a membrane contactor. *International journal of pharmaceutics*, 423(2), 419-427. DOI: 10.1016/j.ijpharm.2011.12.016.
70. Kim, B., & Peppas, N. A. (2003). Poly (ethylene glycol)-containing hydrogels for oral protein delivery applications. *Biomedical Microdevices*, 5(4), 333-341.

71. Kim, S. W., Bae, Y. H., & Okano, T. (1992). Hydrogels: swelling, drug loading, and release. *Pharmaceutical research*, 9(3), 283-290.
72. Kolarsick, P. A., Kolarsick, M. A., & Goodwin, C. (2011). Anatomy and physiology of the skin. *Journal of the Dermatology Nurses' Association*, 3(4), 203-213.
73. Kreuter, J. (1983). Physicochemical characterization of polyacrylic nanoparticles. *International Journal of Pharmaceutics*, 14(1), 43-58.
74. Krizek, R. J., & Pepper, S. F. (2004). Slurries in geotechnical engineering. *The Twelfth Spencer J. Buchanan Lecture*.
75. Kumar, N., & Kumbhat, S. (2016). *Essentials in nanoscience and nanotechnology*.
76. Kuo, C. K., & Ma, P. X. (2001). Ionically crosslinked alginate hydrogels as scaffolds for tissue engineering: Part 1. Structure, gelation rate and mechanical properties. *Biomaterials*, 22(6), 511-521.
77. Kwee, B. J., & Mooney, D. J. (2017). Biomaterials for skeletal muscle tissue engineering. *Current opinion in biotechnology*, 47, 16-22.
78. Labet, M., & Thielemans, W. (2009). Synthesis of polycaprolactone: a review. *Chemical Society Reviews*, 38(12), 3484-3504. DOI: 10.1039/B820162P.
79. Lafuma, A., & Quéré, D. (2003). Superhydrophobic states. *Nature materials*, 2(7), 457.
80. Larson, R. G. (2013). *Constitutive equations for polymer melts and solutions: Butterworths series in chemical engineering*. Butterworth-Heinemann.
81. Lassalle, V., & Ferreira, M. L. (2007). PLA nano-and microparticles for drug delivery: an overview of the methods of preparation. *Macromolecular bioscience*, 7(6), 767-783.
82. Lee, D. S., Yam, K. L., & Piergiovanni, L. (2008). *Food packaging science and technology*. CRC press.
83. Li, G., Wu, L., Li, F., Xu, P., Zhang, D., & Li, H. (2013). Photoelectrocatalytic degradation of organic pollutants via a CdS quantum dots enhanced TiO₂ nanotube array electrode under visible light irradiation. *nanoscale*, 5(5), 2118-2125. DOI: 10.1039/C3NR34253K.

84. Li, S., Xia, Y., Qiu, Y., Chen, X., & Shi, S. (2018). Preparation and property of starch nanoparticles reinforced aldehyde–hydrazide covalently crosslinked PNIPAM hydrogels. *Journal of Applied Polymer Science*, 135(5), 45761.
85. Li, X., Wang, S. Q., & Wang, X. (2009). Nonlinearity in large amplitude oscillatory shear (LAOS) of different viscoelastic materials. *Journal of Rheology*, 53(5), 1255-1274.
86. Li, X.; Chen, S.; Zhang, B.; Li, M.; Diao, K.; Zhang, Z.; Li, J.; Xu, Y.; Wang, X.; Chen, H. In situ injectable nano-composite hydrogel composed of curcumin, N,O-carboxymethyl chitosan and oxidized alginate for wound healing application. *Int. J. Pharm.* 2012, 437, 110–119
87. Lin, C. C., & Metters, A. T. (2006). Hydrogels in controlled release formulations: network design and mathematical modeling. *Advanced drug delivery reviews*, 58(12-13), 1379-1408.
88. M. Schäfer, S. Werner, Oxidative stress in normal and impaired wound repair, *Pharm. Res.* 58 (2008) 165–171.
89. Magenheim, B., Levy, M. Y., & Benita, S. (1993). A new in vitro technique for the evaluation of drug release profile from colloidal carriers-ultrafiltration technique at low pressure. *International journal of pharmaceutics*, 94(1-3), 115-123.
90. Maherani, B., & Wattraint, O. (2017). Liposomal structure: A comparative study on light scattering and chromatography techniques. *Journal of Dispersion Science and Technology*, 38(11), 1633-1639.
91. Manbeck, A. E., Aldrich, C. G., Alavi, S., Zhou, T., & Donadelli, R. A. (2017). The effect of gelatin inclusion in high protein extruded pet food on kibble physical properties. *Animal Feed Science and Technology*, 232, 91-101. DOI: 10.1016/j.anifeedsci.2017.08.010.
92. Mariod, A. A., & Fadul, H. (2013). gelatin, source, extraction and industrial applications. *Acta Scientiarum Polonorum Technologia Alimentaria*, 12(2), 135-147.
93. Mark, J. E. (1999). *Polymer Data Handbook*: Oxford University Press. New York.

94. Maynard, T., & Baxter, D. (2007). *Nanotechnology: Recent Development, Risks and Opportunities*.
95. Mazzarino, L., Travelet, C., Ortega-Murillo, S., Otsuka, I., Pignot-Paintrand, I., Lemos-Senna, E., & Borsali, R. (2012). Elaboration of chitosan-coated nanoparticles loaded with curcumin for mucoadhesive applications. *Journal of colloid and interface science*, 370(1), 58-66.
96. Mejía, E. S., Mendoza, A. J., Gálvez, L. R., & Aguilar, A. A. (2015). Úlceras por presión en diversos servicios de un hospital de segundo nivel de atención. *Enfermería Universitaria*, 12(4), 173-181. DOI: 10.1016/j.reu.2015.08.004.
97. Menzies, K. L., & Jones, L. (2010). The impact of contact angle on the biocompatibility of biomaterials. *Optometry and Vision Science*, 87(6), 387-399.
98. Meyers, M. A., Chen, P. Y., Lin, A. Y. M., & Seki, Y. (2008). Biological materials: structure and mechanical properties. *Progress in Materials Science*, 53(1), 1-206.
99. Mi, F. L., Wu, Y. B., Shyu, S. S., Schoung, J. Y., Huang, Y. B., Tsai, Y. H., & Hao, J. Y. (2002). Control of wound infections using a bilayer chitosan wound dressing with sustainable antibiotic delivery. *Journal of Biomedical Materials Research: An Official Journal of The Society for Biomaterials, The Japanese Society for Biomaterials, and The Australian Society for Biomaterials and the Korean Society for Biomaterials*, 59(3), 438-449.
100. Miladi, K., Sfar, S., Fessi, H., & Elaissari, A. (2016). Nanoprecipitation process: from particle preparation to in vivo applications. In *Polymer Nanoparticles for Nanomedicines* (pp. 17-53). Springer, Cham.
101. Mironova, M. M., & Kovaleva, E. L. (2017). Comparative Analysis of Quality Assessment Requirements for Gelatin Used in Drug Production. *Pharmaceutical Chemistry Journal*, 50(12), 820-825. DOI: 10.1007/s11094-017-1540-4.
102. Mohanty, A. K., Misra, M., & Drzal, L. T. (2005). *Natural fibers, biopolymers, and biocomposites*. CRC press.
103. Monsonís, B. (2013). *Abordaje en las heridas de difícil cicatrización* (Doctoral dissertation). Universitat de Lleida, España.

104. Mora-Huertas, C. E., Fessi, H., & Elaissari, A. (2010). Polymer-based nanocapsules for drug delivery. *International journal of pharmaceutics*, 385(1-2), 113-142.
105. Moseley, R., Hilton, J. R., Waddington, R. J., Harding, K. G., Stephens, P., & Thomas, D. W. (2004). Comparison of oxidative stress biomarker profiles between acute and chronic wound environments. *Wound repair and regeneration*, 12(4), 419-429.
106. Mu, L., & Feng, S. S. (2002). Vitamin E TPGS used as emulsifier in the solvent evaporation/extraction technique for fabrication of polymeric nanospheres for controlled release of paclitaxel (Taxol®). *Journal of Controlled Release*, 80(1-3), 129-144.
107. Muid, S., Ali, A. M., Yusoff, K., & Nawawi, H. (2013). Optimal antioxidant activity with moderate concentrations of Tocotrienol rich fraction (TRF) in in vitro assays. *International Food Research Journal*, 20(2). DOI: 10.1007/s11274-015-1903-5.
108. Nafee, N., Youssef, A., El-Gowell, H., Asem, H., & Kandil, S. (2013). Antibiotic-free nanotherapeutics: hypericin nanoparticles thereof for improved in vitro and in vivo antimicrobial photodynamic therapy and wound healing. *International journal of pharmaceutics*, 454(1), 249-258.
109. Nagasawa, N., Yagi, T., Kume, T., & Yoshii, F. (2004). Radiation crosslinking of carboxymethyl starch. *Carbohydrate Polymers*, 58(2), 109-113. DOI: 10.1016/j.carbpol.2004.04.021.
110. Ng, T. S., McKinley, G. H., & Ewoldt, R. H. (2011). Large amplitude oscillatory shear flow of gluten dough: A model power-law gel. *Journal of Rheology*, 55(3), 627-654.
111. Nguyen, K. T., & West, J. L. (2002). Photopolymerizable hydrogels for tissue engineering applications. *Biomaterials*, 23(22), 4307-4314.
112. Nho, Y. C., Park, J. S., & Lim, Y. M. (2014). Preparation of poly (acrylic acid) hydrogel by radiation crosslinking and its application for mucoadhesives. *Polymers*, 6(3), 890-898. DOI: 10.3390/polym6030890.

113. Niekraszewicz, B., & Niekraszewicz, A. (2009). The structure of alginate, chitin and chitosan fibres. In *Handbook of Textile Fibre Structure* (pp. 266-304). Woodhead Publishing.
114. Noronha, C. M., Granada, A. F., de Carvalho, S. M., Lino, R. C., de OB Maciel, M. V., & Barreto, P. L. M. (2013). Optimization of α -tocopherol loaded nanocapsules by the nanoprecipitation method. *Industrial Crops and Products*, 50, 896-903.
115. Nyanhongo, G. S., Sygmund, C., Ludwig, R., Prasetyo, E. N., & Guebitz, G. M. (2013). An antioxidant regenerating system for continuous quenching of free radicals in chronic wounds. *European journal of pharmaceutics and biopharmaceutics*, 83(3), 396-404.
116. Ogawa, Y., Ogawa, K., & Kokufuta, E. (2004). Swelling– shrinking behavior of a polyampholyte gel composed of positively charged networks with immobilized polyanions. *Langmuir*, 20(7), 2546-2552.
117. Pal, S. L., Jana, U., Manna, P. K., Mohanta, G. P., & Manavalan, R. (2011). Nanoparticle: An overview of preparation and characterization. *Journal of applied pharmaceutical science*, 1(6), 228-234.
118. Pavot, V., Rochereau, N., Primard, C., Genin, C., Perouzel, E., Lioux, T., ... & Verrier, B. (2013). Encapsulation of Nod1 and Nod2 receptor ligands into poly (lactic acid) nanoparticles potentiates their immune properties. *Journal of controlled release*, 167(1), 60-67.
119. Peppas, N. A., Bures, P., Leobandung, W., & Ichikawa, H. (2000). Hydrogels in pharmaceutical formulations. *European journal of pharmaceutics and biopharmaceutics*, 50(1), 27-46. DOI: 10.1016/S0939-6411(00)00090-4.
120. Pérez-García, L. J. (2004). Metaloproteinasas y piel. *Actas Dermo-Sifiliográficas*, 95(7), 413-423. DOI: 10.1016/S0001-7310(04)76850-7.
121. Pevere, A., Guibaud, G., Van Hullebusch, E., Lens, P., & Baudu, M. (2006). Viscosity evolution of anaerobic granular sludge. *Biochemical Engineering Journal*, 27(3), 315-322.

122. Pohlmann, A. R., Fonseca, F. N., Paese, K., Detoni, C. B., Coradini, K., Beck, R. C., & Guterres, S. S. (2013). Poly (ϵ -caprolactone) microcapsules and nanocapsules in drug delivery. *Expert opinion on drug delivery*, 10(5), 623-638.
123. Quintanar-Guerrero, D., Allémann, E., Fessi, H., & Doelker, E. (1998). Preparation techniques and mechanisms of formation of biodegradable nanoparticles from preformed polymers. *Drug development and industrial pharmacy*, 24(12), 1113-1128.
124. Raffaini, G., & Ganazzoli, F. (2007). Understanding the performance of biomaterials through molecular modeling: crossing the bridge between their intrinsic properties and the surface adsorption of proteins. *Macromolecular bioscience*, 7(5), 552-566.
125. Remminghorst, U., & Rehm, B. H. (2006). Bacterial alginates: from biosynthesis to applications. *Biotechnology letters*, 28(21), 1701-1712. DOI: 10.1007/s10529-006-9156-x.
126. Rigotti, A. (2007). Absorption, transport, and tissue delivery of vitamin E. *Molecular aspects of medicine*, 28(5), 423-436. DOI: 10.1016/j.mam.2007.01.002.
127. Rizwan, M., Yahya, R., Hassan, A., Yar, M., Azzahari, A. D., Selvanathan, V., ... & Abouloula, C. N. (2017). pH sensitive hydrogels in drug delivery: Brief history, properties, swelling, and release mechanism, material selection and applications. *Polymers*, 9(4), 137.
128. Roxana Sava, O., Florin Sava, D., Radulescu, M., Georgiana Albu, M., Ficai, D., Fernanda Veloz-Castillo, M., ... & Ficai, A. (2017). Trends in Materials Science for Ligament Reconstruction. *Current stem cell research & therapy*, 12(2), 145-154.
129. Saarai, A., Sedlacek, T., Kasparikova, V., Kitano, T., & Saha, P. (2012). On the characterization of sodium alginate/gelatine-based hydrogels for wound dressing. *Journal of Applied Polymer Science*, 126(S1). DOI: 10.1002/app.36590.
130. Saarai, A., Sedlacek, T., Kasparikova, V., Kitano, T., & Saha, P. (2012). On the characterization of sodium alginate/gelatine-based hydrogels for wound dressing. *Journal of Applied Polymer Science*, 126(S1). DOI: 10.1002/app.36590.

131. Saladin, K. S., Sullivan, S. J., & Gan, C. A. (2015). *Anatomy & physiology: The unity of form and function*.
132. San-Miguel, A., & Martin-Gil, F. J. (2009). Importancia de las especies reactivas al oxígeno (radicales libres) y los antioxidantes en clínica. *Gaceta Médica de Bilbao*, 106(3), 106-113. DOI: 10.1016/S0304-4858(09)74661-X.
133. Sen, C. K., Gordillo, G. M., Roy, S., Kirsner, R., Lambert, L., Hunt, T. K., ... & Longaker, M. T. (2009). Human skin wounds: a major and snowballing threat to public health and the economy. *Wound repair and regeneration*, 17(6), 763-771.
134. Sewell-Loftin, M. K., Chun, Y. W., Khademhosseini, A., & Merryman, W. D. (2011). EMT-inducing biomaterials for heart valve engineering: taking cues from developmental biology. *Journal of cardiovascular translational research*, 4(5), 658.
135. Seyssiecq, I., Ferrasse, J. H., & Roche, N. (2003). State-of-the-art: rheological characterisation of wastewater treatment sludge. *Biochemical Engineering Journal*, 16(1), 41-56.
136. Shah, U., Joshi, G., & Sawant, K. (2014). Improvement in antihypertensive and antianginal effects of felodipine by enhanced absorption from PLGA nanoparticles optimized by factorial design. *Materials Science and Engineering: C*, 35, 153-163.
137. Shih, W. Y., & Shih, W. H. (2005). *Nanosensors for Environmental Applications. Nanotechnologies for the Life Sciences*. DOI: 10.1002/9783527610419.ntls0058.
138. Silva, M. F., Ciciliatti, M. A., Hechenleitner, A. A. W., Peñalva, R., Agüeros, M., Irache, J. M., ... & Pineda, E. A. (2014). Superparamagnetic maghemite loaded poly (ϵ -caprolactone) nanocapsules: characterization and synthesis optimization. *Matéria (Rio de Janeiro)*, 19(1), 40-52.
139. Singh, B., Varshney, L., & Francis, S. (2016). Designing tragacanth gum based sterile hydrogel by radiation method for use in drug delivery and wound dressing applications. *International journal of biological macromolecules*, 88, 586-602.

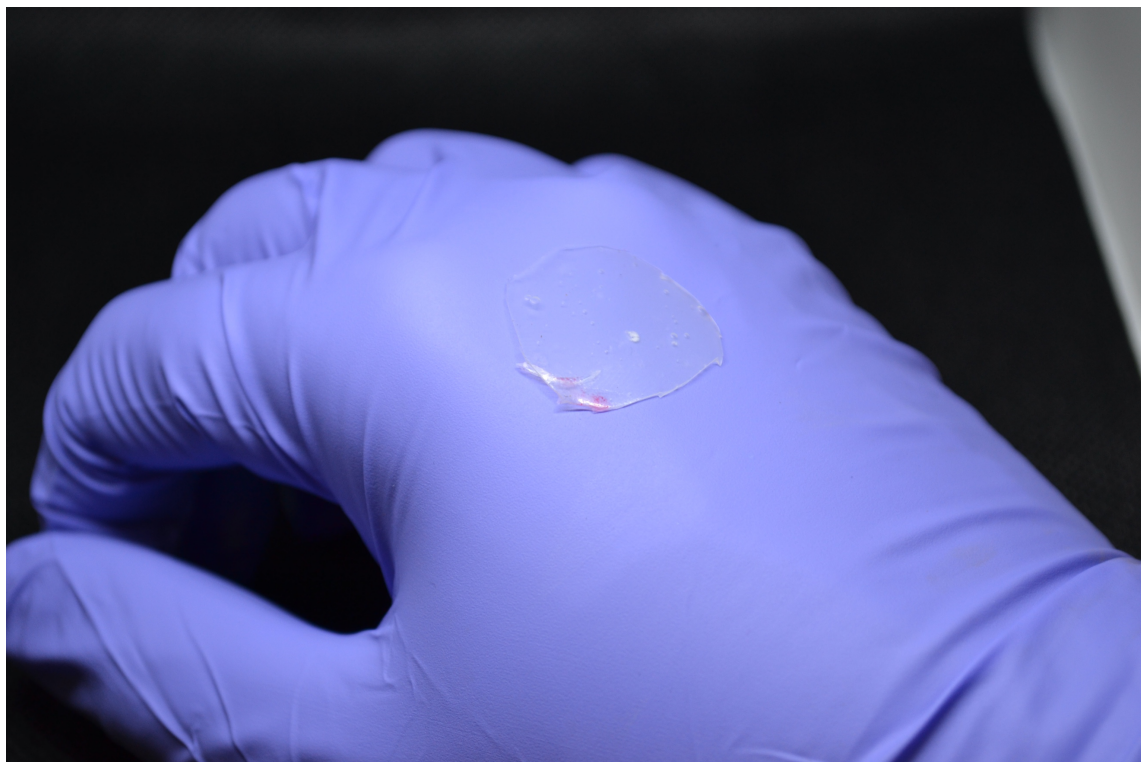
140. Singh, T. R. R., Laverty, G., & Donnelly, R. (Eds.). (2018). *Hydrogels: design, synthesis and application in drug delivery and regenerative medicine*. CRC Press.
141. Siqueira-Moura, M. P., Primo, F. L., Espreafico, E. M., & Tedesco, A. C. (2013). Development, characterization, and photocytotoxicity assessment on human melanoma of chloroaluminum phthalocyanine nanocapsules. *Materials Science and Engineering: C*, 33(3), 1744-1752.
142. Siracusa, V. (2012). Food packaging permeability behaviour: A report. *International Journal of Polymer Science*, 2012.
143. Soldevilla Agreda, J. J., Verdú, J., & Torra i Bou, J. E. (2008). Impacto social y económico de las úlceras por presión.
144. Sravanthi, R. (2009). Preparation and characterization of poly (ϵ -caprolactone) PCL scaffolds for tissue engineering applications. *Mater of Technology*, National Institute of Technology of Rourkela.
145. Suen, W. L. L., & Chau, Y. (2013). Specific uptake of folate-decorated triamcinolone-encapsulating nanoparticles by retinal pigment epithelium cells enhances and prolongs antiangiogenic activity. *Journal of controlled release*, 167(1), 21-28.
146. Szekalska, M., Puciłowska, A., Szymańska, E., Ciosek, P., & Winnicka, K. (2016). Alginate: Current Use and Future Perspectives in Pharmaceutical and Biomedical Applications. *International Journal of Polymer Science*, 2016. DOI: 10.1155/2016/7697031.
147. Talens Belén, F. (2016). Formación y prevención en úlceras por presión: prevalencia en el Hospital General de Elche. *Gerokomos*, 27(1), 33-37.
148. Thiele, J. J., Hsieh, S. N., & Ekanayake-Mudiyanselage, S. (2005). Vitamin E: critical review of its current use in cosmetic and clinical dermatology. *Dermatologic surgery*, 31(s1), 805-813. DOI: 10.1111/j.1524-4725.2005.31724.
149. Thomas, S., Ninan, N., Mohan, S., & Francis, E. (Eds.). (2012). *Natural polymers, biopolymers, biomaterials, and their composites, blends, and IPNs*. CRC press.

150. Tokiwa, Y., Calabia, B. P., Ugwu, C. U., & Aiba, S. (2009). Biodegradability of plastics. *International journal of molecular sciences*, 10(9), 3722-3742. DOI: 10.3390/ijms10093722.
151. Ulery, B. D., Nair, L. S., & Laurencin, C. T. (2011). Biomedical applications of biodegradable polymers. *Journal of polymer science Part B: polymer physics*, 49(12), 832-864. DOI: 10.1002/polb.22259.
152. Valles, E., Durando, D., Katime, I., Mendizábal, E., & Puig, J. E. (2000). Equilibrium swelling and mechanical properties of hydrogels of acrylamide and itaconic acid or its esters. *Polymer bulletin*, 44(1), 109-114.
153. van Dijk-Wolthuis, W. N. E., Franssen, O., Talsma, H., Van Steenberg, M. J., Kettenes-Van Den Bosch, J. J., & Hennink, W. E. (1995). Synthesis, characterization, and polymerization of glycidyl methacrylate derivatized dextran. *Macromolecules*, 28(18), 6317-6322.
154. Vashuk, E. V., Vorobieva, E. V., Basalyga, I. I., & Krutko, N. P. (2001). Water-absorbing properties of hydrogels based on polymeric complexes. *Material Research Innovations*, 4(5-6), 350-352.
155. Vela-Anaya G. (2013). Magnitud del Evento Adverso. Úlceras por presión. *Rev Enferm Inst Mex Seguro Soc.*;21(01): 3-8.
156. Voorhaar, L., & Hoogenboom, R. (2016). Supramolecular polymer networks: hydrogels and bulk materials. *Chemical Society Reviews*, 45(14), 4013-4031.
157. Walden, G., Liao, X., Donell, S., Raxworthy, M. J., Riley, G. P., & Saeed, A. (2017). A clinical, biological, and biomaterials perspective into tendon injuries and regeneration. *Tissue Engineering Part B: Reviews*, 23(1), 44-58.
158. Wang, W., Zhang, M., Lu, W., Zhang, X., Ma, D., Rong, X., ... & Jin, Y. (2009). Cross-linked collagen–chondroitin sulfate–hyaluronic acid imitating extracellular matrix as scaffold for dermal tissue engineering. *Tissue Engineering Part C: Methods*, 16(2), 269-279. DOI: 10.1089/ten.tec.2009.0161.

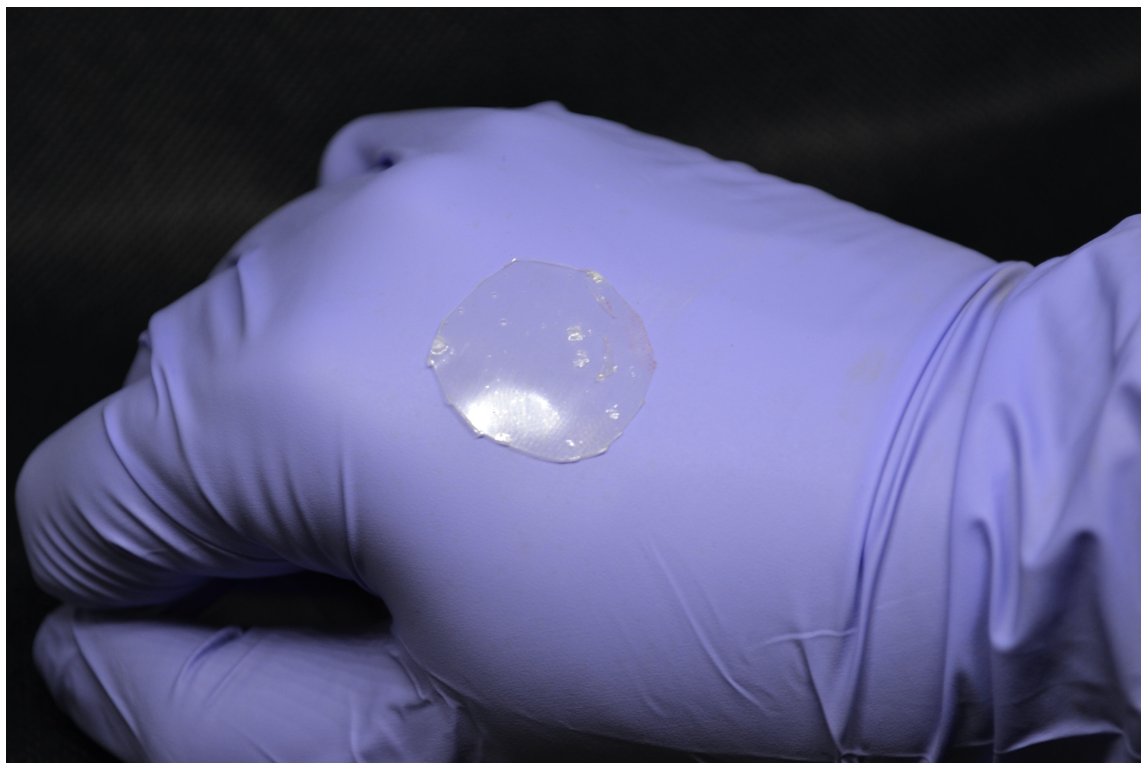
159. Whang, K., Healy, K. E., Elenz, D. R., Nam, E. K., Tsai, D. C., Thomas, C. H., ... & Sprague, S. M. (1999). Engineering bone regeneration with bioabsorbable scaffolds with novel microarchitecture. *Tissue engineering*, 5(1), 35-51.
160. Widgerow, A. D. (2011). Wound fluid intervention: influencing wound healing from the outside: chronic wounds. *Wound Healing Southern Africa*, 4(1), 12-15.
161. Williams, C. G., Malik, A. N., Kim, T. K., Manson, P. N., & Elisseeff, J. H. (2005). Variable cytocompatibility of six cell lines with photoinitiators used for polymerizing hydrogels and cell encapsulation. *Biomaterials*, 26(11), 1211-1218.
162. Winter, G. D. (1962). Formation of the scab and the rate of epithelization of superficial wounds in the skin of the young domestic pig.
163. Winter, G. D. (1963). Effect of air exposure and occlusion on experimental human skin wounds. *Nature*, 200, 378-379.
164. Xu, R., Xia, H., He, W., Li, Z., Zhao, J., Liu, B., ... & Yao, Z. (2016). Controlled water vapor transmission rate promotes wound-healing via wound re-epithelialization and contraction enhancement. *Scientific reports*, 6, 24596.
165. Yang, J. S., Xie, Y. J., & He, W. (2011). Research progress on chemical modification of alginate: A review. *Carbohydrate polymers*, 84(1), 33-39. DOI: 10.1016/j.carbpol.2010.11.048.
166. Yu, H., Xu, X., Chen, X., Hao, J., & Jing, X. (2006). Medicated wound dressings based on poly (vinyl alcohol)/poly (N-vinyl pyrrolidone)/chitosan hydrogels. *Journal of Applied Polymer Science*, 101(4), 2453-2463.
167. Yue, K., Trujillo-de Santiago, G., Alvarez, M. M., Tamayol, A., Annabi, N., & Khademhosseini, A. (2015). Synthesis, properties, and biomedical applications of gelatin methacryloyl (GelMA) hydrogels. *Biomaterials*, 73, 254-271.
168. Zhai, M., Chen, Y., Yi, M., & Ha, H. (2004). Swelling behaviour of a new kind of polyampholyte hydrogel composed of dimethylaminoethyl methacrylate and acrylic acid. *Polymer international*, 53(1), 33-36.

APPENDIX

Appendix A. Thermo crosslinked hydrogels



Appendix A.1 Photo crosslinked hydrogels



Appendix B. Effect on the swelling behavior of Thermal crosslinked Alginate or Gelatin hydrogels

Samples	Time (Hours)					
	1 H *	2 H *	4 H *	8 H *	12 H *	24 H *
G2 *	A 40 ± 16 ^b	B 123 ± 12 ^{cd}	A 140 ± 8 ^d	A 100 ± 8 ^c	A 40 ± 16 ^b	A 0 ± 0.0 ^a
G3 *	B 81 ± 9 ^b	AB 105 ± 13 ^b	B 193 ± 10 ^c	C 202 ± 2 ^c	C 179 ± 13 ^c	B 38 ± 12 ^a
A3 *	A 29 ± 4 ^b	A 81 ± 10 ^c	A 111 ± 15 ^d	B 143 ± 7 ^e	B 115 ± 4 ^d	A 0 ± 0.0 ^a

An ANOVA was performed, where * is equal to $p < 0.05$. A post-hoc (Tukey) was carried out, where the upper-case indices (left) (e.g. ^A) represent the vertical groups (between the same treatments) and the lower case-letters indices (right) (e.g. ^a), represent the horizontal groups (different treatments by hour).

Appendix C. Effect on the solubility behavior of the Alginate or Gelatin hydrogels

Hydrogels	Time (Hours)					
	1 H *	2 H *	4 H *	8 H *	12 H	24 H
G2 *	B -0.4 ± 2 ^b	B -30 ± 16 ^a	B 9 ± 11 ^b	B 36 ± 20 ^c	A 100 ± 0 ^d	100 ± 0 ^d
G3 *	A -40 ± 16 ^{bc}	AB -61 ± 26 ^{ab}	A -110 ± 16 ^a	A -62 ± 20 ^{ab}	B 32 ± 13 ^c	100 ± 0 ^d
A3 *	A -66 ± 7 ^c	A -92 ± 10 ^b	A -124 ± 4 ^a	A -82 ± 7 ^{bc}	B 100 ± 4 ^d	100 ± 0 ^d

An ANOVA was performed, where * is equal to $p < 0.05$. A post-hoc (Tukey) was carried out, where the upper-case indices (left) (e.g. ^A) represent the vertical groups (between the same treatments) and the lower case-letters indices (right) (e.g. ^a), represent the horizontal groups (different treatments by hour).

Appendix D. Effect on the swelling behavior of Thermal and Photo crosslinked hydrogels

Hydrogels	Time (Hours)					
	1 H *	2 H	4 H *	8 H	12 H *	24 H *
AG1 WoPi *	B 134 ± 17 ^b	131 ± 15 ^b	A 135 ± 5 ^b	152 ± 7 ^b	B 131 ± 15 ^b	AB 34 ± 5 ^a
AG WoPi *	C 180 ± 7 ^{cd}	179 ± 38 ^{cd}	B 187 ± 26 ^d	116 ± 9 ^{bc}	B 99 ± 1 ^{ab}	B 39 ± 14 ^a
GA1 WoPi *	A 91 ± 8 ^b	140 ± 5 ^{bc}	AB 170 ± 8 ^c	145 ± 38 ^{bc}	A 97 ± 9 ^b	AB 0 ± 9 ^a
AG1 WPi *	B 133 ± 5 ^{bc}	136 ± 14 ^{bc}	AB 145 ± 10 ^d	118 ± 4 ^{bc}	AB 109 ± 6 ^b	A 5 ± 10 ^a
AG WPi*	B 141 ± 9 ^{cd}	170 ± 12 ^{de}	AB 180 ± 24 ^e	114 ± 15 ^{bc}	A 92 ± 11 ^b	AB 22 ± 6 ^a
GA1 WPi*	B 137 ± 12 ^c	160 ± 10 ^{cd}	AB 178 ± 7 ^d	103 ± 12 ^b	A 82 ± 6 ^b	AB 16 ± 7 ^a

An ANOVA was performed, where * is equal to $p < 0.05$. A post-hoc (Tukey) was carried out, where the upper-case indices (left) (e.g. ^A) represent the vertical groups (between the same treatments) and the lower case-letters indices (right) (e.g. ^a), represent the horizontal groups (different treatments by hour).

Appendix E. Effect on the solubility behavior of Thermal and Photo crosslinked hydrogels

Time (Hours)						
Hydrogels	1 H	2 H *	4 H *	8 H *	12 H *	24 H *
AG1 WoPi *	-26 ± 3 ^c	^A -61 ± 5 ^{cd}	^A -74 ± 4 ^{ab}	^B -30 ± 6 ^a	^B 1 ± 8 ^d	^D 100 ± 0.0 ^e
AG WoPi*	-28 ± 9 ^c	^B -34 ± 4 ^{bc}	^B -61 ± 9 ^{ab}	^B -73 ± 14 ^a	^B 8 ± 5 ^d	^B 100 ± 0.0 ^e
GA1 WoPi *	-27 ± 9 ^b	^B -38 ± 8 ^a	^C -14 ± 21 ^a	^B 17 ± 23 ^b	^B 40 ± 33 ^c	^D 100 ± 0.0 ^e
AG1 WoPi *	-17 ± ^a	^B -38 ± 3 ^a	^{AB} -51 ± 4 ^{ab}	^A -83 ± 7 ^{ab}	^A -61 ± 9 ^{bc}	^C 100 ± 0.4 ^e
AG WoPi *	-28 ± 8 ^d	^B -34 ± 8 ^c	^B -48 ± 1 ^{bc}	^A -56 ± 5 ^a	^C -68 ± 10 ^b	^A 100 ± 0.0 ^e
GA1 WoPi *	-13 ± 3 ^{cd}	^B -30 ± 8 ^b	^{BC} -47 ± 4 ^a	^B -21 ± 7 ^{bc}	^D -6 ± 2 ^d	^D 100 ± 0.1 ^e

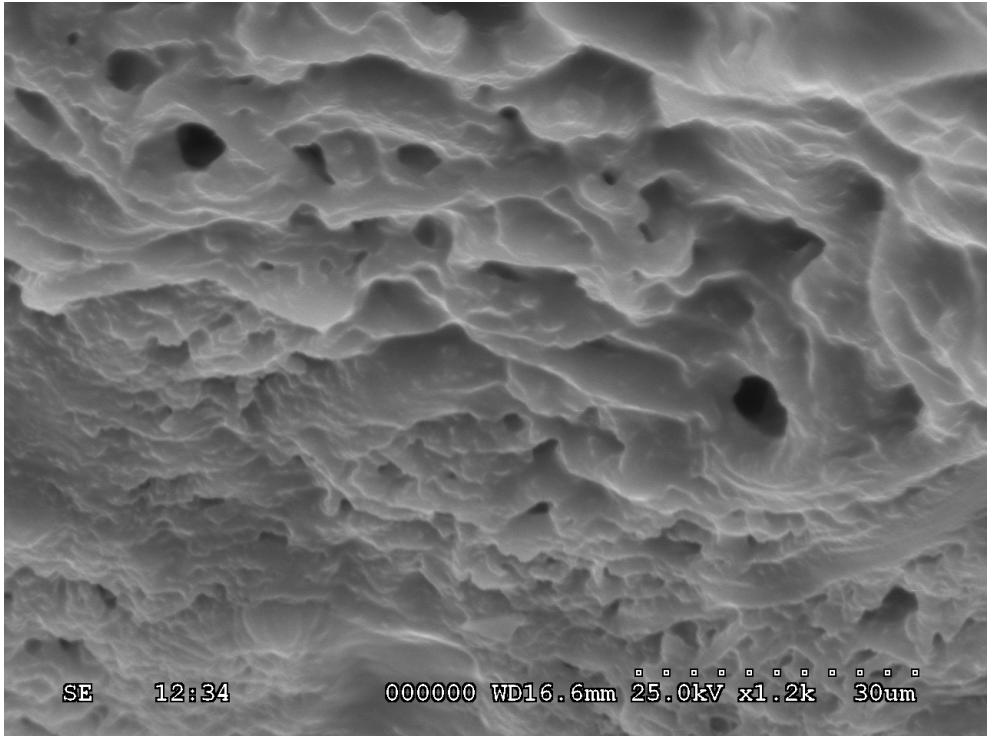
An ANOVA was performed, where * is equal to $p < 0.05$. A post-hoc (Tukey) was carried out, where the upper-case indices (left) (e.g. ^A) represent the vertical groups (between the same treatments) and the lower case-letters indices (right) (e.g. ^a), represent the horizontal groups (different treatments by hour).

Appendix F. Effect on the water vapor permeability on the Thermal and photo crosslinked hydrogels.

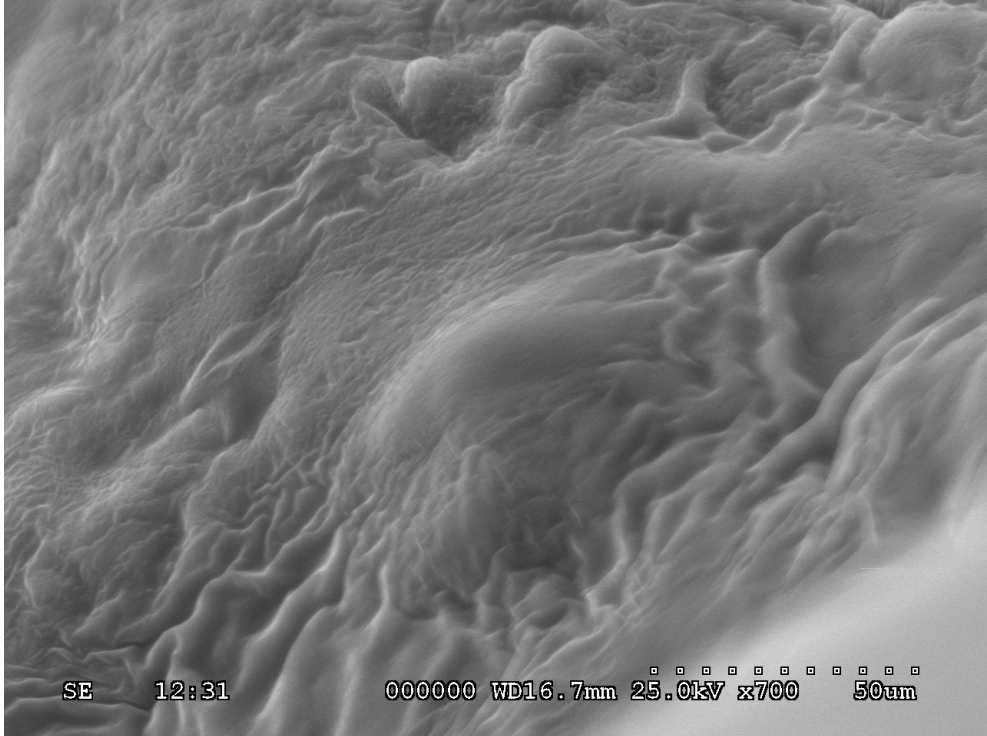
Water Vapor Permeability (gH₂O/mm²)						
Sample	1 H	2 H	4 H	8 H	12 H	24 H
AG1 WoPi *	0.28 ± 0.06 ^a	0.56 ± 0.11 ^{ab}	1.12 ± 0.23 ^{ab}	2.24 ± 0.45 ^{bc}	3.36 ± 0.68 ^c	6.72 ± 1.35 ^d
AG WoPi *	0.61 ± 0.34 ^a	1.22 ± 0.67 ^a	2.43 ± 1.35 ^a	4.04 ± 2.69 ^{ab}	7.30 ± 4.05 ^{ab}	14.59 ± 8.08 ^c
GA1 WoPi *	0.51 ± 0.24 ^a	1.01 ± 0.47 ^a	2.02 ± 0.95 ^a	4.04 ± 1.89 ^a	6.06 ± 2.84 ^{ab}	12.13 ± 5.67 ^b
AG1 WPi *	0.30 ± 0.07 ^a	0.59 ± 0.15 ^a	1.19 ± 0.30 ^a	2.38 ± 0.60 ^{ab}	3.57 ± 0.89 ^b	7.14 ± 1.79 ^c
AG WPi *	0.29 ± 0.11 ^a	0.58 ± 0.22 ^a	1.16 ± 0.43 ^a	2.32 ± 0.86 ^a	3.32 ± 0.07 ^a	6.30 ± 2.57 ^b
GA1 WPi *	0.53 ± 0.06 ^a	1.06 ± 0.17 ^a	2.12 ± 0.23 ^a	4.23 ± 0.47 ^b	6.35 ± 0.69 ^c	12.70 ± 1.39 ^d

An ANOVA was performed, where * is equal to $p < 0.05$. A post-hoc (Tukey) was carried out, where the upper-case indices (left) (e.g. ^A) represent the vertical groups (between the same treatments) and the lower case-letters indices (right) (e.g. ^a), represent the horizontal groups (different treatments by hour).

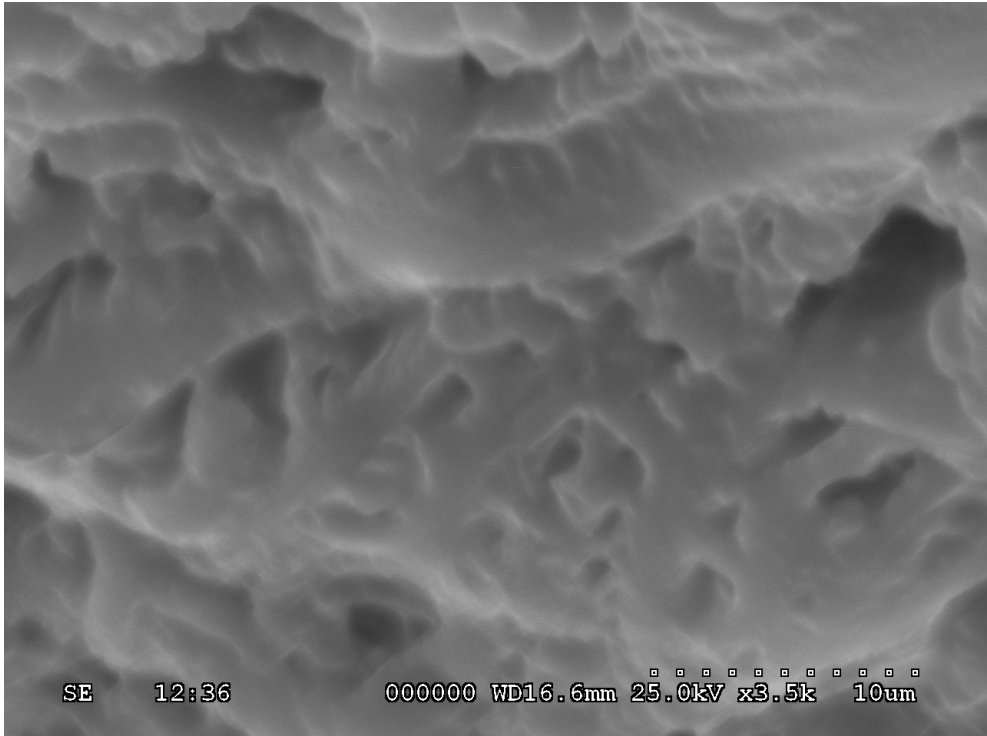
Appendix G. Microscopic analysis of AG1 Thermal crosslinked hydrogels



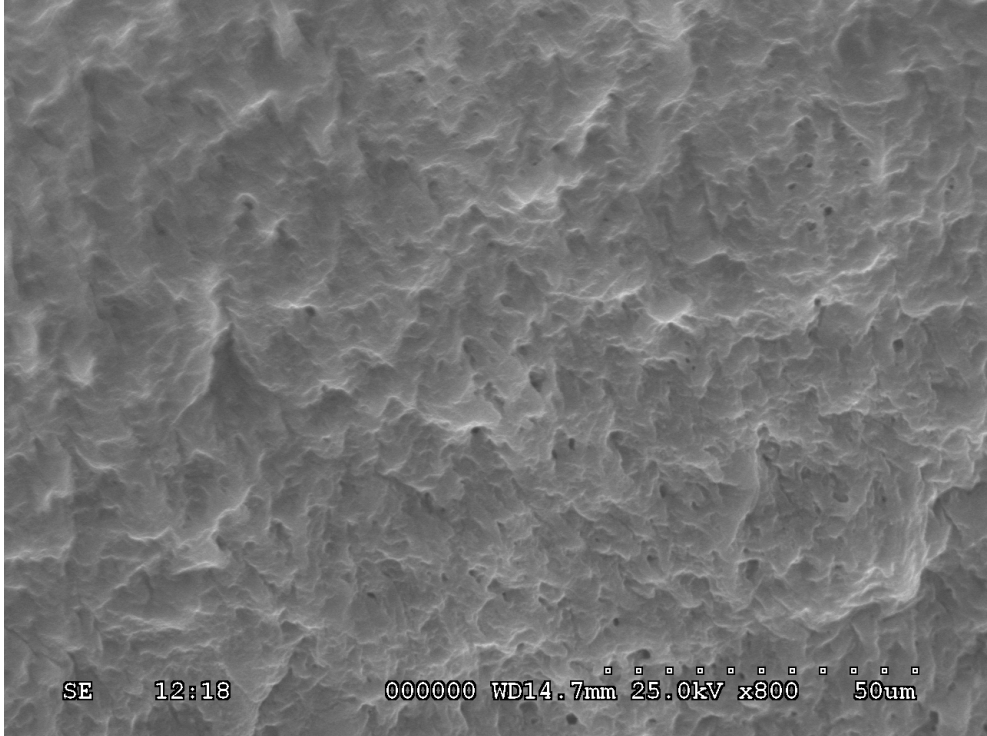
Appendix G.1 Microscopic analysis of AG1 Photo crosslinked hydrogels



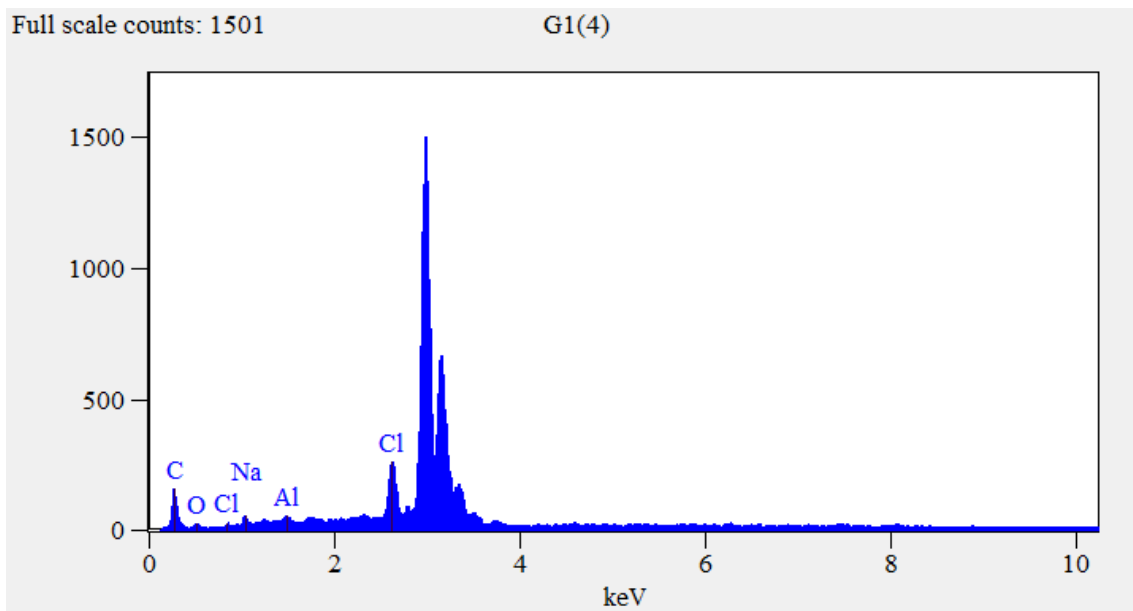
Appendix H. Microscopic analysis of GA1 Thermal crosslinked hydrogels



Appendix H.1. Microscopic analysis of GA1 Photo crosslinked hydrogels

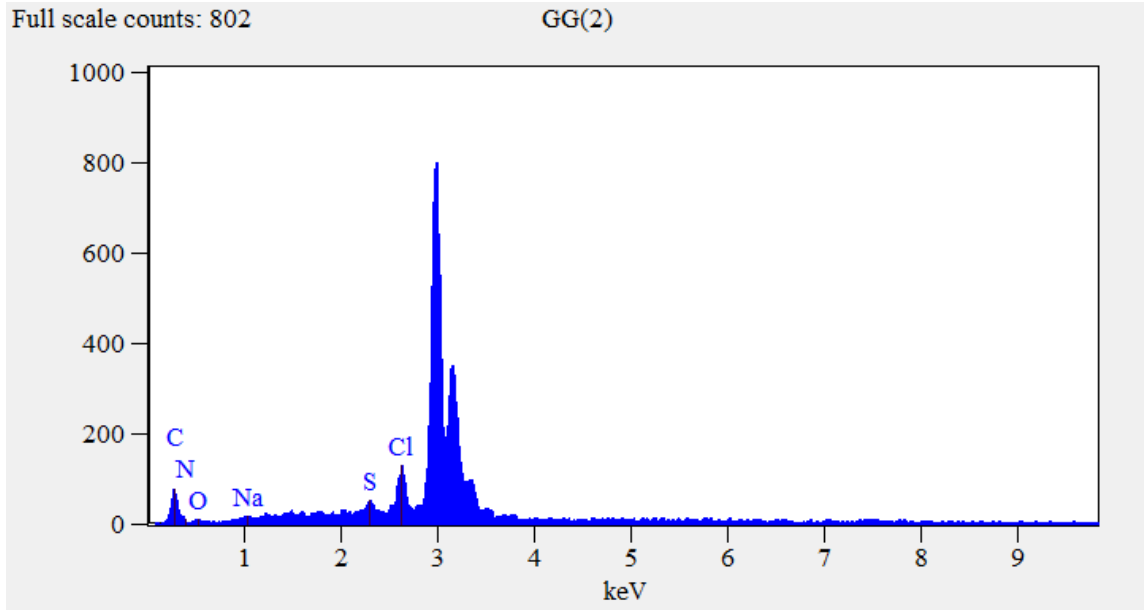


Appendix I. Elemental analysis of Thermo crosslinked hydrogels AG1



<i>Element Line</i>	<i>Net Counts</i>	<i>ZAF</i>	<i>Weight %</i>	<i>Norm. Wt.%</i>	<i>Atom %</i>
<i>C K</i>	1119	5.150	72.93	72.93	85.03
<i>O K</i>	109	11.796	7.81	7.81	6.84
<i>Na K</i>	170	2.905	1.79	1.79	1.09
<i>Al K</i>	259	1.625	1.12	1.12	0.58
<i>Cl K</i>	4108	1.157	16.35	16.35	6.46
Total			100.00	100.00	100.00

Appendix J. Elemental analysis of Photo crosslinked hydrogels GA1

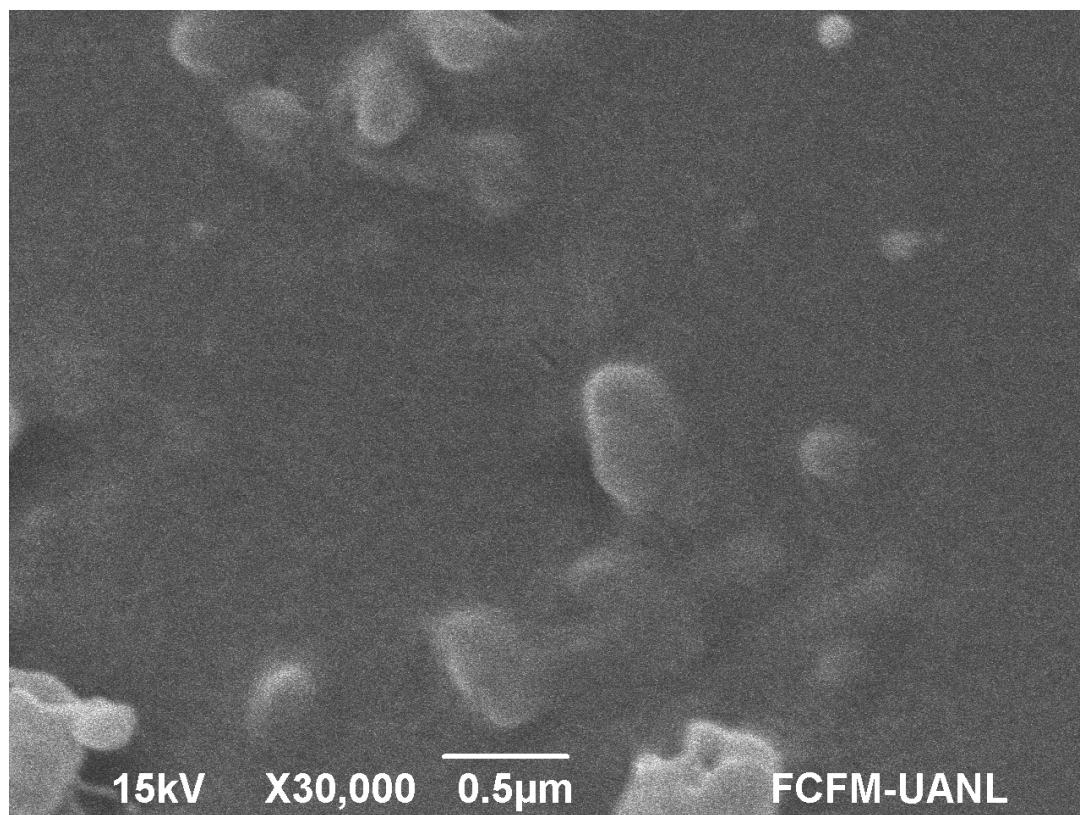


<i>Element Line</i>	<i>Net Counts</i>	<i>ZAF</i>	<i>Weight %</i>	<i>Norm. Wt.%</i>	<i>Atom %</i>
<i>C K</i>	601	4.154	49.86	49.86	58.24
<i>N K</i>	149	12.096	30.23	30.23	30.28
<i>O K</i>	76	13.690	7.02	7.02	6.16
<i>Na K</i>	53	3.295	0.70	0.70	0.43
<i>S K</i>	439	1.138	1.78	1.78	0.78
<i>Cl K</i>	2269	1.194	10.40	10.40	4.12
<i>Total</i>			100.00	100.00	100.00

Appendix K. Nanocapsule batch



Appendix L. Nanocapsules microscopic (SEM) analysis



Resumen Biográfico

José Ernesto Palacios Santos



Candidato a Doctor en Ciencias con Orientación en Biotecnología

Tesis: Síntesis y caracterización fisicoquímica de hidrogeles foto entrecruzados de Alginato/Gelatina y nanocápsulas cargadas con α -tocoferol para su potencial uso como un biomaterial.

Campo de estudio: Biotecnología

Datos personales: Nacido en Monterrey, Nuevo León el 27 de Octubre de 1991, hijo de la Sra. Nelly Santos García y del Sr. José Ernesto Palacios Lerma.

Educación: Egresado de la Facultad de Enfermería de la Universidad Autónoma de Nuevo León con el título de Licenciado en Enfermería.

Experiencia Profesional: Enfermero General en el ISSSTE UNIDAD “A” CONSTITUCION en el área de urgencias, cuidados intensivos y ginecología (2014-2015). Enfermero Industrial en **VCIP, SOLUCIONES (2015)**.

Presentaciones en congresos: “Desarrollo de hidrogeles nanoestructurados para ingeniería de tejidos” en VIII Congreso Nacional de Ciencia e Ingeniería en Materiales (2017). “Desarrollo de Hidrogeles Fotoresponsivos de Gelatina/Alginato incorporando nanocápsulas de Policaprolactona (PCL) con α -tocoferol para su caracterización Fisicoquímica y Mecánica” en 1er Congreso Internacional de NanoBioIngeniería (2018). “Evaluación de la Eficiencia de Encapsulamiento y Actividad Antioxidante de Nanocápsulas de α -tocoferol mediante nanoprecipitado” en XVIII Congreso Nacional de Biotecnología y Bioingeniería (2019).